EXPERIMENTAL INVESTIGATION OF THE DIRECTIONAL DISTRIBUTION OF K_α X-RAYS FROM ELECTRON CONVERSION IN ^{169}Tm

---

A Dissertation
Presented to
the Faculty of the Department of Physics
University of Manitoba

In Partial Fulfillment
of the Requirements for the Degree
Doctor of Philosophy

---

by

David Lester Salie

August 1972

ABSTRACT

Experimental Investigation of the Directional Distribution of K_α X-rays from Electron Conversion in ^{169}Tm - David Lester Salie

The directional correlation coefficients and anisotropies involving the K_α X-rays generated by internal conversion were measured for several cascades in ^{169}Tm. The experimental anisotropies were $A(K_\alpha\text{-}\gamma_{131})=-0.065(19)$, $A(K_\alpha\text{-}\gamma_{110})=-0.038(22)$, $A(K_\alpha\text{-}(e_{177K}+e_{131L}))=-0.031(28)$, $A(K_\alpha\text{-}e_{198K})=-0.006(26)$, $A(K_\alpha\text{-}\gamma_{177})=-0.022(53)$ and $A(K_\alpha\text{-}\gamma_{198})=-0.002(17)$. It is suggested that these anisotropies are caused by a dynamic and possibly a static electric quadrupole interaction between the highly deformed nucleus and the K shell electrons when the nucleus de-excites by the highly retarded 177 keV and 198 keV transitions. The experimental values can be explained if the interaction is assumed to add $d_{3/2}'$ and $d_{5/2}'$ waves to the normal $1s_{1/2}$ K shell electron wavefunction. The measured directional correlation coefficients were consistent with $(4^{+5}_{-4})\%$ $d_{3/2}'$ and $(44\pm24)\%$ $d_{5/2}'$ waves in the $1s_{1/2}$ K shell electron wavefunction during the 177 keV nuclear transition and with $(11\pm10)\%$ $d_{3/2}'$ wave in the $1s_{1/2}$ K shell electron wavefunction during the 198 keV nuclear transition. Eighteen weak gamma-rays previously assigned to $^{169}Yb \rightarrow {}^{169}Tm$ decay were conclusively shown not to be associated with this decay.

PREFACE

Acknowledgements:

- To the National Research Council who started it all by providing a bursary and scholarship and indirectly for financial assistance for equipment.
- To Dr. S.K. Sen, the overseer, who provided the inspiration.
- To Dr. E. Tomchuk, whose equipment was priceless in these measurements.

Notation:

a_i = unnormalized directional correlation coefficients

A = anisotropy

$A_k, A_k()$ = directional correlation coefficients

b_i = electron particle parameters

$B^{\lambda}(Ur)$ = spherical Bessel functions of the first kind

c = speed of light

$C(\underline{l}\underline{l}'L;00)$ = Clebsch-Gordan coefficients

$C(\theta)$ = coincidences at angle θ

$f_i, f(), f'()$ = fractions

$F_i()$ = tabulated directional correlation coefficients

G_k = radial electron wavefunctions

H_k = radial electron wavefunctions

h = Planck's constant

I_i = intensity

j = total atomic spin

J = total nuclear spin

k_m = integer

k = quantum number

$\underline{K}$ = projection of nuclear angular momentum onto the nuclear symmetry axis

$\underline{l}$ = atomic angular momentum

L = multipolarity

m_e = electron mass

p = fraction

P_k = Legendre polynomial

q = electron charge

$Q_{kk'}^{\lambda(\pm)}$ = radial integral

r = electron wavefunction radius

R = random coincidence rate

S_i = single count rate

$T(jj'L)$ = X-ray transition rate

μ_i = coincidence rate

U = X-ray energy

w_i = detector efficiency

$W(\theta)$ = angular distribution function

$W(j\underline{l}j'\underline{l}';\frac{1}{2}L)$ = Wigner coefficients

X_i = area

α_i = conversion coefficient

δ = multipole mixing ratio

θ = angle

ρ = fine structure constant

τ = resolving time

TABLE OF CONTENTS

TABLE OF CONTENTS (continued)

The foolish and the dead alone
never change their opinion
... Lowell

CHAPTER I

INTRODUCTION

Many researchers have examined the interaction of the nuclear surroundings on the nucleus (see for example references 1,3) and the interaction of the nucleus on the valence electrons (see for example reference 2). The present dissertation will deal with the interaction of the nucleus on the K shell electrons toward which only little effort has previously been directed.[4-10] The experimental technique employed will be directional correlation measurements on a radioactive sample.

Directional correlation is the angular distribution of some type of radiation, for instance a gamma-ray, as a function of a coincidental second radiation, for instance an X-ray or another gamma-ray. Each radiation is detected with an appropriate detector and coincidences are recorded with the appropriate electronic instruments.

The technique can be elucidated further by considering Figure 1-1 in which cascade transitions #1 and #2 are shown. Here J_i, J and J_f are the spins of the initial, intermediate and final states. These three states are usually representative of three nuclear levels and transitions #1 and #2 are typically gamma-rays although they may be any radiation or charged particle. Then the

directional correlation measurement involves detecting transition #1 with detector 1 in coincidence with the detection of transition #2 with detector 2. When these two transitions are detected respectively, one measures the coincidences as a function of the angle θ between the two detectors to get the directional correlation between transitions #1 and #2.

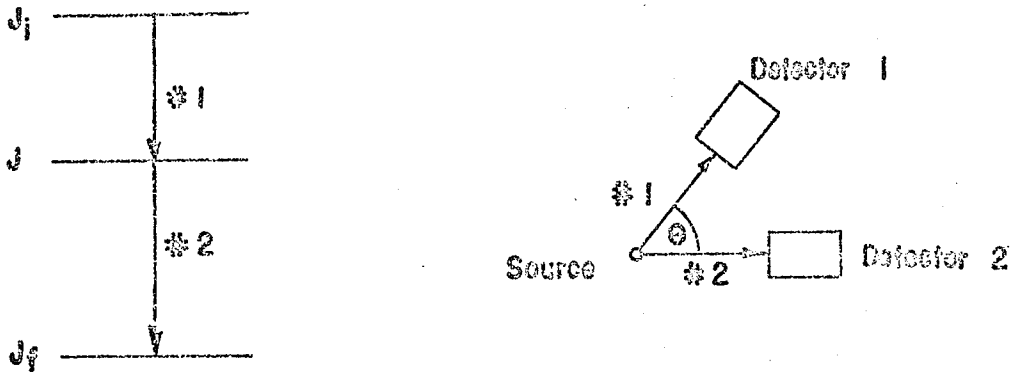

Figure 1-1. Illustration of the cascade transitions which give rise to directional correlation effects and an abbreviated schematic of the geometrical arrangement of the equipment used.

The complete formal theory of directional correlation has been developed in many articles (see for example reference 3). An important point is that if the intermediate spin, J, is 0 or 1/2 then the directional correlation is isotropic, i.e. independent of the angle θ.

Only when the intermediate spin is greater than 1/2 can the directional correlation be anisotropic, i.e. dependent upon the angle θ.

As mentioned previously transitions #1 and #2 are typically gamma-ray transitions between nuclear levels. Instead of the excited nucleus decaying by gamma-ray emission, the excited nucleus can transfer its excess energy to one of the atomic electrons by direct electromagnetic interaction. The atomic electron is ejected and is known as an internal conversion electron or more simply as a conversion electron. The ejection of the electron (largely from the K shell which is nearest to the nucleus) leaves a hole or vacancy in the electron orbit. This hole then decays predominantly through X-radiation.[a)]

It should be pointed out that X-rays can also be generated by electron capture. In electron capture a parent nucleus captures an atomic electron, changing itself into the daughter nucleus and simultaneously creating a hole in one of the atomic electron orbits (an antineutrino is also produced). This hole too decays predominantly through X-radiation as in the conversion electron emission case. The X-rays in both cases are identical. It is only in the manner in which the holes are generated that the two cases are different.

The measurement of the angular distribution of X-rays

a) Auger electron emission accounts for about 7% of the decays.

(following electron conversion of a nuclear transition) with respect to its associated conversion electron or cascading gamma-ray, in practice, differs little from the standard gamma-gamma or electron-gamma directional correlation measurements described in reference 3. The conversion electron-K X-ray directional correlation would involve cascade transitions, shown representatively in Figure 1-2. Here an excited nucleus with spin J_i de-excites through internal conversion of an electron in the K shell. The hole in the K shell is filled, in the figure, by an

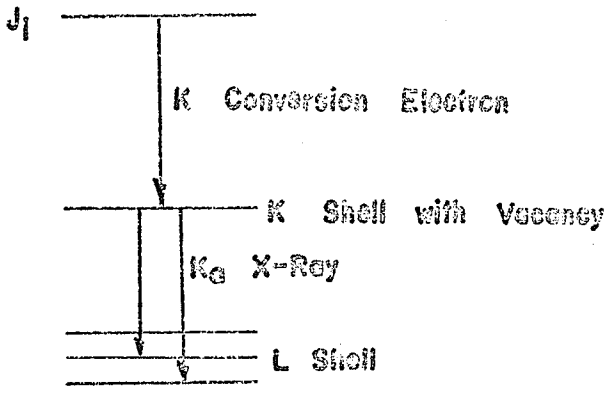

Figure 1-2. Representative diagram of the cascade transitions for a K conversion electron-K_α X-ray directional correlation measurement.

electron from one of the L subshells with the concurrent emission of an K_α X-ray. Hence the K conversion electron-K_α X-ray directional correlation simply involves the detection of a K conversion electron in coincidence with

a K_α X-ray and a measurement of this coincidence rate as a function of the angle between the two detectors.

A.Z. Dolginov's theory[4] generally denies the existence of K X-ray-gamma-ray anisotropy and K X-ray-conversion electron anisotropy either for the K X-ray associated with electron capture or with electron conversion.[a] However, he mentions that for the electric monopole (E0) transitions and partly for the magnetic dipole (M1) transitions the structure of the nucleus will give corrections which may change this.[b] These corrections will be applicable only for the K X-rays associated with electron conversion. Dolginov does not indicate what he feels these corrections will be.

Perepelkin[5] measured the directional correlation between the electron capture K X-rays and the subsequent gamma-rays in the electron capture decay of ^{54}Mn to ^{54}Cr (see Figure 1-3). He obtained an anisotropy of 2.3±0.4%. Fechner et.al.[6] later performed similar measurements on $^{54}Mn \rightarrow {}^{54}Cr$, as well as on $^{139}Ce \rightarrow {}^{139}La$, $^{153}Gd \rightarrow {}^{153}Eu$ and $^{202}Tl \rightarrow {}^{202}Hg$. In all cases, their electron capture

a) Anisotropy, A, is defined as $A = (C(180^\circ)-C(90^\circ))/C(90^\circ)$ where $C(\theta)$ is the coincidences between two detectors at an angle θ to each other.
b) E1 is short for an electric dipole and similarly E2 is short for electric quadrupole.

K X-ray-gamma-ray directional correlation measurements showed isotropy (i.e. no anisotropy) with an accuracy of better than 0.4%.

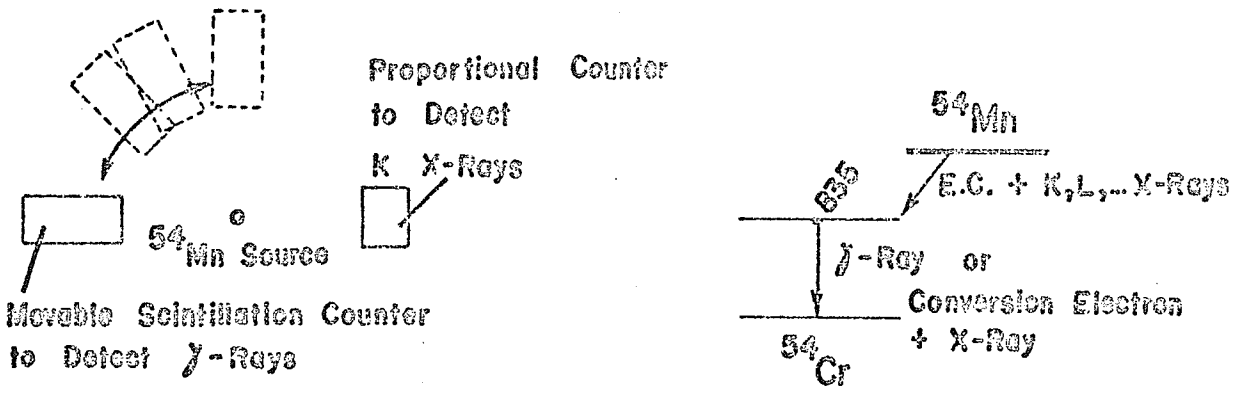

Figure 1-3. Representative diagram of the equipment in Perepelkin's investigation[5] of the K X-ray-gamma-ray directional correlation in the decay of ^{54}Mn and the decay scheme of ^{54}Mn.

Further K X-ray-gamma-ray directional correlation measurements by M.K. Ramaswamy[7] on $^{65}Zn \rightarrow {}^{65}Cu$, $^{85}Sr \rightarrow {}^{85}Rb$, $^{113}Sn \rightarrow {}^{113}In$ and $^{133}Ba \rightarrow {}^{133}Cs$ yielded isotropic distributions to typically 1%. The measurement on $^{113}Sn \rightarrow {}^{113}In$ was repeated by Murty et.al.[8] and they too, obtained an isotropic distribution with an accuracy of about 0.6%. It was generally concluded that within the experimental error, there was no correlation between the

K X-ray from electron capture and the succeeding gamma-ray - as predicted by the theory of Dolginov.[4)]

Of course all these measurements involved the K X-ray associated with electron capture and a subsequent gamma-ray. However in McDonnell and Ramaswamy's experiment[9)] on $^{133}Ba \rightarrow {}^{133}Cs$ (see Figure 1-4) they point out that part

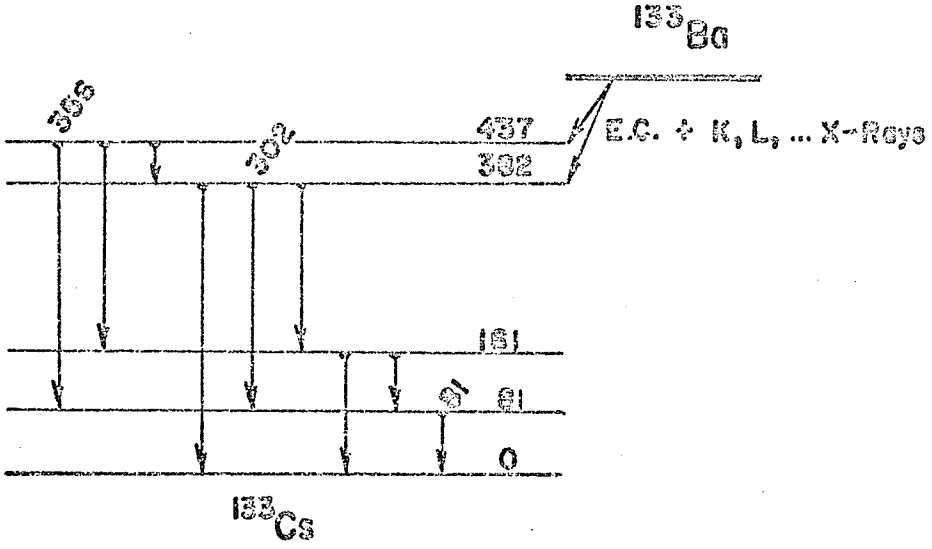

Figure 1-4. Decay scheme of $^{133}Ba \rightarrow {}^{133}Cs$.[9)]

of the K X-rays originated from the internal conversion of the 81 keV gamma-ray. Since they measured an isotropic distribution for K X-ray-gamma-ray, they interpreted their result as implying that there was also no correlation between the gamma-ray and the succeeding K X-ray arising from internal conversion. Rightfully they had only set

an upper limit. Since less than half the K X-rays would originate from the internal conversion of the 81 keV transition, the upper limit of the anisotropy would be about 2-3%.

Brannan[10] looked for the existence of a directional correlation between K X-rays and internal conversion electrons in the electron capture decay of $^{145}Sm \rightarrow {}^{145}Pm$ and $^{195}Hg \rightarrow {}^{195}Pt$ and the β^- decay of $^{203}Hg \rightarrow {}^{203}Tl$. He compared the count rate of electrons that were in coincidence with the K X-rays emitted at 180° relative to the direction of electron emission with the coincidence count rate of emission at 90°. For ^{145}Sm and ^{195}Hg the K X-ray-L conversion electron distributions were isotropic to 2% and 1% respectively. In these two cases the K X-rays would be primarily from K electron capture. For ^{203}Hg the K X-rays would be from K electron conversion. In this case the distribution was isotropic to about 2%.

In 1968 Sen[11] suggested that, in some special cases, a small anisotropy could be detected in the directional correlation measurements between the K conversion electrons and the accompanying K X-rays. He suggested that the perturbation of the K shell due to the static dipole and static quadrupole moments of the nucleus could add in states to the unperturbed K shell. Occasionally a K conversion electron would be ejected from such a state,

leaving an intermediate state with spin greater than 1/2. As mentioned previously, when the intermediate spin in a cascade is greater than 1/2 the directional correlation can be anisotropic. In such a case the directional distribution of the K X-rays would be determined by both the population of the perturbed states and the probability of electron conversion from these states.

Church and Weneser[12] state that the effect of the static magnetic dipole and static electric quadrupole moments on the electron wave functions and so on the conversion process have not been very deeply explored. They say that on the basis of first order perturbation calculations of the nuclear static dipole moment effect on the K shell one would not expect to see any anisotropy. They add however that a large static quadrupole moment could produce a percent or so change in the K conversion coefficients for M1 and E2 transitions. In first order the quadrupole perturbation of the bound K shell wave function, which could be written symbolically as $(1s_{1/2}^2, J=0)$, would be to add in $(d_{3/2}', 1s_{1/2}, J=2)$ and $(d_{5/2}', 1s_{1/2}, J=2)$ components to the unperturbed K shell wave function.[12]

Sen[11] suggested that if 1% of the ejected conversion electrons come from a perturbed K shell with a spin of 5/2, then the anisotropy in the directional correlation would be about 0.2%. On the other hand, if 1% of the conversion

electrons come from a 3/2 spin K shell, the anisotropy would be about 0.06%.

Naturally the perturbation should be greatest for a nucleus which interacts strongly with the K shell atomic electrons and which has a large electric quadrupole moment. Strong interaction should occur if the K shell atomic electrons penetrate the nuclear volume.

I. ISOTOPE ^{169}TM

To measure the existence of any interaction, a suitable isotope had to be selected. The isotope selected on which to perform the directional correlation measurements was ^{169}Yb (see Figure 1-5). Here is a deformed nucleus which decays by electron capture to another deformed nucleus, ^{169}Tm. Thulium-169 has an isomeric level of 0.66 μsec and retarded M1 transitions.[14] The significance of the isomeric level will be explained later. Retardation is usually associated with nuclear penetration.[15,16] Hence there should be a strong interaction between the nucleus and the K shell electrons. The first excited state has an electric quadrupole moment of $-1 \times 10^{-24} cm^2$ [17,18] (the negative sign indicates an oblate charge symmetry). The more energetic excited levels would likely have the same or even larger electric

Figure 1-5. Decay scheme of $^{169}Yb \rightarrow {}^{169}Tm$ taken from reference 13.

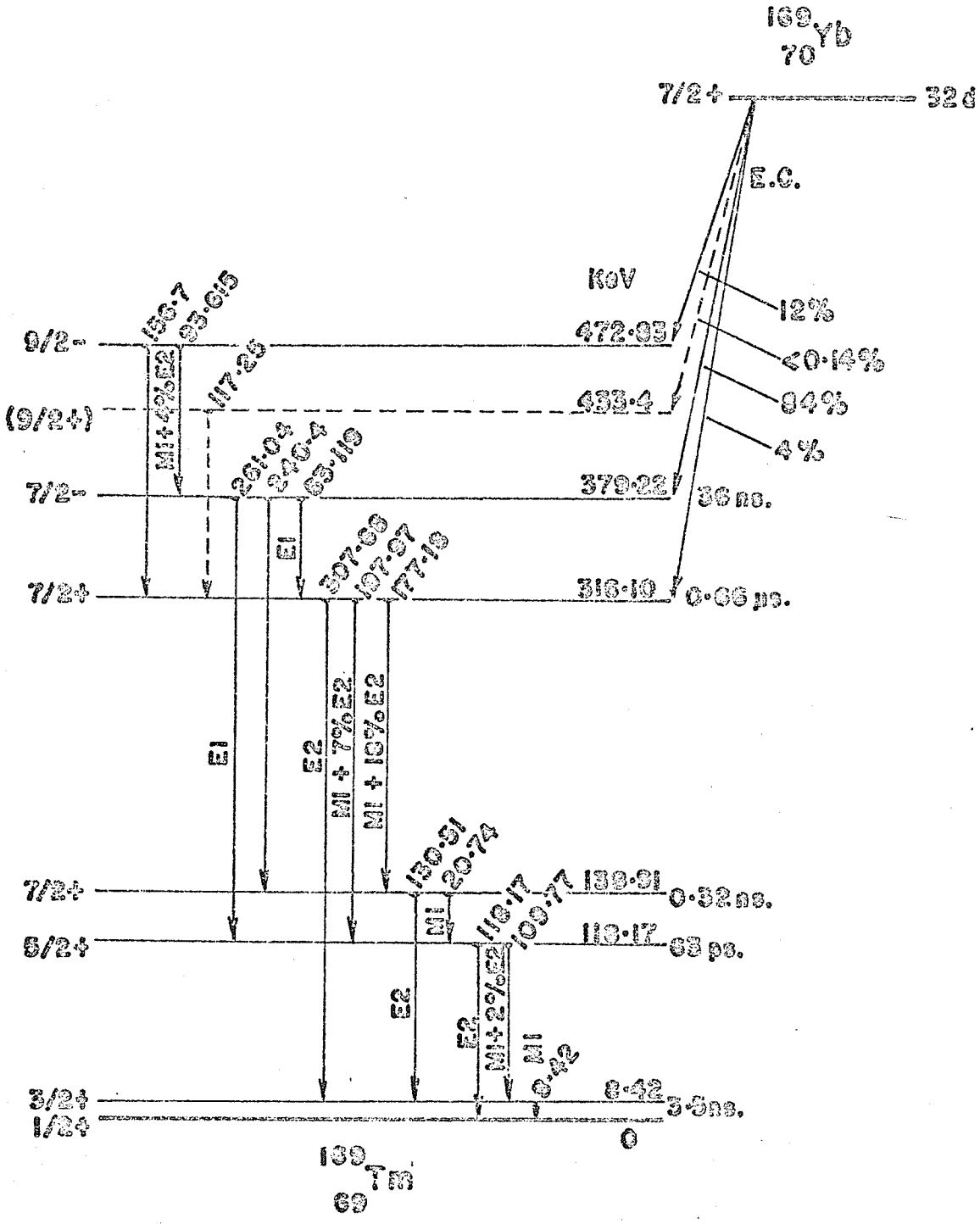
169 70 Yb
7/2+
32 d
E.C.
KeV
12%
<0·14%
84%
4%
9/2-
472·93
(9/2+)
432·4
7/2-
379·22
36 ns.
7/2+
316·10
0·66 ps.
7/2+
139·31
0·32 ns.
5/2+
113·17
68 ps.
3/2+
1/2+
0·42
3·5 ns.
0
169 69 Tm
150·7
93·615
M1+4%E2
117·25
261·04
240·4
63·19
E1
307·03
197·97
177·19
E1
E2
M1 + 7%E2
M1 + 10%E2
150·51
20·74
M1
116·17
109·77
E2
E2
M1+20%E2
M1
0·42

quadrupole moments. In fact the 139 keV level has the same quadrupole moment as the 118 keV level.[33] So the situation is ripe for nuclear perturbation of the K shell electron wave function.

Electron capture of ^{169}Yb feeds levels only above the 0.66 μsec isomeric level or that level itself. This enables one to separate events above from those below when a coincidence experiment involving X-rays is performed. In particular, it isolates the K_α X-rays after conversion electron emission of transitions below the level from the K_α X-rays associated with electron capture. In other words, when a K_α X-ray is detected in the coincidence experiment, it is known that it is a result of conversion electron emission and not from electron capture. In this respect, the isomeric level is extremely valuable.

This isotope is unique in that the isomeric level can decay to another level with the same spin. In fact the $7/2^+$ isomeric level decays predominantly to two levels - another $7/2^+$ level and to a $5/2^+$ level. The $7/2^+ \rightarrow 7/2^+$ (177 keV) transition and the $7/2^+ \rightarrow 5/2^+$ (198 keV) transition are both M1 transitions and both are strongly retarded by the K-selection rule.[14,19]

Of course an explanation of the K-selection rule is in order. For the Bohr-Mottelson rotational model of the nucleus, which is used to describe heavy deformed nuclei,

the emission of electric quadrupole (E2) or magnetic dipole (M1) radiation is dependent upon a parameter $\underline{K}$. $\underline{K}$ is the value of the projection of the total angular momentum of the nucleus, J, onto the nuclear symmetry axis. $\underline{K}$ also indicates which rotational band one is referring to. Consequently, the transition is governed by what is known as the $\underline{K}$-selection rule - the matrix element giving a meaasure of the intensity of the transition, vanishes unless $\Delta\underline{K}=|\underline{K}_i-\underline{K}_f|=0$ or 1, where i indicates a level in the initial rotational band and f refers to a level in the final rotational band. Thus if $\Delta\underline{K}=2,3,\ldots$ this transition would be forbidden and retarded. In the case of ^{169}Tm, the isomeric level belongs to a $\underline{K}=7/2$ band which decays to levels in a $\underline{K}=1/2$ band. Since $\Delta\underline{K}=3$, the transitions are retarded.

So here is a nucleus for which the nuclear quadrupole interaction on the K shell, if it is sufficiently strong, should be experimentally detectable.

Although ^{169}Tm has the features which should maximize the static quadrupole interactions with the K shell, it has a number of shortcomings. For one thing the nucleus itself is rather complicated with a number of transitions. The dozen or so transitions are all crowded within a 300 keV energy range. Hence in selecting any peaks for coincidence purposes, care must be exercised to see that

no adjacent peaks are accepted in the energy window of interest. This problem is especially acute for the case of K X-ray-electron directional correlation measurements. Here the K, L, M, ... lines more than triple the original dozen transitions.[a)]

Another ^{169}Tm shortcoming is the half-life of the isomeric level. Although the isomeric level has a half-life of 660 nanoseconds, it would be more advantageous if it were longer. A longer lifetime would prevent even more of the K X-rays associated with electron capture from "leaking through" and appearing as legitimate coincidences with a gamma-ray or conversion electron below the level. This is not a serious problem however.

Of course since the magnitude of the anisotropy is expected to be small - of the order of a few percent at the most - the measurements must not be influenced by any small systematic geometrical or electronic error. A systematic error of say 2% in measuring directional correlations involving a 20% anisotropy would be insignificant; in anisotropies of 1%, it would be catastrophic.

a) If the conversion electron comes from the K shell it falls in the K line; similarly if it comes from the L shell or M shell, it falls in the L or M lines respectively. The energies of the respective lines are the energy of the transition less the binding energy of the appropriate shell.

Coincidence counting for several hours at each angle could be sensitive to electronic drifts in the electronic equipment. Properly the results of short scans (say half an hour or less) must be taken. They should yield the same results as the long runs in order to establish the credibility of the long runs.

It must also be pointed out that very thin sources are required for the electron-K X-ray work in order to eliminate or at least minimize excessive electron scattering in the source.

Certainly crystalline structure must be avoided in the solid sources in order to rule out the possibility that any crystal-atom interaction will distort or generate anisotropy. This could be achieved by subliming (vacuum depositing) the original radioactive material onto a conductive backing. This should yield a thin noncrystalline source.

II. ISOTOPE ^{207}PB

In addition to ^{169}Tm, some directional correlation measurements were performed on ^{207}Bi $\rightarrow$ ^{207}Pb (see Figure 1-6). This nucleus is beyond the deformed region and has higher multipole transitions than those in ^{169}Tm. It has a small electric quadrupole moment and the K shell

Figure 1-6. The decay scheme of $^{207}Bi \rightarrow ^{207}Pb$ taken from reference 13.

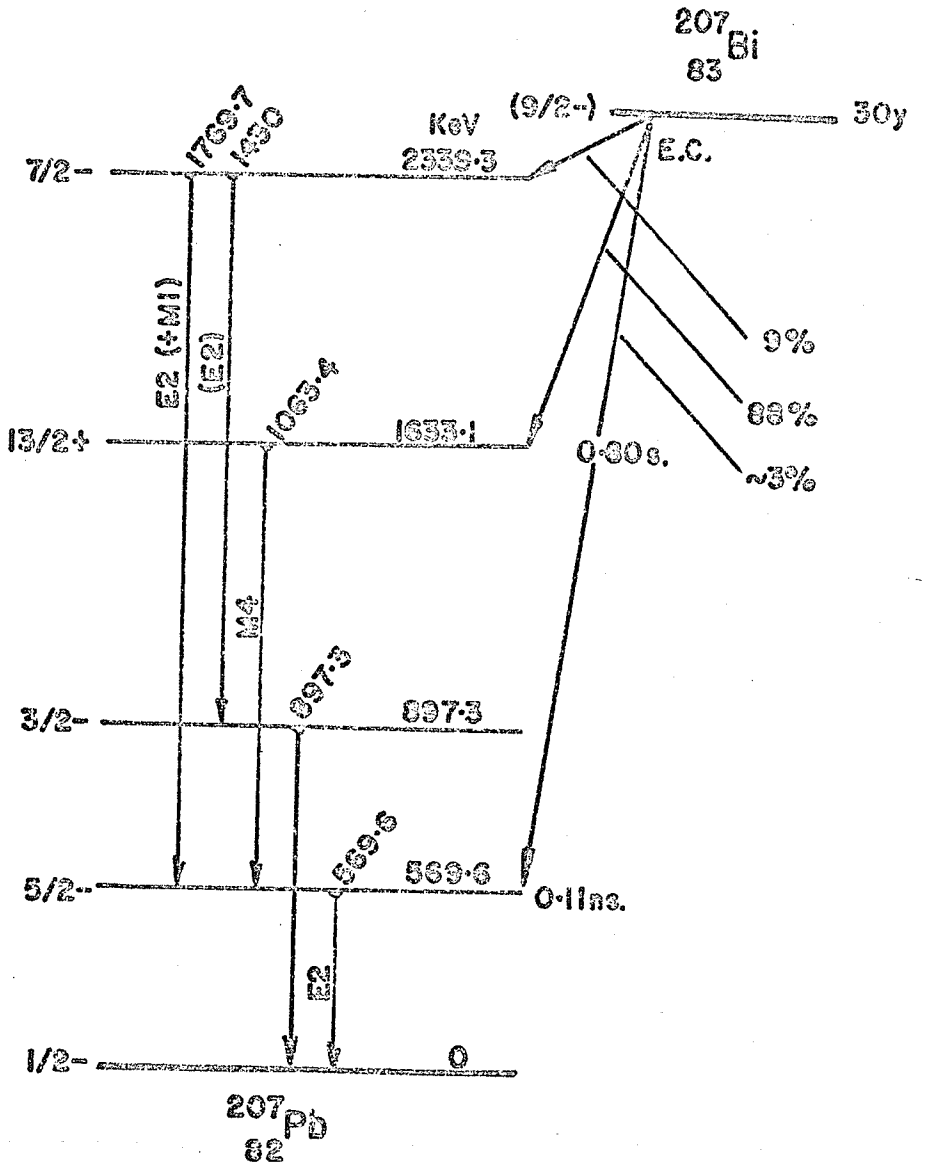
207 Bi 83
(9/2-)
30y
KeV
2339·3
E.C.
7/2-
1769·7
1430
E2 (+M1)
(E2)
1065·4
1633·1
9%
88%
~3%
0·30s.
13/2+
M4
897·3
897·3
3/2-
669·6
569·6
0·11ns.
5/2-
E2
1/2-
0
207 Pb 82

electrons do not penetrate the nuclear volume. These qualities should make any measurements of K X-ray-conversion electrons nearly, if not completely, isotropic.

In ^{207}Pb (as in ^{169}Tm) there is an isomeric level of 0.80 second half-life which enables one to separate K X-rays after conversion electron emission of the 1064 keV transition from the K X-rays associated with electron capture. Although the two nuclei are similar, one isotope, ^{169}Tm, has a structure favourable to nuclear interactions with the K shell electrons, while the other, ^{207}Pb, has not.

CHAPTER II

EQUIPMENT AND ELECTRONICS

I. INSTRUMENTATION FOR DIRECTIONAL CORRELATION MEASUREMENTS ON ^{169}TM

The geometrical configuration of the experimental apparatus for the directional correlation measurements on $^{169}Yb \rightarrow {}^{169}Tm$ is shown in Figure 2-1. The electron detector as well as the source (suspended in the source holder) were in a chamber evacuated to about 10^{-5} torr. The aluminum source chamber had three beryllium windows, each 10 mil thick. The size of the beryllium windows were such that at the three angles of interest (specifically 90°, 135° and 180°) the X-ray detector saw the source strictly through the beryllium windows. The cap with the beryllium windows along with the source holder were removed when measurements on a liquid were performed.

All of the detectors and the electronics were commercial products.

The electron detector was a 50 mm^2 X 3 mm Si(Li) detector cooled to liquid nitrogen temperature. The electron detection system resolution was typically 2.0 keV FWHM (full width at half maximum)[a] for electrons with an

a) The resolution of a gamma-ray or electron detector is usually specified by the full width at half the peak

Figure 2-1. The geometrical arrangement of the experimental apparatus for the directional correlation measurements on $^{169}Yb \rightarrow {}^{169}Tm$.

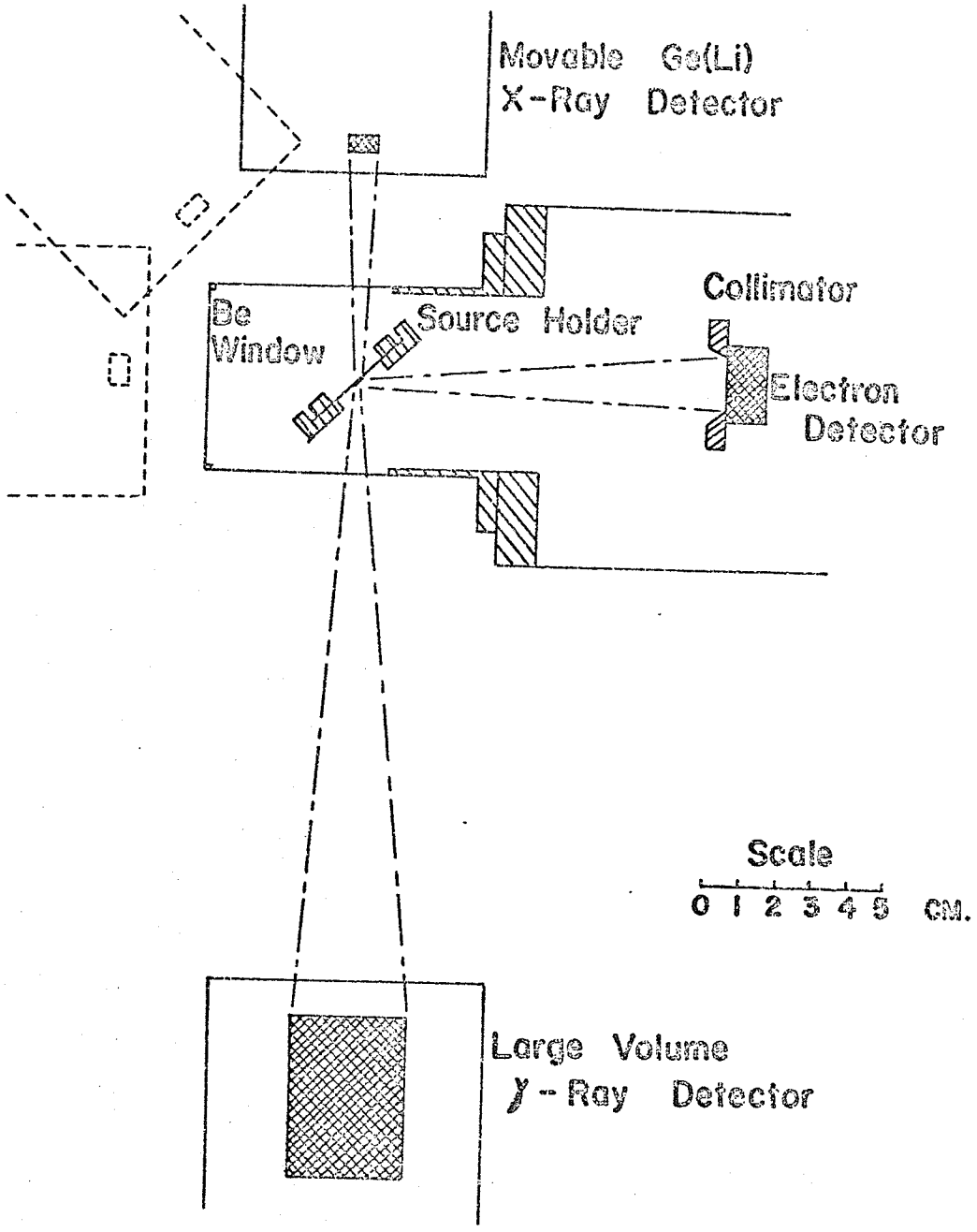
Movable Ge(Li)
X-Ray Detector
Collimator
Be
Window
Source Holder
Electron
Detector
Scale
0 1 2 3 4 5 CM.
Large Volume
γ-Ray Detector

energy of about 130 keV.

A small volume Ge(Li) detector acted as the X-ray detector. Its resolution was about 750 eV for 60 keV X-rays. It was positioned on a movable platform which in turn was pivoted at a point directly below the source. The center of the detector's circular motion was the radioactive source.

The gamma-ray detector was a 40 cc coaxial Ge(Li) detector. Its resolution was 1.95 keV FWHM for 122 keV gamma-rays. It was positioned at right angles to the electron detector.

The detectors were aligned to within 1^{o} of the designated angles of 90^{o}, 135^{o} and 180^{o}.[b] Their heights, i.e. the position of the center of the detectors, were also aligned in the same horizontal plane to within 1 mm. The K X-ray single count rate varied by less than a half of a percent as the X-ray detector was moved from 90^{o} to 135^{o} and then to 180^{o} (or back again). This was indicative of the accuracy with which the X-ray detector was positioned

height that the detector yields when it is activated by a mono-energetic gamma-ray or electron.

b) These angles are the angles between the electron detector and the X-ray detector at which coincidences were recorded. Since the gamma-ray detector was at right angles to the electron detector, these angles were the complementary angles between the gamma-ray detector and the X-ray detector.

with respect to the radioactive source.

The electronic system for the K X-ray-gamma-ray directional correlation measurements is shown in Figure 2-2. The same system was utilized for the K X-ray-conversion electron measurements. For this latter case, the gamma-ray detector was replaced with the electron detector.

All the low voltage and high voltage power supplies have not been shown in the diagram. The lettering adjacent to the 'AND' gates are standard Boolean algebra expressions. For instance, the expression AB+AC represents an output of A and B or A and C.

The system registered an energy-dependent analog signal from the X-ray detector whenever an X-ray or gamma-ray entered the X-ray detector simultaneously with the entrance of an unique gamma-ray into the gamma-ray detector. The unique gamma-ray would be any gamma-ray whose energy was within the energy range specified by the single channel analyzer. The system registered separately the coincidence spectra for two gamma-ray energy ranges. Each energy range was set with one of the single channel analyzers (SCA) positioned after the gamma-ray linear amplifier (LA).

The system's time resolution for the K X-ray-conversion electron coincidences was about 30 nanoseconds and for the K X-ray-gamma-ray coincidences, it was about 40 nanoseconds.

Figure 2-2. The electronic system for the K X-ray-gamma-ray directional correlation measurements on $^{169}Yb \rightarrow {}^{169}Tm$.

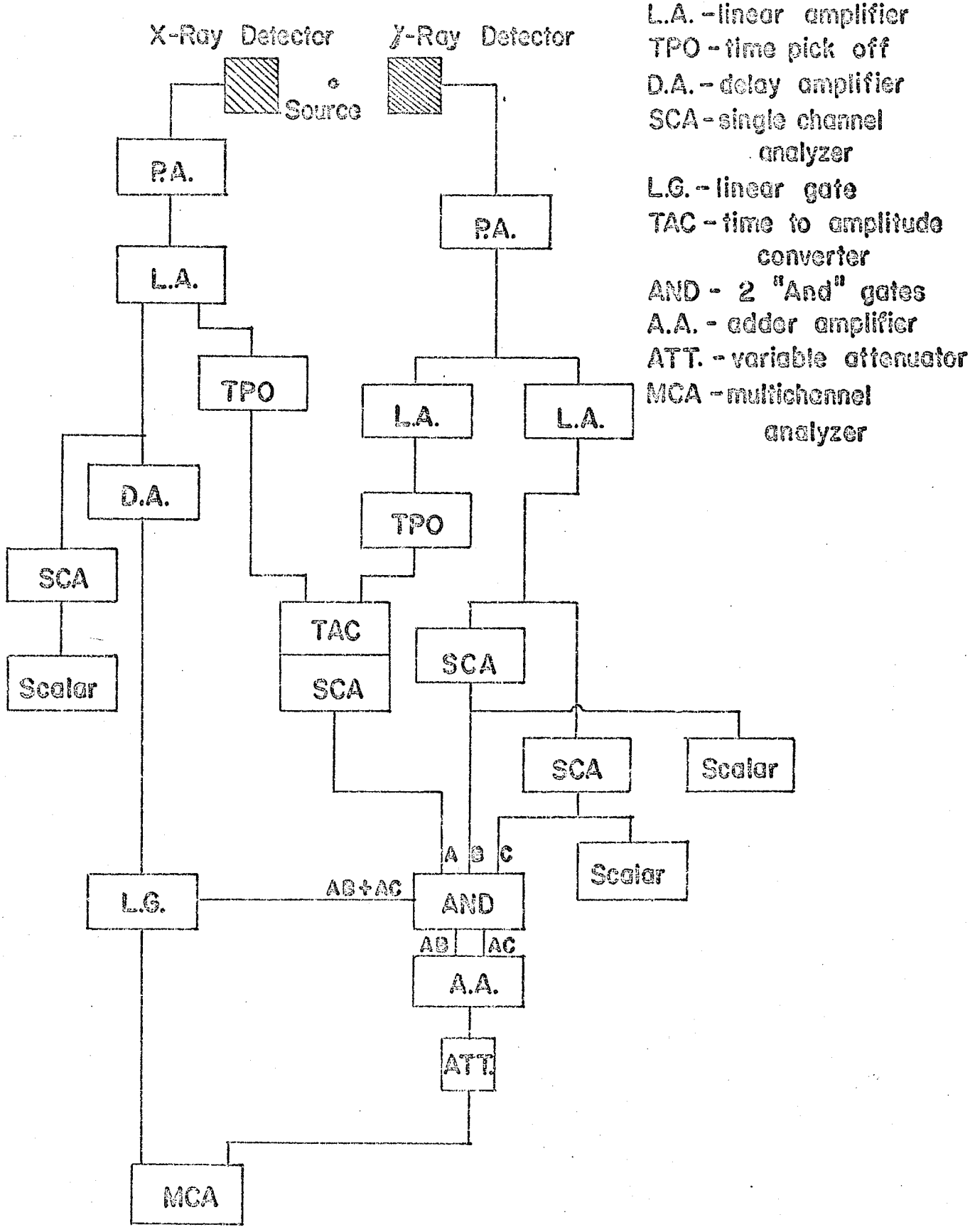
X-Ray Detector
γ-Ray Detector
Source
P.A.
P.A.
L.A.
TPO
L.A.
L.A.
D.A.
TPO
SCA
Scalar
TAC
SCA
SCA
SCA
Scalar
Scalar
A B C
L.G.
AB+AC
AND
AB
AC
A.A.
ATT.
MCA
P.A. - preamplifier
L.A. - linear amplifier
TPO - time pick off
D.A. - delay amplifier
SCA - single channel analyzer
L.G. - linear gate
TAC - time to amplitude converter
AND - 2 "And" gates
A.A. - adder amplifier
ATT. - variable attenuator
MCA - multichannel analyzer

Leading edge pick-off on the non-integrated amplified signals were employed. The actual coincidence electronics was the time-to-amplitude converter (TAC) coupled to a single channel analyzer (SCA).

The scalars on the outputs of the single channel analyzers gave the gated singles from which the random coincidences were calculated.[a] In addition the gated K_α X-ray singles were used in the singles correction; but this will be discussed later.

No intimate description of the electronic system will be given which hopefully will be a welcome relief to the reader since such a description serves no useful purpose.

II. INSTRUMENTATION FOR DIRECTIONAL CORRELATION MEASUREMENTS ON ^{207}PB

The geometrical arrangement for the directional correlation measurements on $^{207}Bi \rightarrow {}^{207}Pb$ was slightly different from the measurements conducted on $^{169}Yb \rightarrow {}^{169}Tm$. The configuration is shown in Figure 2-3. The same small volume Ge(Li) detector was utilized but the electron detector was a liquid-nitrogen-cooled, 100 mm^2 x 3 mm Si(Li)

a) The random coincidences rate R using a time-to-amplitude converter is $R=\tau S_1 S_2$ where τ is the resolution of the coincidence circuit and S_1 and S_2 are the singles count rates.

Figure 2-3. The geometrical arrangement for the directional correlation measurement on $^{207}Bi \rightarrow ^{207}Pb$.

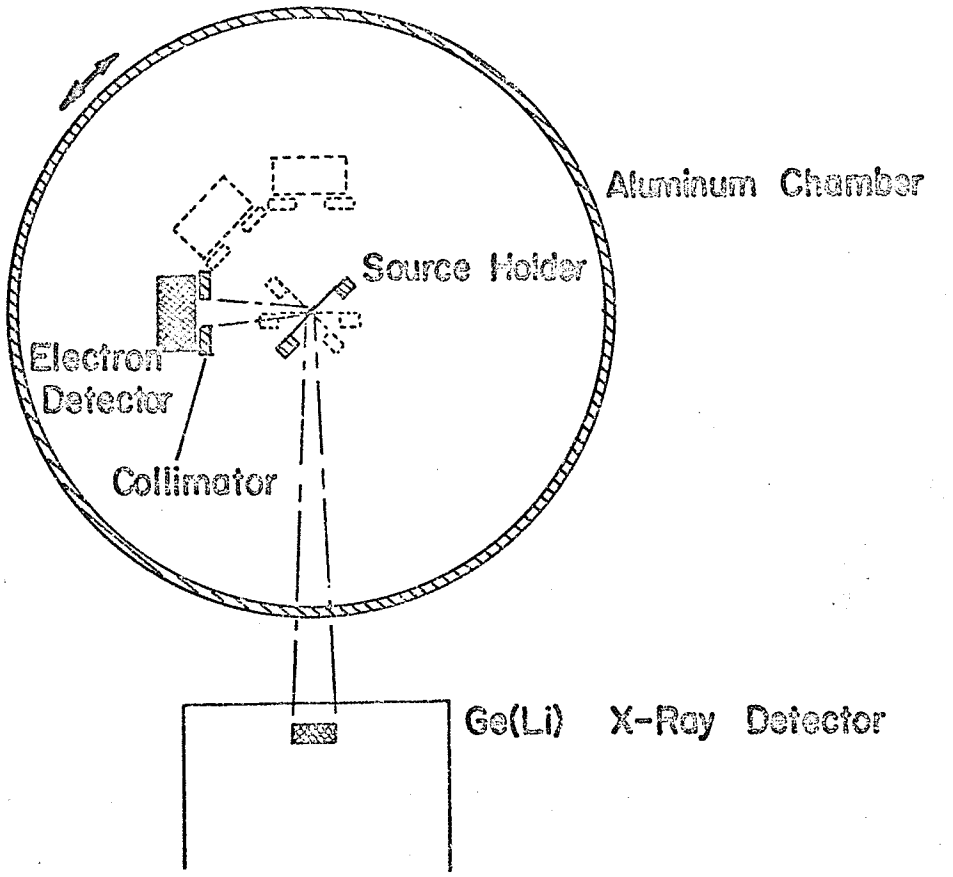
Aluminum Chamber
Source Holder
Electron Detector
Collimator
Ge(Li) X-Ray Detector
Scale
0 1 2 3 4 5 CM.

detector with a typical resolution of 8 keV for electrons of an energy of about 1000 keV.

Rather than move the X-ray detector, the entire chamber with the electron detector and source was rotated. This technique was more practical than moving the X-ray detector. Again the K_α singles counting rate differed by less than 1% at 90°, 135° and 180° (with respect to the electron detector).

The electronic system used is shown in Figure 2-4. The principle of the system was essentially the same as the system described four pages previously.

Figure 2-4. The electronic system for the directional correlation measurements on $^{207}Bi \rightarrow {}^{207}Pb$.

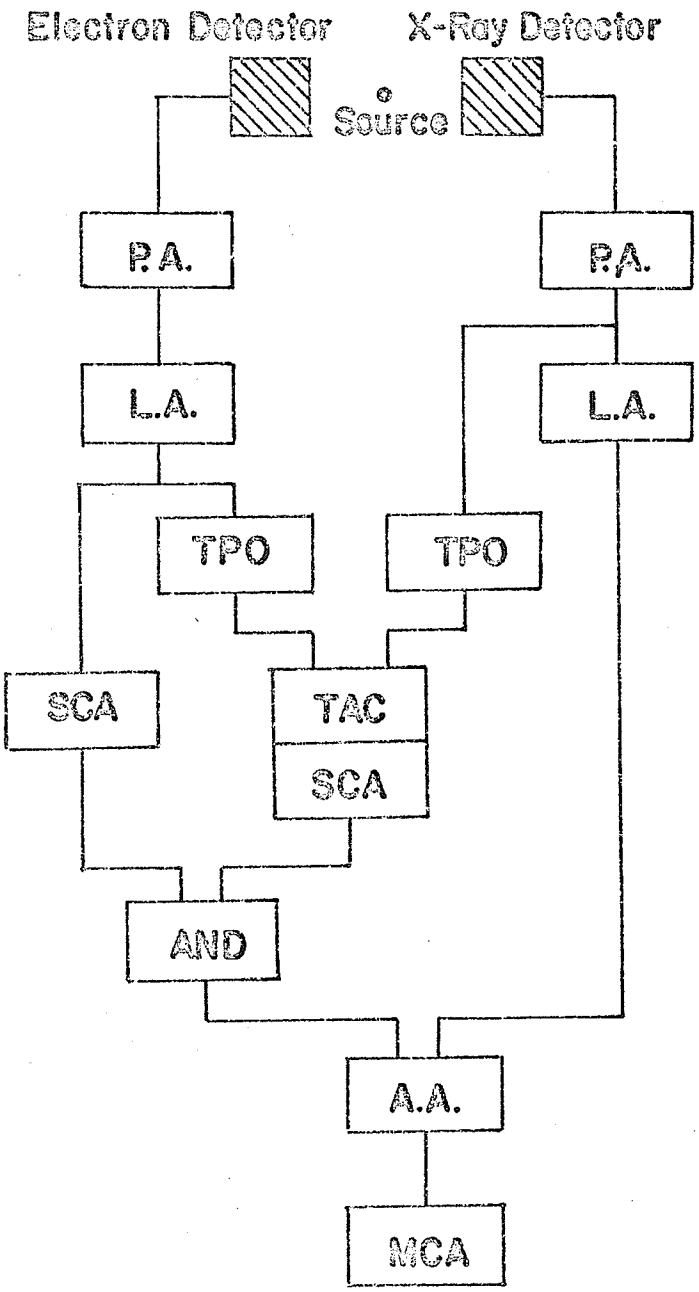

P.A. - preamplifier
L.A. - linear amplifier
TPO - time pick off
SCA - single channel analyzer
TAC - time to amplitude converter
AND - "And" gate
A.A. - adder amplifier
MCA - multichannel analyzer

CHAPTER III

EXPERIMENT

I. GAMMA-RAY TRANSITIONS IN THE DECAY OF $^{169}YB \rightarrow ^{169}TM$

Before the directional correlation measurements are revealed and discussed, the decay scheme of $^{169}Yb \rightarrow ^{169}Tm$ will be examined.

The generally accepted levels in ^{169}Tm were as shown in Figure 1-5.[13] Recently numerous weak transitions, observed in the gamma-ray singles spectrum and attributed to $^{169}Yb \rightarrow ^{169}Tm$ decay, have been reported.[20,21] In order to incorporate these transitions additional levels were introduced in ^{169}Tm and assumed to be populated in the decay of ^{169}Yb. To verify or deny the existence of these transitions (and the population of the proposed levels) several gamma-ray singles spectra of ^{169}Yb decay were taken.

Four Ge(Li) gamma-ray detectors were used. Three were large volume detectors - 50 cc, 40 cc and 35 cc - and one was a small 0.25 cc volume one. Thus any scattering, summing[a] or escape[b] peak would have an intensity

a) A sum peak occurs when two cascade gamma-rays enter the Ge(Li) detector at the same time. Then the total energy deposited is the sum of the two individual gamma-rays.
b) An escape peak occurs when a germanium K X-ray escapes

(relative to a known ^{169}Tm transition) that would change as the different detectors were utilized.

Furthermore several original commercial sources were used to make the radioactive sources from which the gamma-ray singles spectra were obtained. The solid sources were sublimed from the original liquid material supplied. The liquid sources received no special treatment. They were simply a small quantity of the mother liquid pipetted into thin-walled plastic tubes. Three different sources from New England Nuclear Corporation, each purchased a year apart, and one from Amersham/Searle were used. Thus the impurity concentration and their intensities (relative to a known ^{169}Tm gamma-ray) would vary as the different sources were looked at.

The relative gamma-ray intensities were determined from the standard relation

$$\frac{I_1}{I_2} = \frac{X_1}{X_2} \cdot \frac{w_2}{w_1}$$

where I_1 was the intensity of gamma-ray #1 relative to the intensity I_2 of gamma-ray #2; X_1 and X_2 were the areas under the total absorption peaks of gamma-rays #1 and #2, respectively; w_1 and w_2 were the absorption peak

from the Ge(Li) detector after an incident gamma-ray has interacted with the germanium K electrons by the photoelectric process.

efficiencies of the detector for gamma-rays #1 and #2. The efficiency of each gamma-ray detector was determined using standard radioactive sources.

0-200 keV Range. The gamma-rays that were investigated were those that had all been reported as arising from electron capture decay of ^{169}Yb.[20,21,22] Figure 3-1 is the gamma-ray singles spectrum in the energy range 0-200 keV taken with the 0.25 cc Ge(Li) detector. The firmly established gamma-rays of ^{169}Yb decay are labelled with their accepted energies.[13] The first gamma-ray in question is the one at 117 keV. The region around 118 keV is enlarged in Figure 3-2 in order to show the composite peaks of 117.3 keV and 118.2 keV (the 117.3 keV transition was reported by Alexander et.al.[22]). The shape of the 118.2 keV photopeak was determined from the 130.5 keV photopeak. The latter was not plagued by adjoining peaks. As is evident in Figure 3-2, there was a 117.3 keV gamma-ray. The relative intensities of this gamma-ray as well as the others that were examined, are listed in Table I on page 52.

Figure 3-3 is the gamma-ray singles spectrum in the energy range 130-800 keV taken with the 50 cc Ge(Li) detector. Important portions of the spectrum are expanded in Figures 3-4, 3-7, 3-9, 3-11 and 3-14. Figure 3-4 is the

Figure 3-1. Gamma-ray singles spectrum in the energy range 20-200 keV with the 0.25 cc Ge(Li) detector.

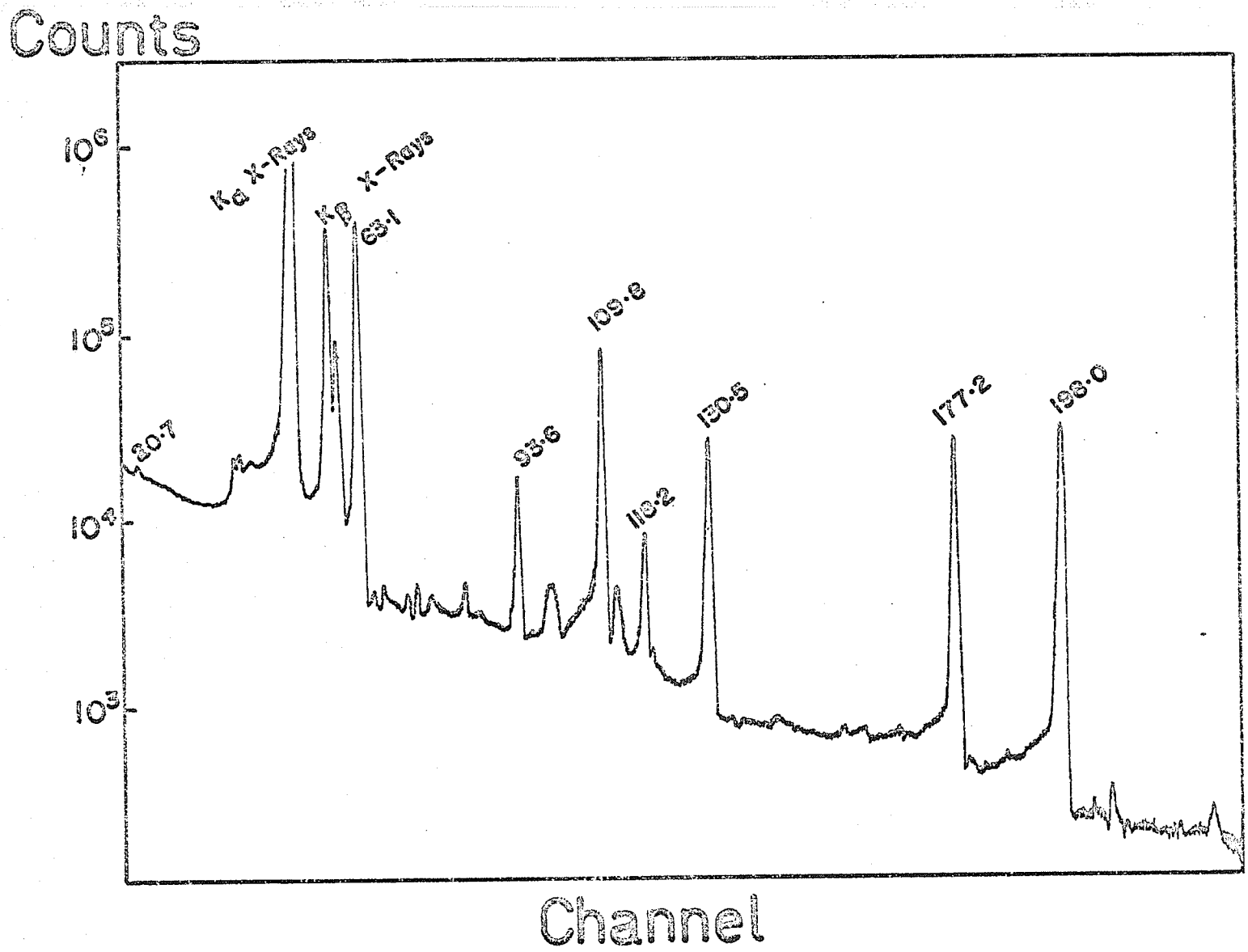
Counts
10^6
10^5
10^4
10^3
Ka X-Rays
Kβ X-Rays
63.1
20.7
53.6
109.8
118.2
130.5
177.2
198.0
Channel

Figure 3-2. The region around the 118 keV gamma-ray taken with the 0.25 cc Ge(Li) detector.

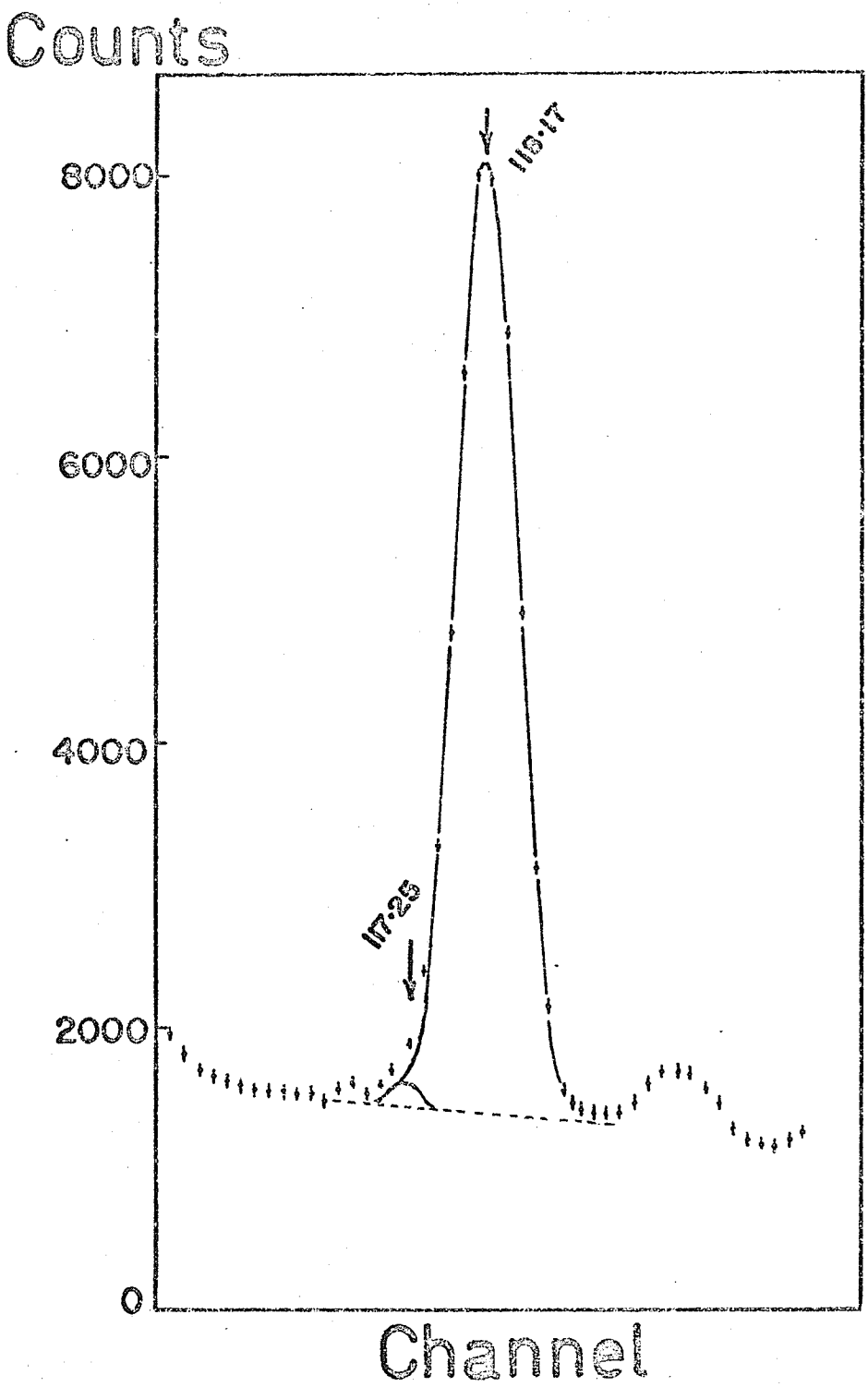
Counts
8000
6000
4000
2000
0
115·17
117·28
Channel

Figure 3-3. Gamma-ray singles spectrum in the energy range 130-800 keV taken with the 50 cc Ge(Li) detector.

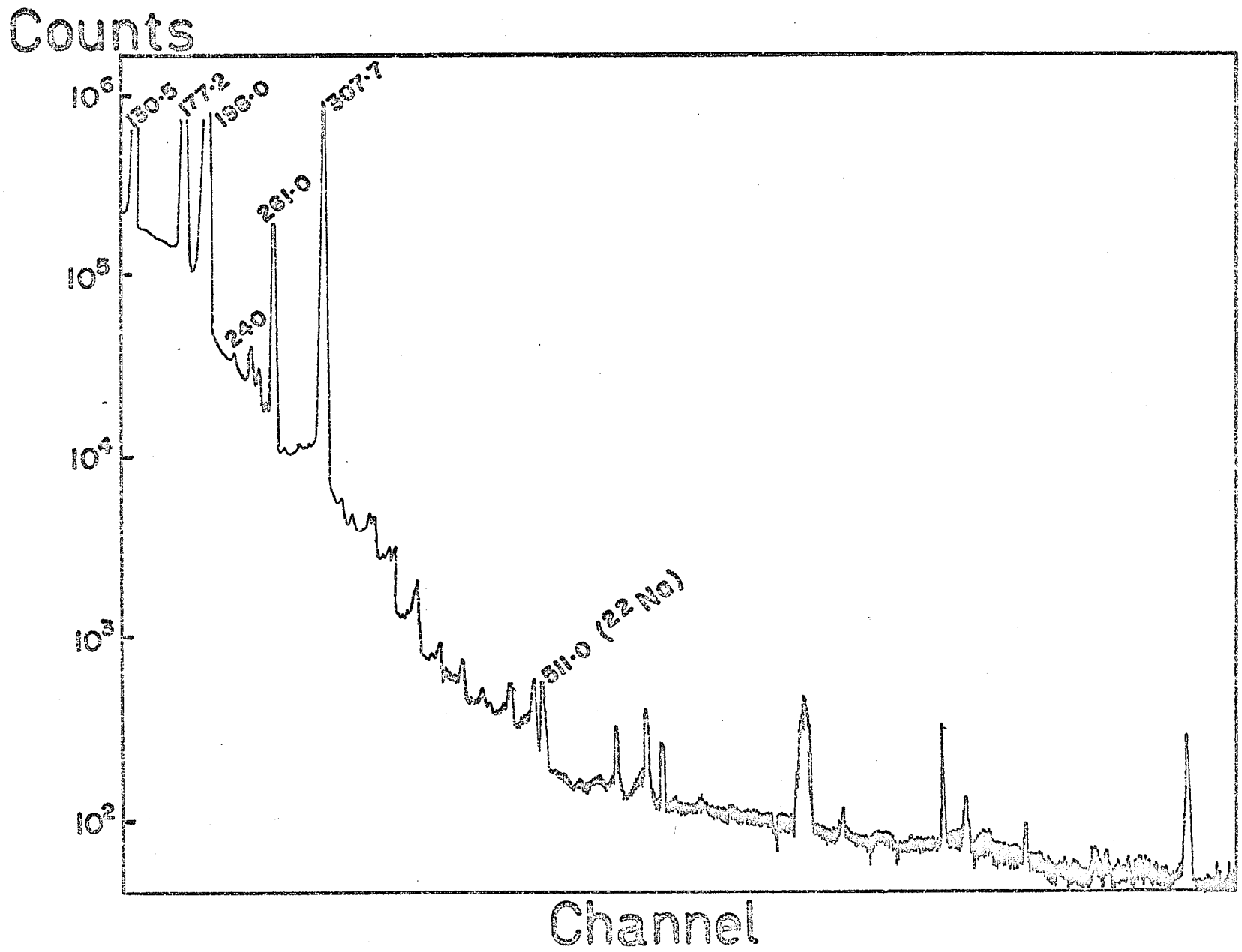
Counts
10^6
10^5
10^4
10^3
10^2
80·5
177·2
198·0
240
261·0
307·7
511·0 (22 Na)
Channel

region containing the reported 156.7 keV[22] and 160 keV[20] transitions. In this case the 160 keV gamma-ray was virtually nonexistent (compare its height to that of the 156.7 keV gamma-ray). In another experimental run, using the 0.25 cc detector (see Figure 3-5) the 160 keV gamma-ray was as intense as the 156.7 keV gamma-ray. In both cases, the 156.7 keV gamma-ray intensity was essentially constant with respect to the well-known 198.0 keV gamma-ray in ^{169}Tm. Hence it could be concluded that the 160 keV gamma-ray did not originate from transitions in ^{169}Tm. Miminoshvili et.al.[21] suggested that there might be a 140 keV transition in ^{169}Tm. In the present investigation the intensity of the 140 keV gamma-ray in Figure 3-5 may be compared with the 140 keV gamma-ray in another source, shown in Figure 3-6. The spectrum in Figure 3-6 was acquired with a 35 cc Ge(Li) detector. The intensities of the 140 keV gamma-rays (relative to the 198.0 keV gamma-ray in ^{169}Tm) were very different in the two cases. Thus the origin of the 140 keV gamma-ray could not have been ^{169}Tm.

200-250 keV Range. Figure 3-7 is the 205-250 keV region of the spectrum taken with the 50 cc detector. Of particular interest is the reported 207±0.5 keV gamma-ray.[21] Here it is very weak, nearly nonexistent, whereas in a spectrum taken with the 0.25 cc detector, it was quite

Figure 3-4. 150-160 keV region of the gamma-ray spectrum taken with the 50 cc Ge(Li) detector.

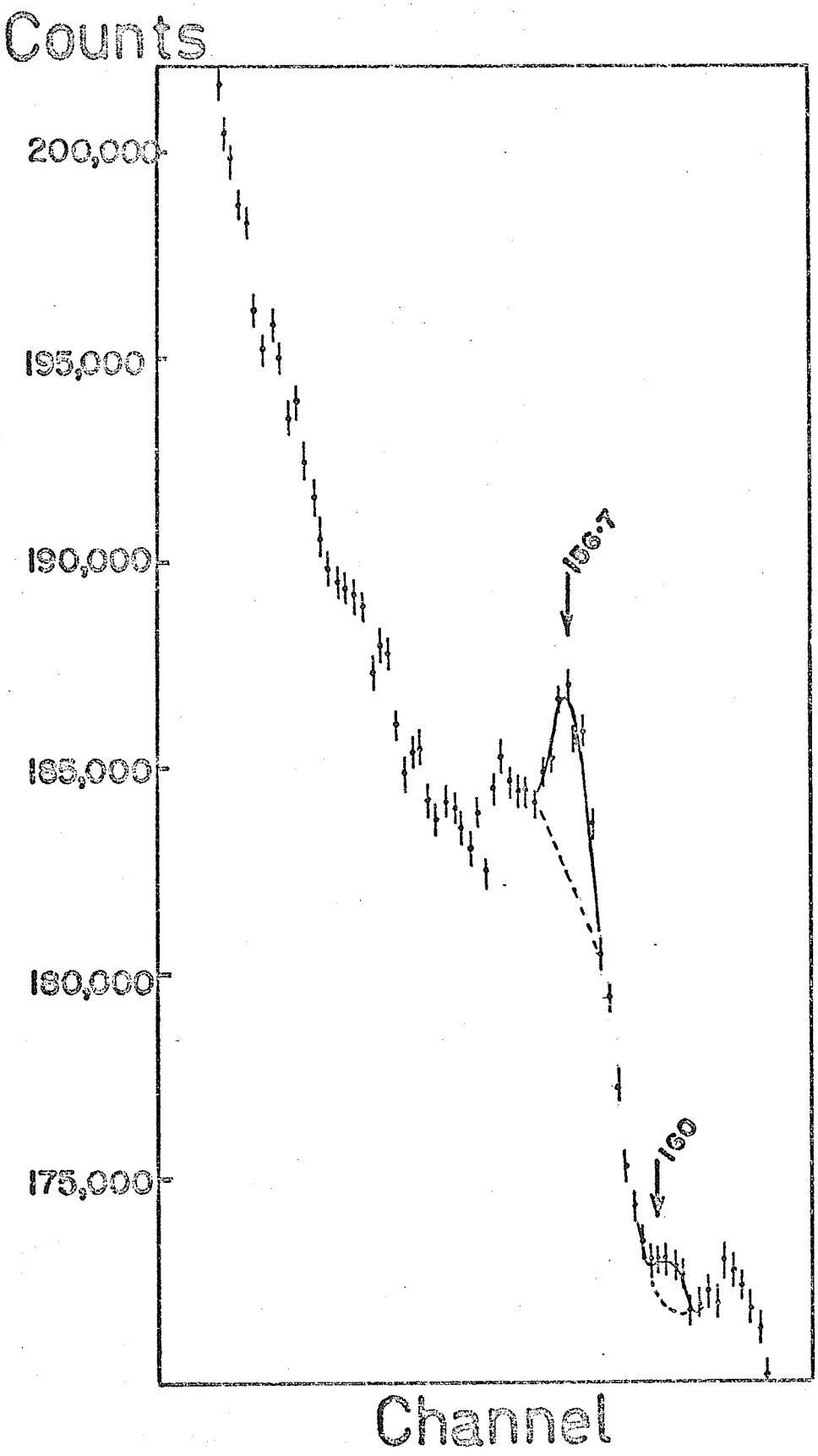
Counts
200,000
195,000
190,000
185,000
180,000
175,000
156.7
160
Channel

Figure 3-5. 140-160 keV region of the gamma-ray spectrum taken with the 0.25 cc Ge(Li) detector.

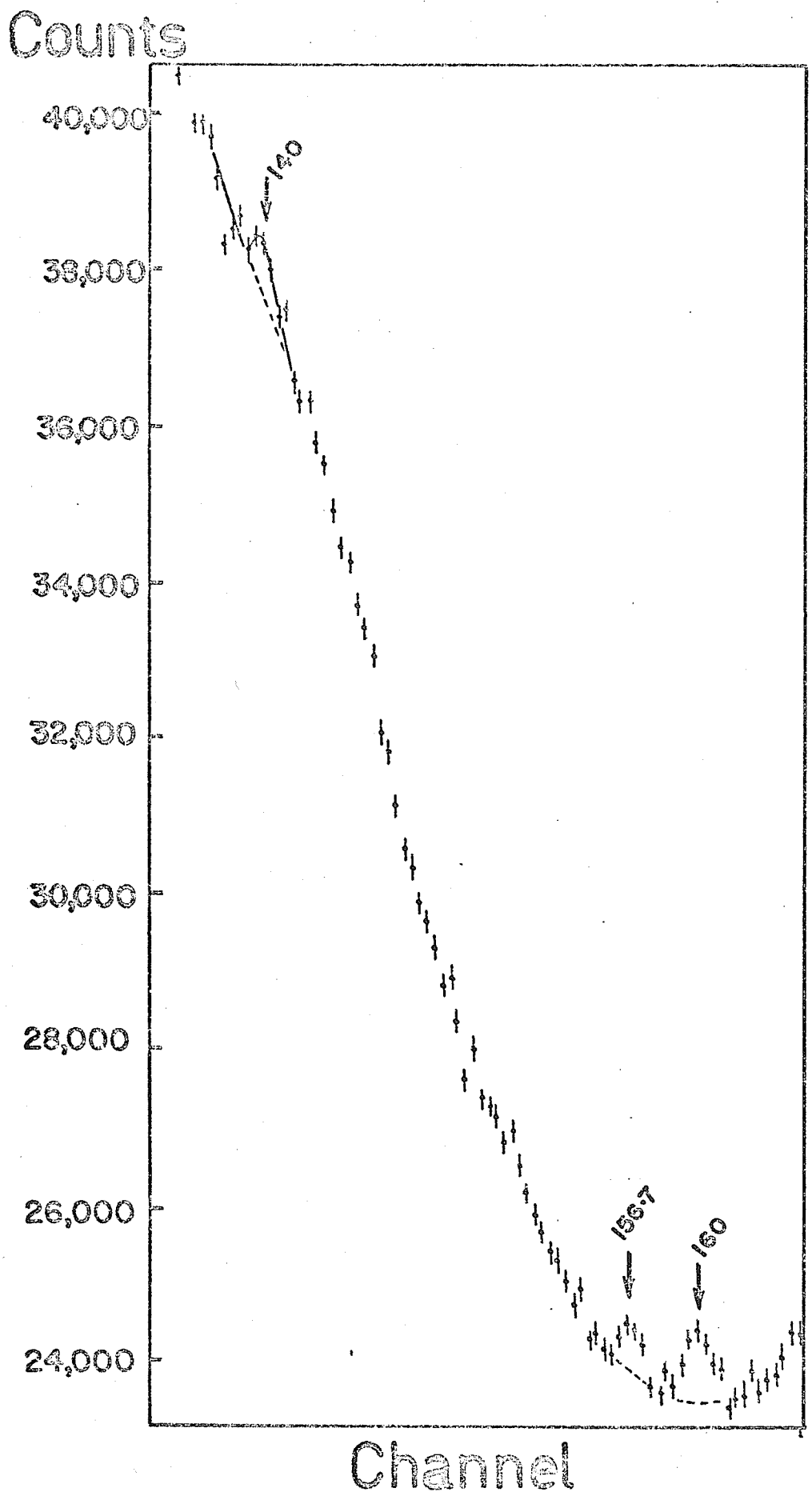
Counts
40,000
38,000
36,000
34,000
32,000
30,000
28,000
26,000
24,000
140
156.7
160
Channel

Figure 3-6. Gamma-ray singles spectrum in the energy range 140-160 keV taken with the 35 cc Ge(Li) detector.

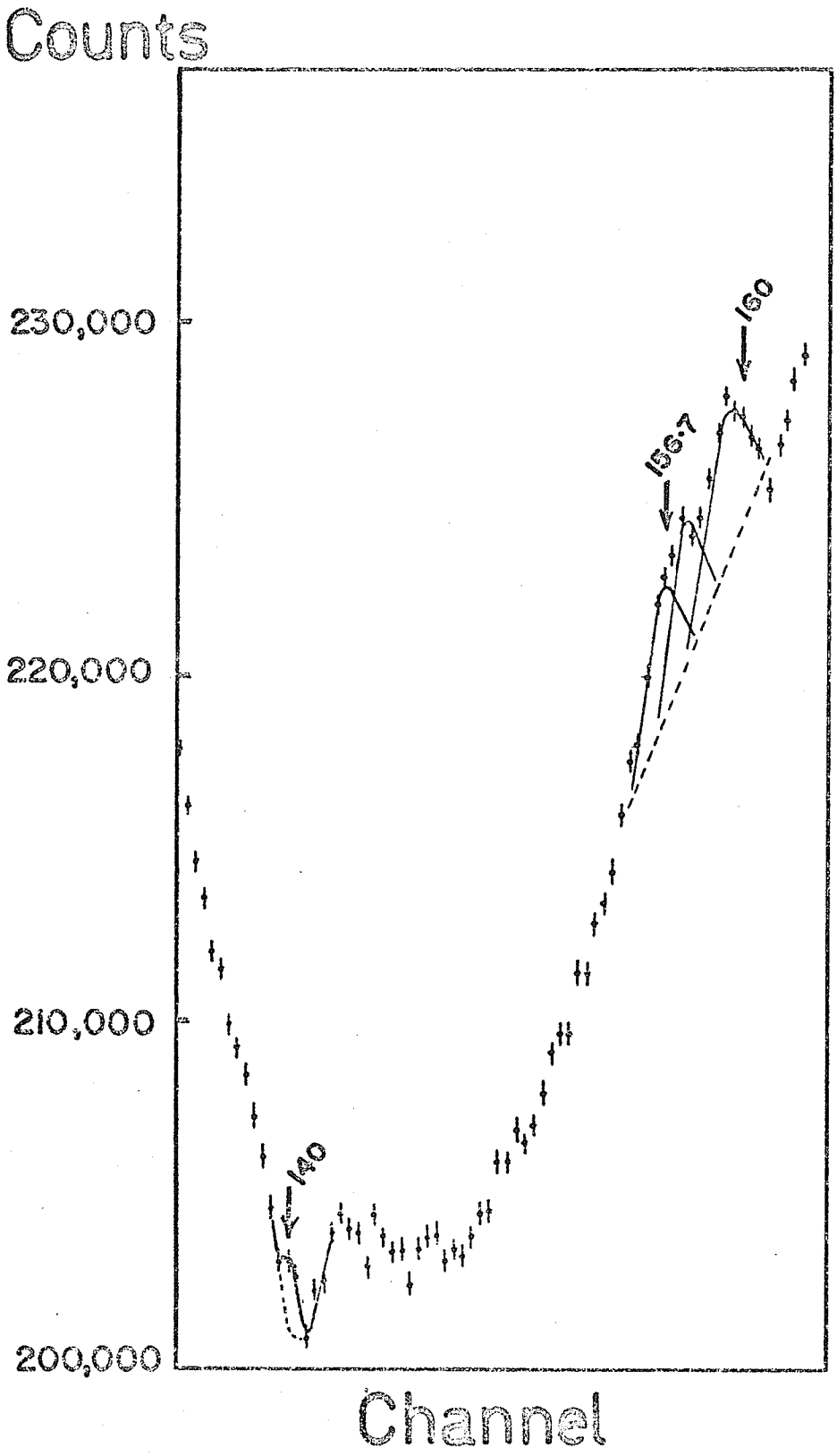
Counts
230,000
220,000
210,000
200,000
140
156.7
160
Channel

prominent (see Figure 3-8). The 207 keV peak is probably the summing of 198 keV gamma-rays and L X-rays (9 keV). Since the 0.25 cc detector was very responsive to L X-rays whereas the 50 cc detector was not, the sum peak should be larger in the former case and it was.

The next peak reported was one at 218±0.5 keV.[21] From Figure 3-7 an upper limit may be placed on the intensity of this peak. There was a peak at 219.3±0.2 keV but this was beyond the energy range reported.

From Figure 3-7 it was impossible to determine whether a 229±0.5 keV peak existed. Miminoshvili et.al.[21] detected the existence of such a gamma-ray. However Figure 3-8, gotten with the 0.25 cc detector, easily separates the sum peak of the 177 keV gamma-ray and K_α X-ray (50 keV) from the location where the 229±0.5 keV peak should be. Only an upper limit may be set on the relative intensity of the purported 229 keV peak.

<u>250-310 keV Range</u>. The next weak gamma-rays reported were those by Miminoshvili et.al.[21] at 285±0.5 keV and 295±1 keV. Figure 3-9 is the 270-305 keV region taken with the 50 cc detector. There was no evidence of a peak at 285±0.5 keV (the peak to the right in the figure is at 288 keV). Hence only an upper limit on the relative intensity may be set. As for the 295±1 keV peak, it could

Figure 3-7. 205-250 keV region of the gamma-ray spectrum taken with the 50 cc Ge(Li) detector.

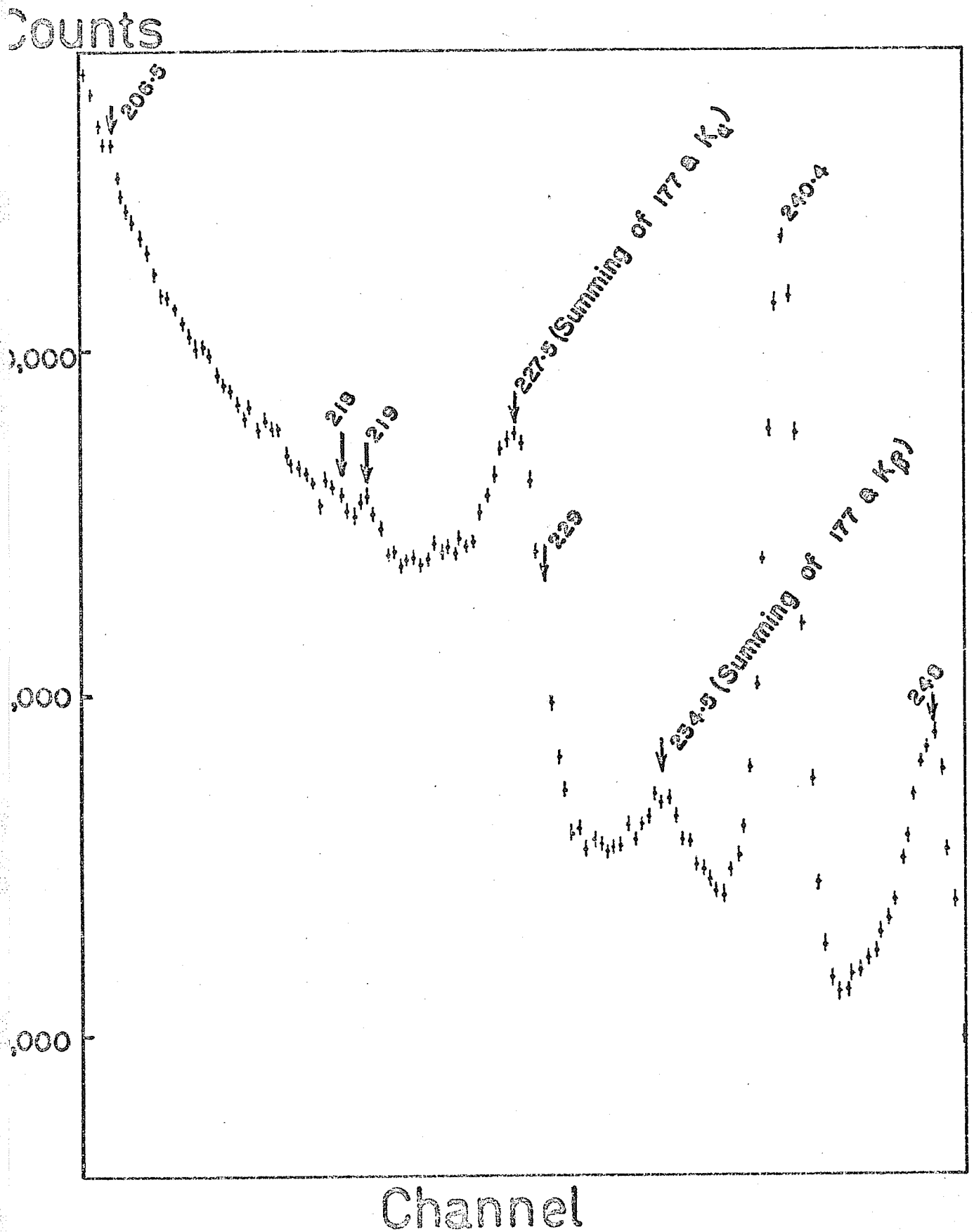
Counts
206.5
219
219
227.5 (Summing of 177 & Kα)
229
234.5 (Summing of 177 & Kβ)
240.4
240
Channel

Figure 3-8. 200-250 keV region of the gamma-ray spectrum taken with the 0.25 cc Ge(Li) detector.

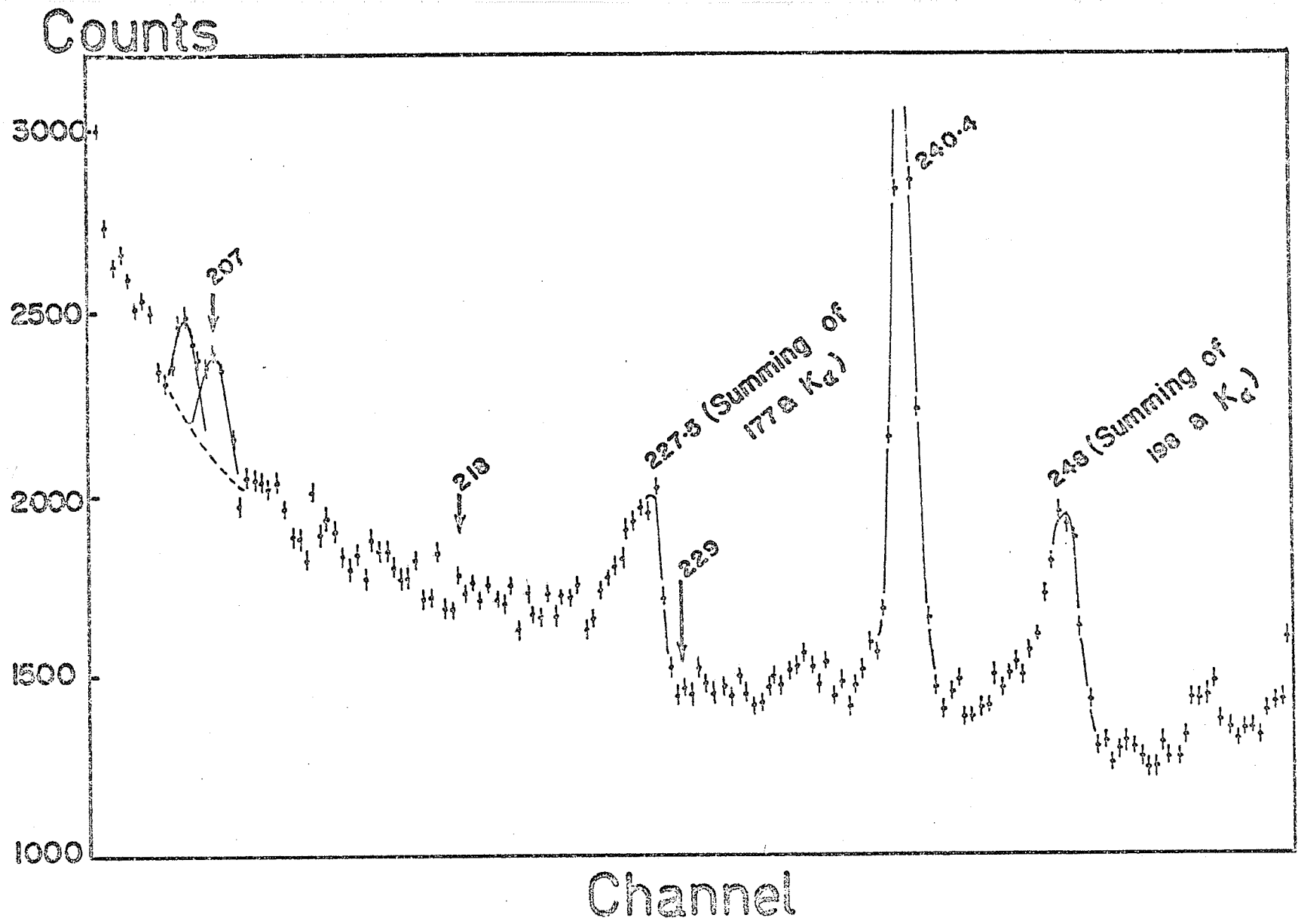
Counts
3000
2500
2000
1500
1000
207
218
227.3 (Summing of 177 & Kα)
229
240.4
243 (Summing of 198 & Kα)
Channel

be the peak at 296.2±0.3 keV. But its intensity (relative to the 198 keV transition of ^{169}Tm) in this run was three times smaller than in a run with the 0.25 cc detector (see Figure 3-10). This peak is likely the germanium escape peak of the 307.7 keV photopeak. That this is so is suggested by the fact that the 296 keV peak was larger when the small detector was used. This is characteristic of escape peaks.

From Figure 3-10 an upper limit may be placed on the relative intensity of the 304 keV peak seen by Miminoshvili et.al.[21]

310-360 keV Range. The next region of interest was the 310-360 keV region. Figure 3-11 shows such a region taken with the 50 cc detector. A 316 keV gamma-ray was reported by George[20] and such a gamma-ray is barely evident here. As for the 320±1.5 keV gamma-ray reported by Miminoshvili et.al.[21] only an upper limit on its relative intensity could be given. There was however a 328 keV peak. Miminoshvili et.al.[21] stated that they found one at 328±1.5 keV. Its relative intensity was however three times as great in another run (see Figure 3-12) in which the 35 cc Ge(Li) detector was used. As is evident in Figure 3-12, peaks are quite prominent at 316 and 320 keV. Since the spectrum of Figure 3-12 was from an "aged" source,

Figure 3-9. 270-305 keV region of the gamma-ray spectrum taken with the 50 cc Ge(Li) detector.

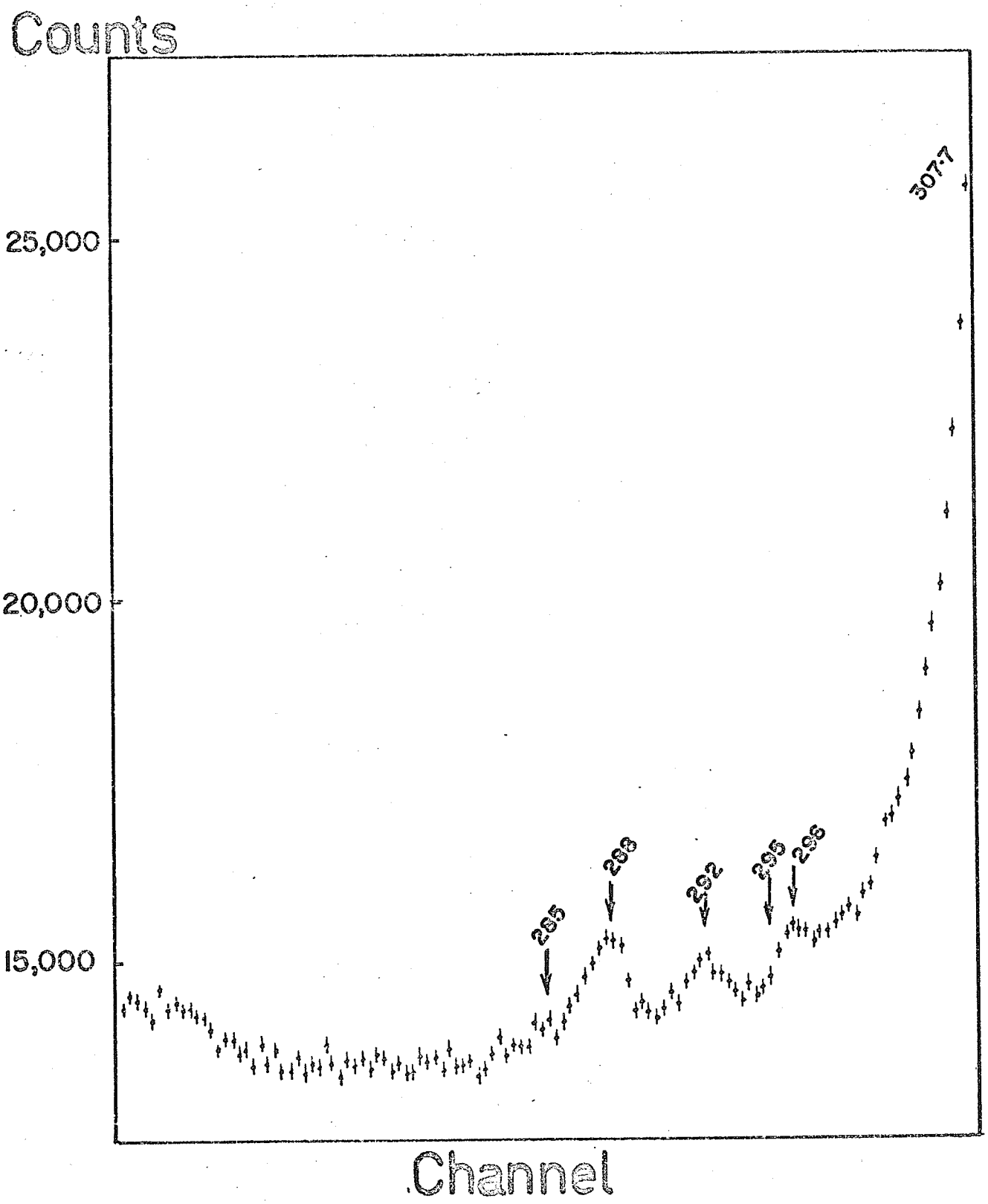
Counts
25,000
20,000
15,000
285
288
292
295
298
307.7
Channel

Figure 3-10. 270-310 keV region of the gamma-ray spectrum taken with the 0.25 cc Ge(Li) detector.

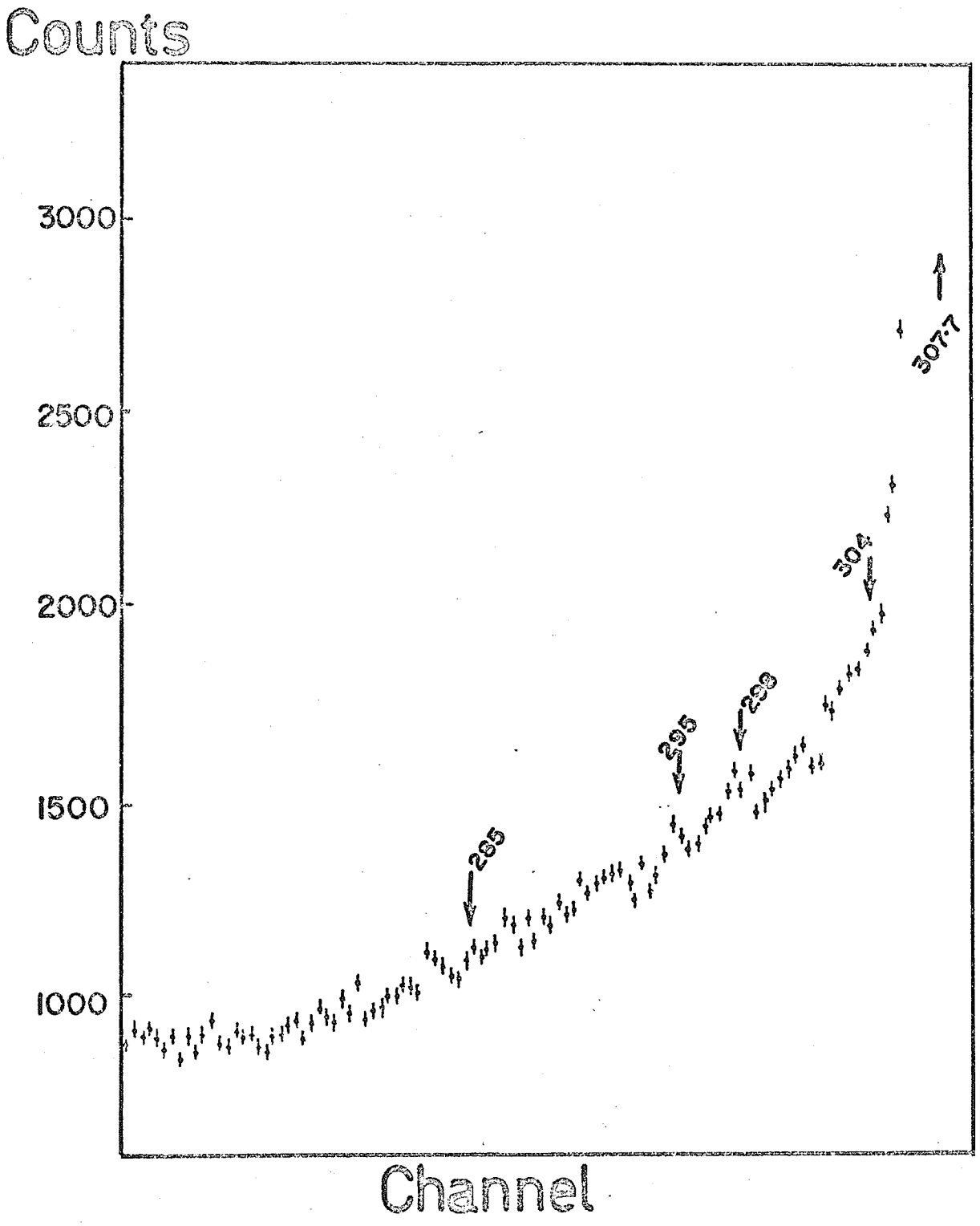
Counts
3000
2500
2000
1500
1000
265
295
299
304
307.7
Channel

Figure 3-11. 310-360 keV region of the gamma-ray spectrum taken with the 50 cc Ge(Li) detector.

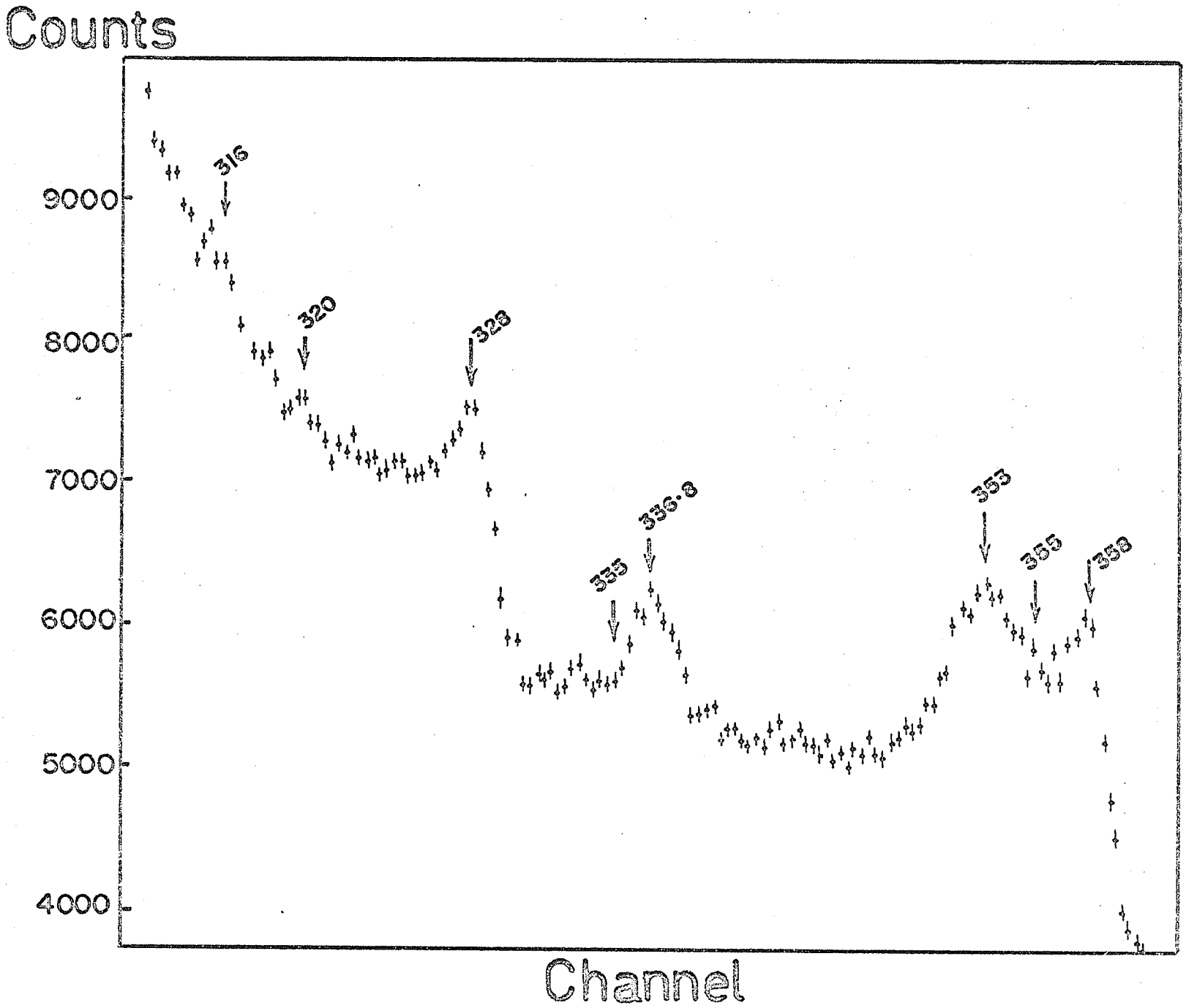
Counts
9000
8000
7000
6000
5000
4000
316
320
328
333
336.8
353
355
358
Channel

Figure 3-12. 310-360 keV region of the gamma-ray spectrum taken with the 35 cc Ge(Li) detector.

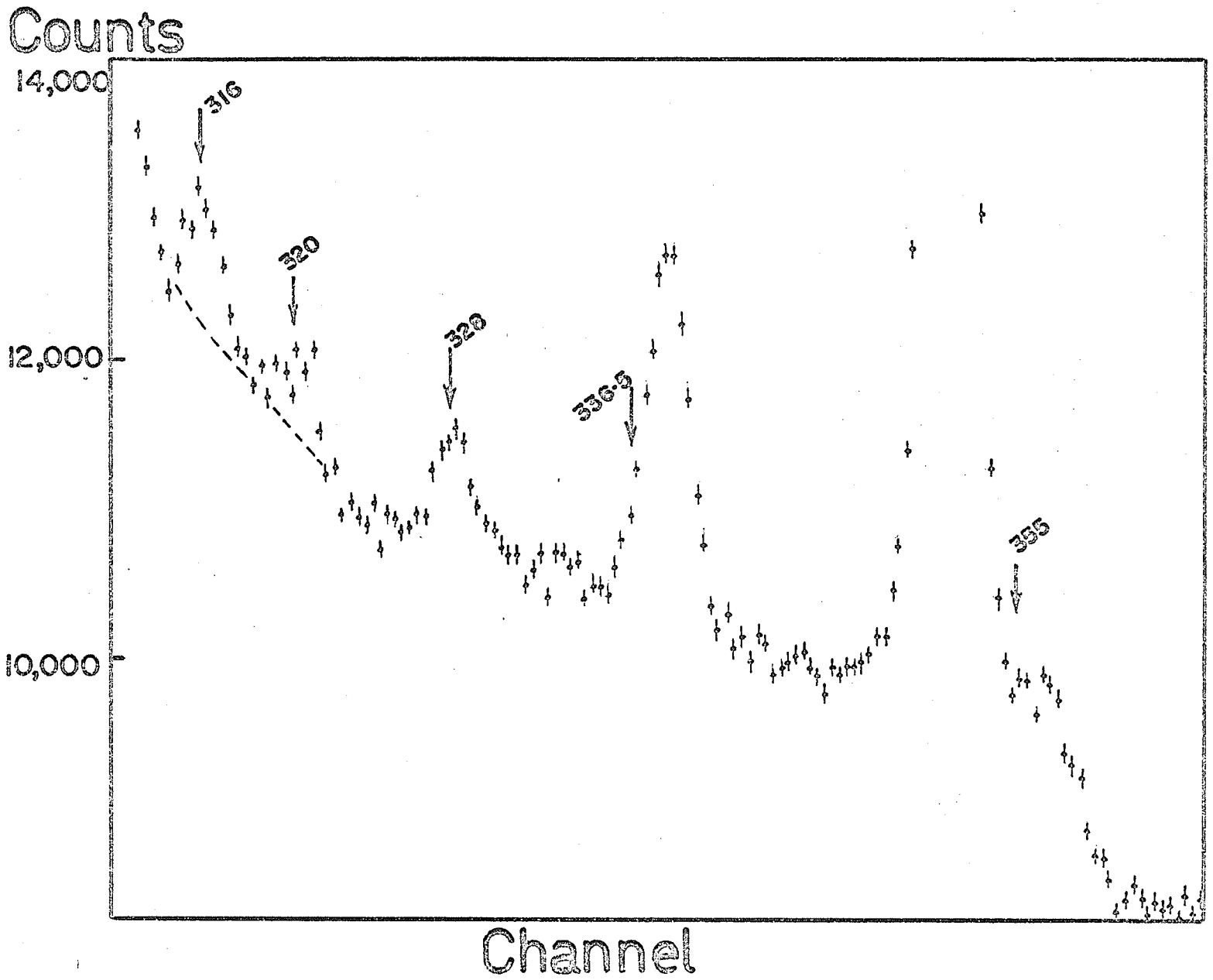
Counts
14,000
12,000
10,000
316
320
328
336.5
355
Channel

it would support the belief that the 328 keV as well as the 320 keV and 316 keV peaks were all gamma-rays due to long-lived impurities in the original source. Their presence was observed only after a large majority of ^{169}Yb atoms had decayed.

Another gamma-ray seen in the 310-360 keV region was the one at 337 keV (see Figure 3-12). Miminoshvili et.al.[21] found it at 335±1.5 keV while Alexander et.al.[22] gave its energy as 336.5±1.2 keV. With the 50 cc detector, its measured intensity was twice as large as when it was measured with the 35 cc detector and with another source (see Figure 3-13). One would have to say that the 337 keV gamma-ray was due to an impurity.

The last gamma-ray of interest in the 310-360 keV region was the one at 355 keV (reported by Miminoshvili et.al.[21] as 355±1.5 keV). In Figure 3-12, it was difficult to decipher its presence. However Figure 3-13 shows it a little more plainly. Since its relative intensity was measured only once it could not be conclusively determined whether it belonged to ^{169}Yb decay.

360-450 keV Range. Figure 3-14 displays the 370-430 keV region taken with the 50 cc detector. Only upper limits on the relative intensities of gamma-rays reported[21] at 388 keV, 411±2 keV and 425±2 keV could be given. The

Figure 3-13. Gamma-ray singles spectrum in the energy range 310-370 keV with the 35 cc Ge(Li) detector.

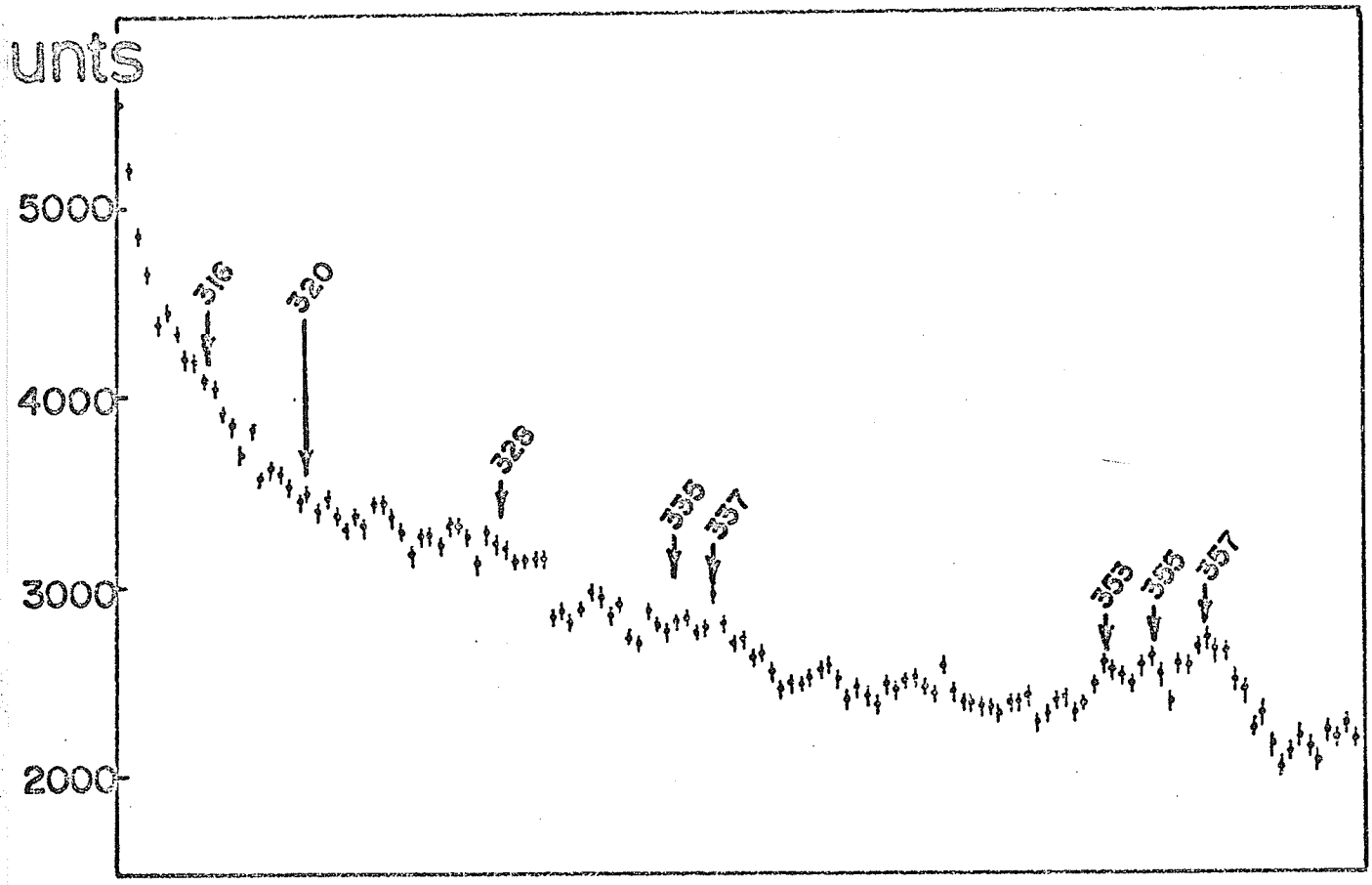
unts
5000
4000
3000
2000
316
320
328
335
337
353
355
357
Channel

Figure 3-14. 370-430 keV region of the gamma-ray spectrum taken with the 50 cc Ge(Li) detector.

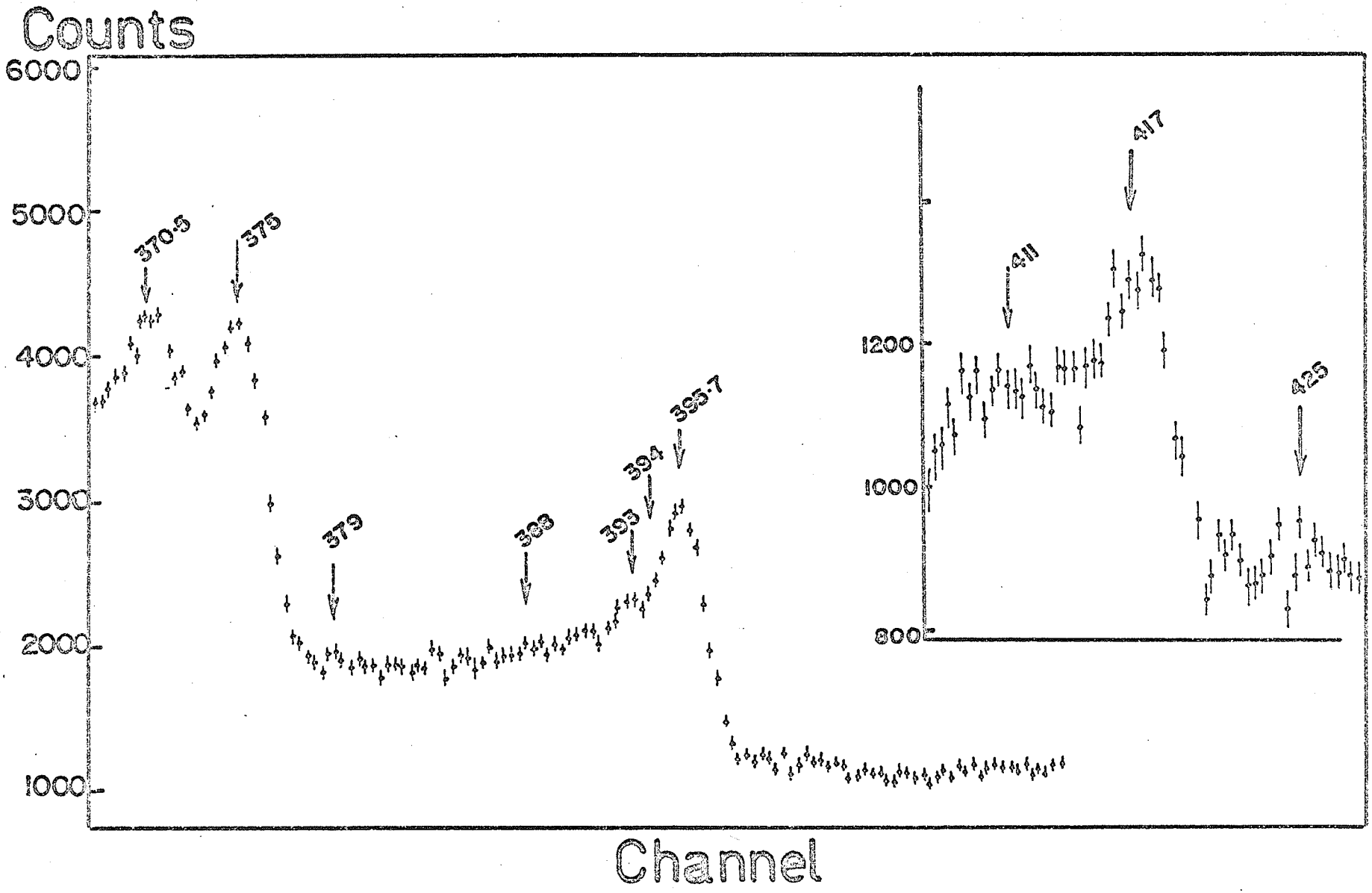
Counts
6000
5000
4000
3000
2000
1000
370·5
375
379
388
393
394
395·7
1200
1000
800
411
417
425
Channel

379 keV peak (seen by Miminoshvili et.al.[21]) had an intensity here which was more than twice that measured with a new source and the 40 cc detector but less than half on another run with an old source and the 35 cc detector. This fluctuating relative intensity supported the conclusion that the 379 keV gamma-ray came from a long-lived impurity.

The remaining two gamma-rays reported in the 370-430 keV region were the 394±2 keV and 417±2 keV ones.[21] Both were detected with the 50 cc detector (see Figure 3-14) as well as with the 35 cc detector. Since both measurements were done with new sources, it could not be said that the 394 keV and 417 keV lines were from impurities or from ^{169}Yb decay. These measurements were inconclusive.

450-650 keV Range. The last two weak gamma-rays at 515 keV and 625 keV were reported by George[20] and by Potnis et.al.[32] Figure 3-15 shows these two gamma-rays as detected with the 40 cc detector. Although very weak, they were also detected with the 35 cc and the 50 cc detectors. The possibility that they were contaminants could not be ruled out. George also came to the same conclusion. Moreover George's reported intensities of these gamma-rays were six times as great as the intensity currently measured. Even Potnis et.al.'s[32] measured

Figure 3-15. Gamma-ray singles spectrum in the energy range 500-650 keV taken with the 40 cc Ge(Li) detector.

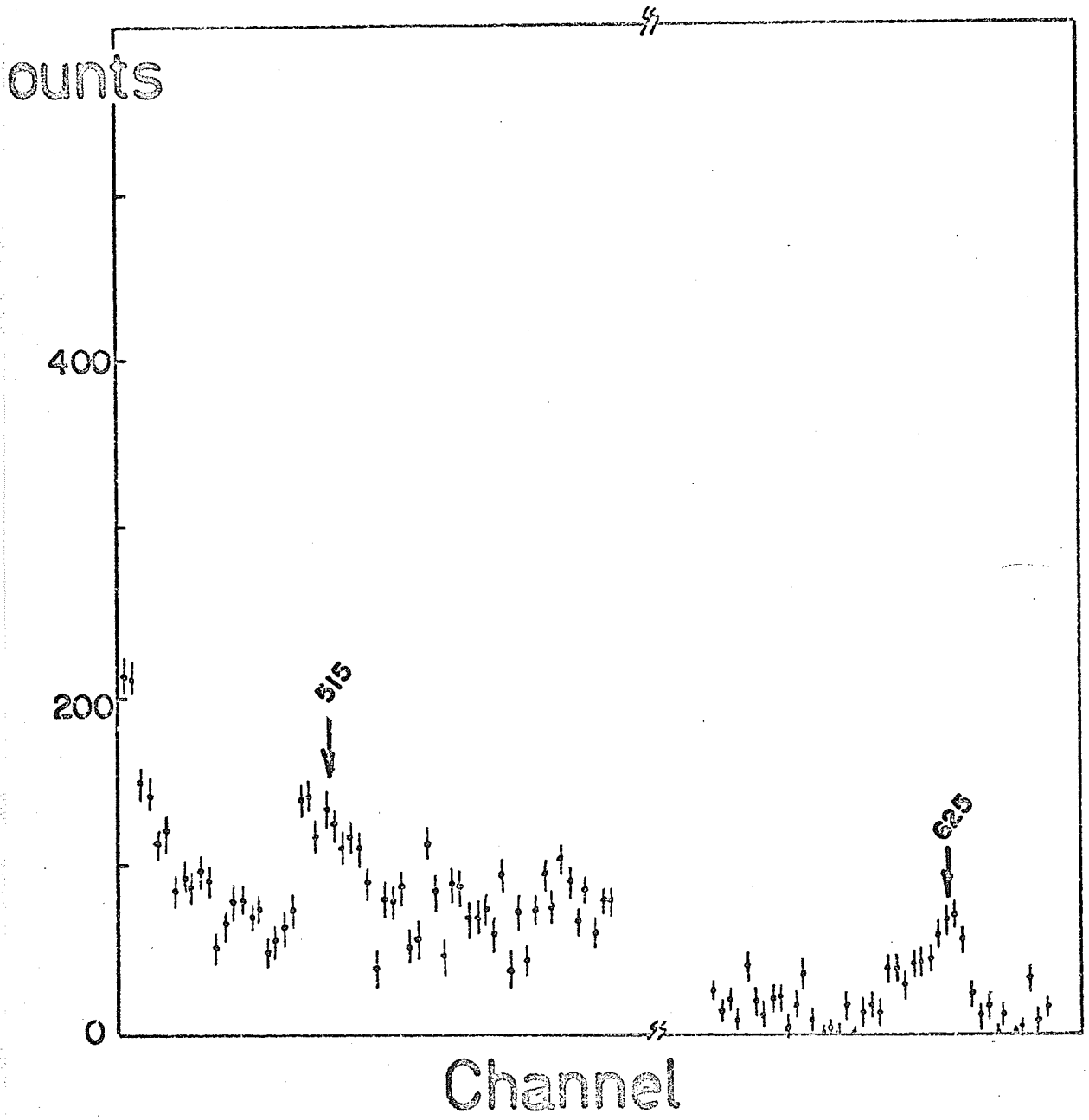
ounts
400
200
0
515
625
Channel

relative intensities differed from the current measurements.

Summary. Table I on page 52 lists the relative intensities of numerous gamma-rays as measured from nine separate gamma-ray spectra. All the gamma-rays listed were those reported to be due to ^{169}Yb decay.[20,21,22] No other peaks were followed systematically through the many runs. The summary (last column in the table) either rules out the peak as belonging to ^{169}Yb decay (written no), gives an upper limit to the gamma-rays' relative intensity, or gives the average intensity as measured in these runs.

The footnotes of Table I list the detector, source, and source age to the nearest month from the time it was purchased. Since the half-life of ^{169}Yb is 31 days, the age of the source has a one-to-one correspondence to the number of ^{169}Yb half-lives that have elapsed.

The results of these gamma-ray measurements are combined with the results of other investigations in Table II. The majority of the weak gamma-rays reported were impurities while a few others were actually sum peaks of two gamma-rays. Only for the 117.3 keV and the 156.7 keV gamma-rays were the relative intensities consistent throughout these measurements and agreed with other investigations.

The results of all the gamma-ray measurements showed that the decay scheme of $^{169}Yb \rightarrow {}^{169}Tm$ is no more complicated than that shown in Figure 1-5.

TABLE I

GAMMA-RAY INTENSITIES FROM ^{169}YB SOURCES

Energy keV[a]	Intensities				
	Run #1[b]	Run #2[c]	Run #3[d]	Run #4[e]	Run #5[f]
20.7		0.68(8)	0.66(4)	0.66(4)	
63.1	124(5)				
93.6		7.2(6)	7.2(3)	7.3(3)	
109.8		51(3)	50(2)	50(2)	
117.25	0.07(4)	0.09(4)			
118.2		5.5(8)	5.3(2)	5.5(2)	
130.5		34(2)	33(2)	36(2)	
140				<0.02	
156.7				0.013(14)	
160				<0.02	
177.2			59(3)	58(3)	
198.0	100	100	100	100	100
207					
218					<0.01
229					
240.4					0.31(2)
261.0			5.0(3)		4.6(3)
285					
295					
304					
307.7			29(1)		28(2)
316					
320					<0.01
328					
335					<0.01
337					0.011(3)
355					0.015(2)
379					0.003(2)
388					
394					
411					
417					
425					
515					0.011(2)
625					0.010(2)

a) Energy in accordance with references 20, 21 and 22.
b) The 0.25 cc detector and solid source (1 month old) made from New England Nuclear Corporation source #2.
c) The 0.25 cc detector and solid source (9 months old) made from New England Nuclear Corporation source #1.
d) The 0.25 cc detector and solid source (2 months old) made from Amersham/Searle source.
e) The 0.25 cc detector and solid source (2 months old) made from Amersham/Searle source.
f) The 40 cc detector and solid source (1 month old) made from Amersham/Searle source.

TABLE I (continued)

Energy keV[a]	Intensities				
	Run #6[g]	Run #7[h]	Run #8[i]	Run #9[j]	Summary
20.7					0.66(4)
63.1					124(5)
93.6					7.2(3)
109.8					50(2)
117.25					0.08(4)
118.2					5.4(2)
130.5					34(2)
140	0.016(3)	0.022(5)	0.004(1)	<0.025	No
156.7	0.045(6)[k]	0.034(6)	0.020(4)		0.023(4)
160	<0.004	0.065(9)			No
177.2					59(3)
198.0	100	100			100
207	<0.004	0.018(4)	<0.08		No
218	<0.004	<0.015	<0.02		<0.004
229	<0.02	<0.015	<0.02		<0.015
240.4	0.41(5)[l]	0.36(2)	0.33(2)		0.33(2)
261.0		4.6(2)			4.7(2)
285	<0.01	<0.025			<0.01
295	0.006(2)	0.023(7)	0.007(2)		No
304		<0.1			<0.1
307.7	27(3)	28(1)	28	28	28(1)
316	0.005(1)	<0.03		0.032(4)	No
320	<0.01	<0.04	<0.01		<0.01
328	0.013(4)	<0.04	0.029(3)	0.043(5)	No
335					<0.01
337	0.021(3)		0.013(2)		No
355					0.015(2)
379	0.0013(5)		<0.01	0.030(4)	No
388	<0.005		<0.01		<0.005
394	0.028(9)		0.037(4)		0.035(4)
411	<0.005		<0.015		<0.005
417	0.008(3)		0.0088(15)		0.009(2)
425	<0.005		<0.015		<0.005
515	0.011(2)		0.007(2)		0.008(2)
625	0.012(2)		0.010(2)		0.011(2)

g) The 50 cc detector and liquid source (1 month old) made from New England Nuclear Corporation source #3.
h) The 0.25 cc detector and solid source (1 month old) made from New England Nuclear Corporation source #3.
i) The 35 cc detector and solid source (1 month old) made from New England Nuclear Corporation source #2.
j) The 35 cc detector and solid source (3 months old) made from New England Nuclear Corporation source #2.
k) High because of summing of the 94 keV and 63 keV gamma-rays.
l) High because of summing of the 63 keV and 177 keV gamma-rays.

TABLE II

GAMMA-RAY TRANSITIONS REPORTED IN ^{169}YB DECAY

Energy keV[a]	Intensities		
	Present Work	George[20]	Miminoshvili et.al.[21]
20.7[b]	0.66(4)	-	-
63.1	124(5)	133	-
93.6	7.2(3)	10.3	-
109.8	50(2)	61	-
117.25	0.08(4)	-	-
118.2	5.4(2)	4.3	-
130.5	34(2)	36	-
140	No[c]	-	~0.1
156.7	0.023(4)	0.124	0.03(1)
160	No	0.2	-
177.2	59(3)	57.6	-
198.0	100	100	100
207	No	-	0.03(2)
218	<0.004	-	0.04(2)
229	<0.015	-	0.06(3)
240.4	0.33(2)	0.29	0.36(5)
261.0	4.7(2)	-	-
285	<0.01	-	0.12(4)
295	No	-	0.04(2)
304	<0.1	-	0.5(3)
307.7	28(1)	39	-
316	No	0.08	-
320	<0.01	-	0.06(3)
328	No	-	~0.01
335	<0.01	-	0.03(1)[d]
337	No	-	-
355	0.015(2)	-	0.050(15)
379	No	-	≲0.012
388	<0.005	-	≲0.02
394	0.035(4)[e]	-	~0.02
411	<0.005	-	~0.01
417	0.009(2)[e]	-	~0.01
425	<0.005	-	~0.01
515	0.008(2)	0.066	-
625	0.010(2)	0.06	-

a) Energy in accordance with references 20, 21 and 22.
b) The 20.7 keV transition was seen previously only with a beta-ray spectrometer.
c) "No" indicates that the transition was proven to be not from ^{169}Yb decay.
d) This transition is probably the one measured by Alexander et.al.[22] as 336.5±1.2 keV, by Potnis et.al.[32] as 336.87 keV and presently as 336.8±0.3 keV.
e) Only two measurements on 1 month old sources.
f) Not detected.

TABLE II (continued)

Energy keV[a)]	Intensities Alexander[22)] ±5%	Intensities Potnis et.al.[32)]	Conclusion
20.7	-	-	Yes
63.1	121	145(3)	Yes
93.6	7.2	7.5(6)	Yes
109.8	50	53(2)	Yes
117.25	0.108	n.d.[f)]	Yes
118.2	5.2	6.4(6)	Yes
130.5	31	33(3)	Yes
140	<0.02	-	No
156.7	0.024(6)	-	Yes
160	<0.08	-	No
177.2	62	75(2)	Yes
198.0	100	100(5)	Yes
207	<0.07	-	No
218	<0.03	-	No
229	<0.03	-	No
240.4	0.34	0.36(3)	Yes
261.0	4.8	5.0(1)	Yes
285	<0.1	-	No
295	<0.09	-	No
304	<0.1	-	No
307.7	28	30(1)	Yes
316	<0.05	n.d.[f)]	No
320	<0.05	-	No
328	<0.02	-	No
335	-	-	No
337	0.017(4)	0.028(2)	No
355	<0.02	n.d.	No
379	<0.1	n.d.	No
388	<0.1	n.d.	No
394	<0.1	n.d.	No
411	-	-	No
417	-	-	?
425	-	-	No
515	-	0.0070(9)	?
625	-	0.0073(6)	?

II. DIRECTIONAL CORRELATION EXPERIMENTS

^{169}Yb Source. The ^{169}Yb radioactive sources used in the directional correlation experiments were from two suppliers. The mother liquid ($YbCl_3$ in dilute HCl) for the liquid source was from New England Nuclear Corporation; for the solid source, it was from Amersham/Searle.

The solid source was prepared by subliming dried $YbCl_3$ onto 0.18 mg/cm^2 aluminum foil. The original radioactive strength was about 10 microcuries (μCi) and the specific activity was 35 mCi/mg. Source diameter was 3-4 mm. A singles spectrum revealed only one contaminant, ^{175}Lu → ^{175}Yb, but the gamma-rays associated with it were well-resolved from ^{169}Tm gamma-rays and posed no problems (see Figure 3-16). Furthermore the half-life of ^{175}Yb was 4.2 days as compared to the 31 days for ^{169}Yb → ^{169}Tm. Thus after a few weeks the contaminant was no longer significant (see Figure 3-17).

The liquid source was encapsulated in a plastic (methyl methacrylate) capillary tube with outside diameter of 5.0 mm and wall thickness of 1.1 mm. Specific activity was 24 mCi/mg and source strength was about 20 μCi. No noticeable peaks from contaminants were present in a gamma-ray singles spectrum.

For the directional correlation measurements, the

Figure 3-16. Gamma-ray singles spectrum in the energy range of 0-200 keV taken with the X-ray detector.

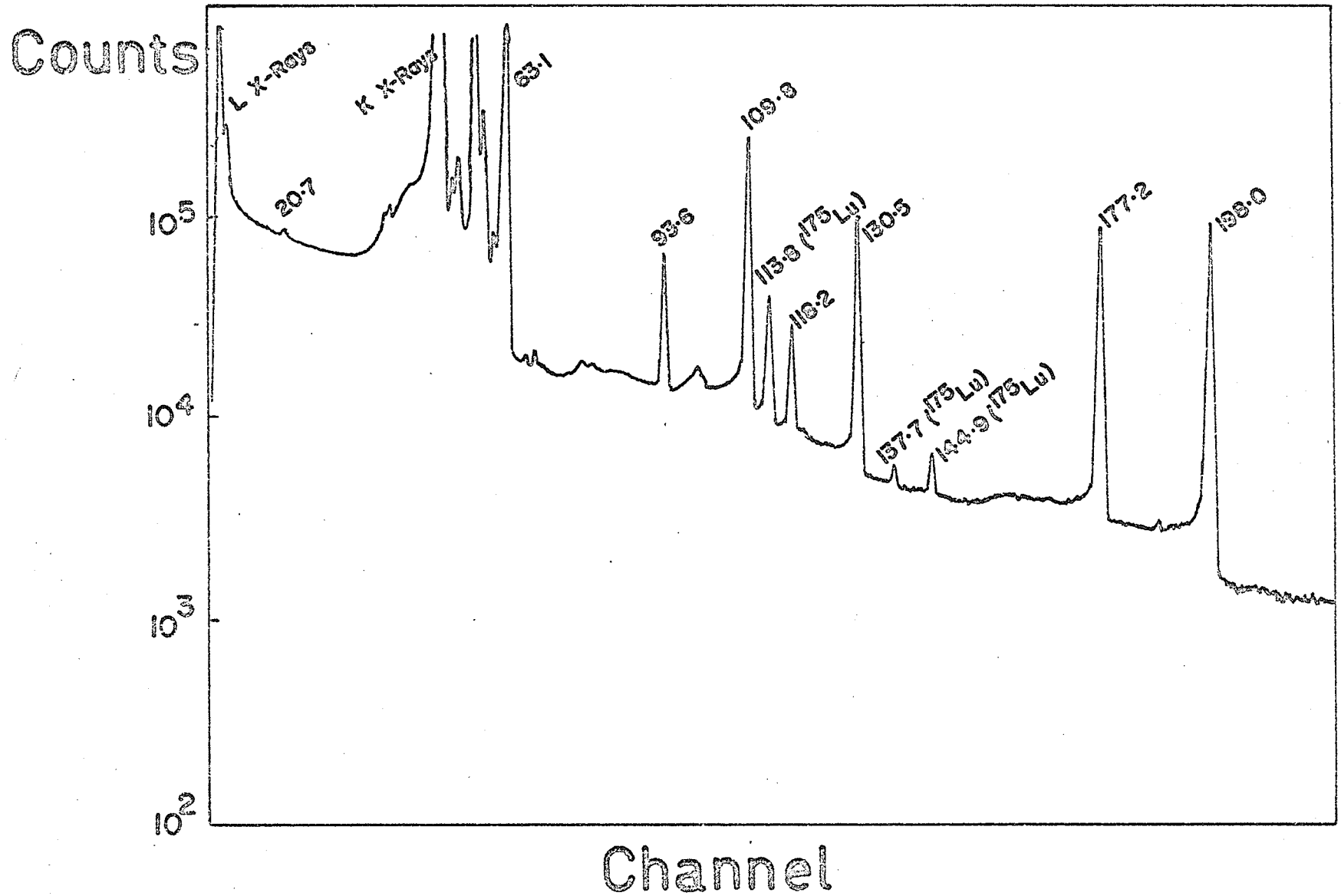
Counts
L X-Rays
K X-Rays
20·7
63·1
93·6
109·8
113·8 (175Lu)
116·2
130·5
137·7 (175Lu)
144·9 (175Lu)
177·2
198·0
10⁵
10⁴
10³
10²
Channel

Figure 3-17. Gamma-ray singles spectrum in the energy range of 0-200 keV taken with the X-ray detector and an "aged" source.

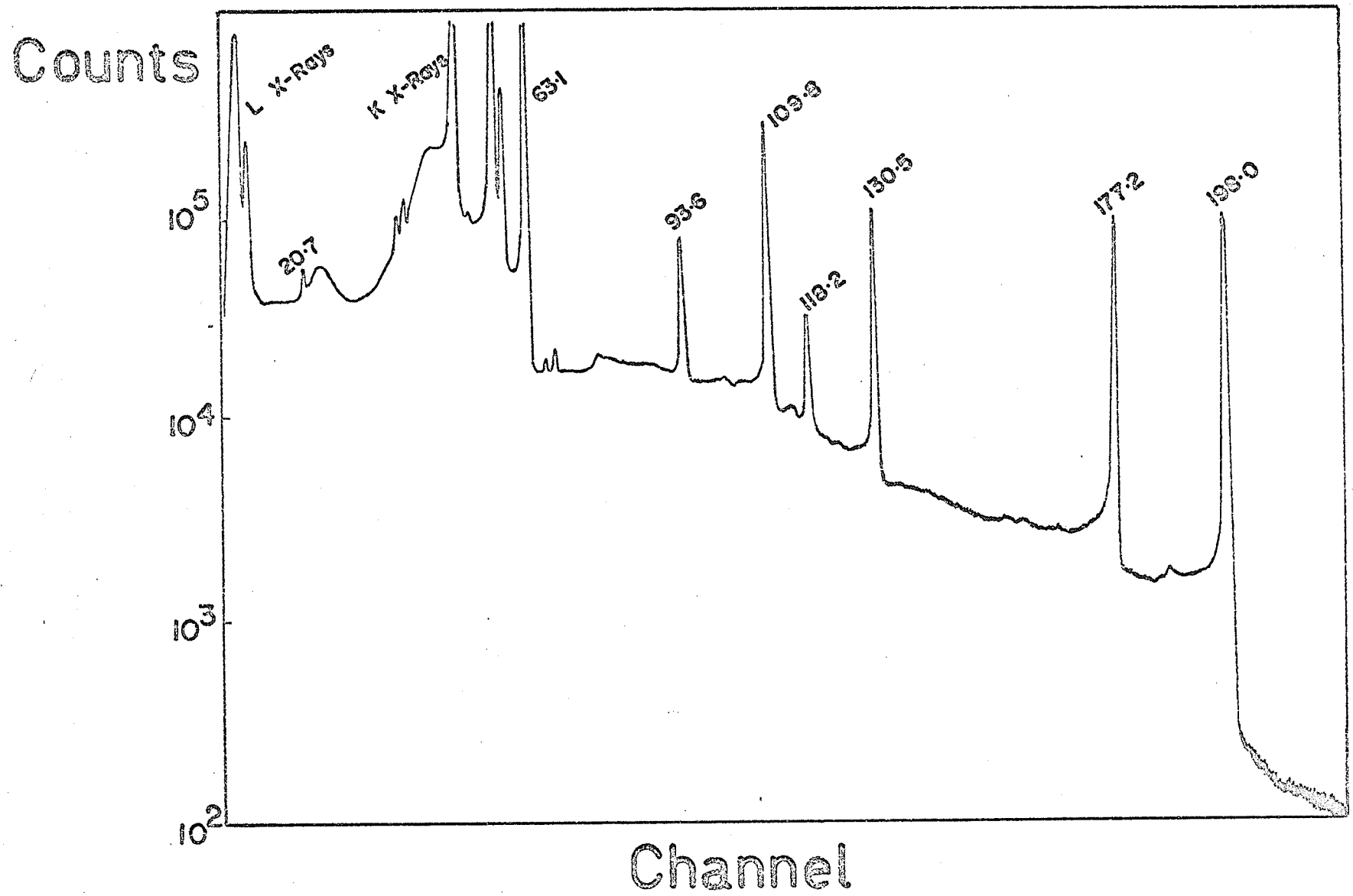
Counts
L X-Rays
K X-Rays
20·7
63·1
93·6
103·8
118·2
130·5
177·2
196·0
10^5
10^4
10^3
10^2
Channel

total coincidence spectra were obtained from many scans in which the X-ray detector was rotated through the angles of 90^{o}, 135^{o} and 180^{o} relative to either the electron detector or to the gamma-ray detector. The order of rotation and the length at each angle were varied in order to minimize any chance of generating systematic errors.

The results of each short scan were analyzed for the A_{22} and A_{44} coefficients. These are the coefficients in the angular distribution function

$$W(\theta) = 1 + A_{22}P_2(\cos\theta) + A_{44}P_4(\cos\theta)$$

where P_2 and P_4 are Legendre polynomials and θ refers to the angle between the two detectors.

Generally,

$$W(\theta) = 1 + \sum_{k=1}^{k_m} A_{2(kk)}P_{2k}(\cos\theta)$$

where the maximum value k_m is given by[23]

$$k_m \leq \text{minimum } (L_1, L_2, J),\ k_m \text{ an integer}$$

The multipole orders of the transitions 1 and 2 in a cascade are L_1 and L_2 respectively and J is the angular momentum of the intermediate nuclear level. Since the conversion electron or gamma-ray in cascade with the K X-ray of interest would be either M1 or E2 (or a mixture of both) the highest order term would be $A_{44}P_4(\cos\theta)$.

The experimental data was fitted by the method of White[24] except that the error calculation was slightly different. The derivation of errors is shown in Appendix A.

Each value of the short scans (from half an hour to two hours per angle) was compared to the average of all the short scans. The criteria for accepting a particular short scan result was that it be within one standard deviation from the average of the short scans. With such a criteria, only one short scan - immediately prior to electronic equipment failure - was rejected.

The long scans of about 10 hours duration per angle were individually analyzed to give A_{22} and A_{44} coefficients. These in turn were accepted only if they were within one standard deviation of the short scan average. Again only knowledgeable equipment failure succeeding the scan gave results which were rejected.

The prepared source was "centered" to less than a half a percent, i.e. the singles counting rate of the movable K_α X-ray detector as a function of the angle θ was constant to less than half a percent. Naturally the coincidences were still corrected for this small singles-counting-rate differences at the different angles.

Random spectra were run at each of the angles and the resolving time τ of the coincidence circuit (a time-to-amplitude converter) was measured with the aid of the

relation

$$R = \tau S_1 S_2$$

where R was the random coincidence counting rate and S_1 and S_2 were the singles counting rates of the two detectors in coincidence. After the resolving time was determined the randoms for all the coincidences were determined from this resolving time and the appropriate singles counting rates. The resolving time of the coincidence circuit was checked periodically throughout the experiment.

The finite solid angle correction for all the detectors was insignificant, i.e. considerably less than 1% to the final directional correlation coefficients. A correction for source size was also not necessary.

Thus the only corrections to the measured coincidences were to subtract random coincidences and correct for the small singles-counting-rate differences at the three angles.

The experimental results will now be presented in detail. The significance of these results will be reserved for a subsequent chapter.

To simplify the discussion of the many coincidences recorded in the directional correlation measurements, the following abbreviations will be adopted. A gamma-ray will be denoted by the Greek letter "γ" and a subscript will indicate its energy. Thus a 131 keV gamma-ray will be

written γ_{131}; similarly a 110 keV gamma-ray will be written γ_{110}. The K_α and K_β X-rays will be shortened to merely K_α and K_β respectively. Conversion electrons will be designated by the letter "e" and a subscript for the appropriate transition and electron shell from which they originated. Thus e_{177K} will indicate K conversion electrons of the 177 keV transition while e_{131L} will indicate L conversion electrons of the 131 keV transition. Coincidences will be designated by hyphened combination of the two things in coincidence. Accordingly K_α-γ_{131} will denote coincidences between K_α X-rays and 131 keV gamma-rays. Similarly γ_{110}-e_{198K} will denote coincidences between 110 keV gamma-rays and K conversion electrons of the 198 keV transition. This nomenclature should simplify the discussion.

Figure 3-18 shows the K X-rays in coincidence with the 131 keV gamma-rays, i.e. K-γ_{131}. This spectrum was the coincidences recorded at 90° during one of the long scans on the solid source. The random coincidences have not yet been subtracted. As is apparent the K_{α_1} X-ray was just partly resolved from the K_{α_2} X-ray but both were well resolved from the K_β X-rays. The unlabeled peak to the right of $K\beta_2$-γ_{131} was γ_{63}-γ_{131}. This peak was a combination of random γ_{63}-γ_{131} and legitimate γ_{63}-γ_{131} through the intermediate 177 keV transition (see Figure 3-19).

Figure 3-18. Spectrum of K X-rays in coincidence with 131 keV gamma-rays.

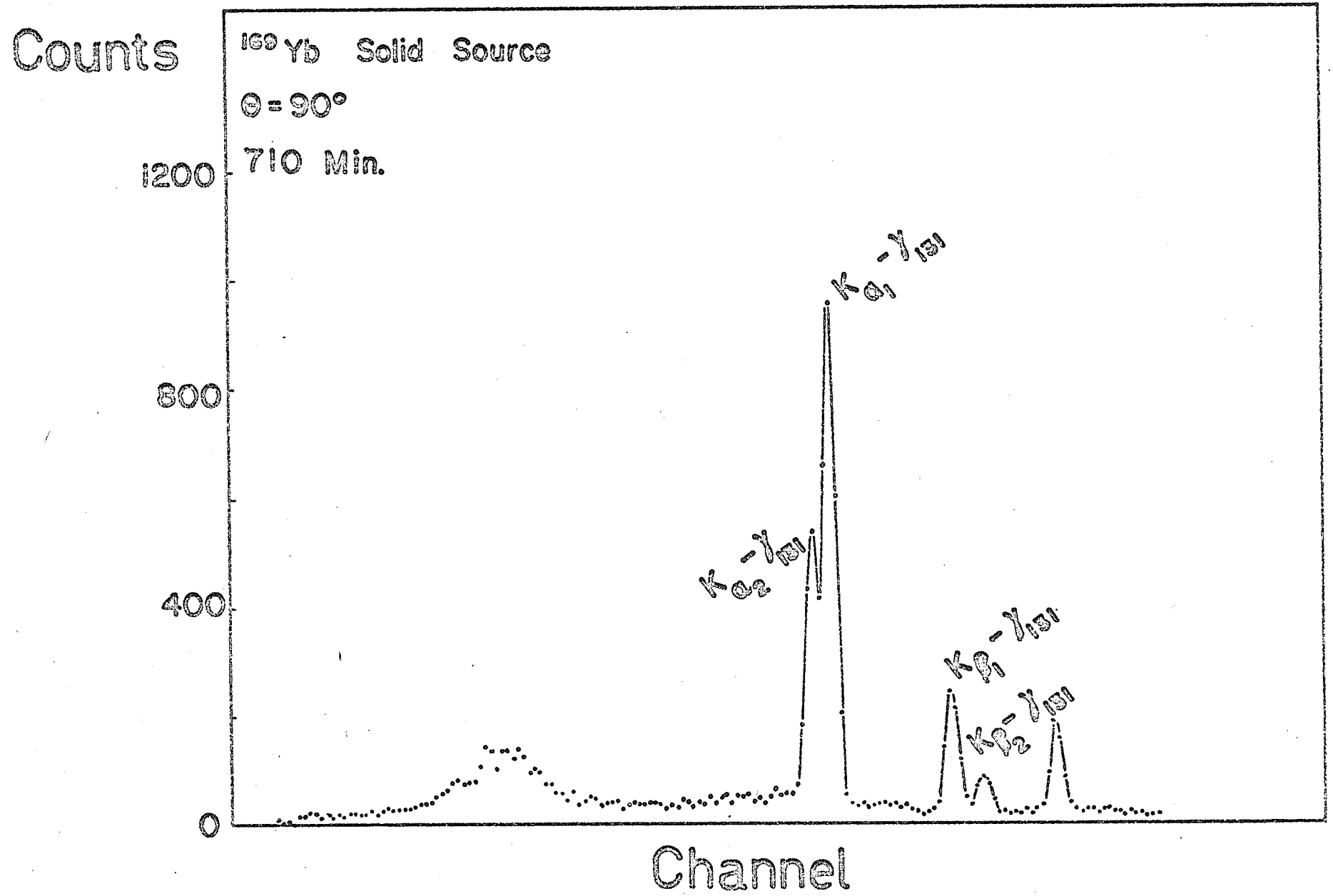
Counts
^{169}Yb Solid Source
θ = 90°
710 Min.
1200
800
400
0
$K_{\alpha_1} - \gamma_{131}$
$K_{\alpha_2} - \gamma_{131}$
$K_{\beta_1} - \gamma_{131}$
$K_{\beta_2} - \gamma_{131}$
Channel

The legitimate γ_{63}-γ_{131} would be due to the chance that after the γ_{63} populated the 0.66 μsec isomeric level, the level depopulated immediately. Of course on the average the isomeric level lived 0.66 μsec. If the isomeric level decayed very shortly (within the resolving time of the electronics in the directional correlation measurements) then it was possible to have a legitimate γ_{63}-γ_{131}.

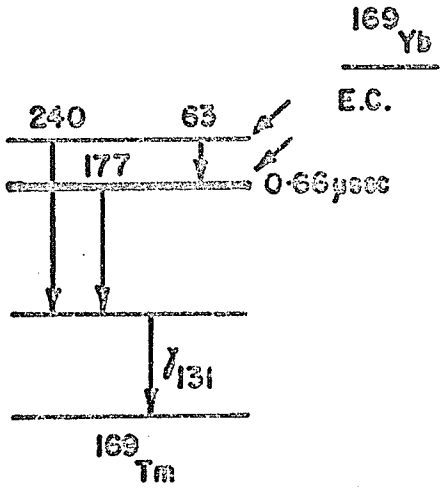

Figure 3-19. Simplified level scheme of ^{169}Tm showing the transitions in cascade with the 131 keV gamma-rays.

By delaying the detection (actually the electronic delay of the signal from the γ_{131} detector) one gets in addition to the random γ_{63}-γ_{131}, a very close measure of the legitimate γ_{63}-γ_{131}. Hence by subtracting the coincidences when γ_{131} detection was delayed from the

total coincidences (with no delay), one obtained only those transitions that were in true coincidence with γ_{131}. After the subtraction of the random coincidences, the peak disappeared. The transitions above the isomeric level gave no evidence of being in true coincidence with γ_{131}. The K X-rays from electron capture which occurred above the isomeric level similarly gave no final evidence of being in coincidence with γ_{131}.

Thus this 0.66 μsec isomeric level isolated events below from those above when coincidences involving K X-rays were performed. In particular, it isolated the K_α X-rays after conversion electron emission from the K_α X-rays associated with electron capture. In other words, when a K_α X-ray was detected, it was known to be a result of conversion electron emission and not from electron capture.

From Figure 3-19 it can be seen that the K_α-γ_{131} arise only from K conversion of the 177 keV and the 240 keV transitions. The intensity ratio of e_{177K} to e_{240K} will be very close to the ratio of $K_\alpha(e_{177K})$ to $K_\alpha(e_{240K})$. Using the relative intensities of γ_{240} and γ_{177} (see Table II on page 54) and the K conversion coefficients[25] one finds

$$\frac{K_\alpha(e_{240K})}{K_\alpha(e_{177K})} \simeq \frac{e_{240K}}{e_{177K}} = \frac{\gamma_{240}}{\gamma_{177}} \cdot \frac{\alpha_{240K}}{\alpha_{177K}} < 0.0005$$

i.e. less than 0.05% and insignificant. Here α_K are the

K conversion coefficients - the ratio of the number of K conversion electrons to the number of gamma-rays from a particular transition.

The directional correlation measurement of K_α-γ_{131} was actually then $K_\alpha(e_{177K})$-γ_{131}, i.e. the K_α's in coincidence with γ_{131} were only from K conversion of the 177 keV transition. With the liquid source the directional correlation coefficients were

$$A_{22}(K_\alpha(e_{177K})\text{-}\gamma_{131}) = -0.053\pm0.013$$

$$A_{44}(K_\alpha(e_{177K})\text{-}\gamma_{131}) = +0.021\pm0.013$$

The measurements taken with a solid source a half year later and with radioactive material from another supplier yielded

$$A_{22}(K_\alpha(e_{177K})\text{-}\gamma_{131}) = -0.051\pm0.023$$

$$A_{44}(K_\alpha(e_{177K})\text{-}\gamma_{131}) = +0.011\pm0.024$$

The notable agreement of the two measurements indicated that there was no attenuation of the anisotropy in the solid source.

The results of all the directional correlation measurements involving K_α X-rays are listed in Table III on page 72. The numerous measurements will nevertheless be discussed individually.

Concurrently with the K_α-γ_{131} directional correlation measurements, the K_α-γ_{110} directional correlation was

measured. One single channel analyzer was set on the 131 keV gamma-ray and another on the 110 keV gamma-ray (see Figure 3-20). The K_{α}-γ_{110} directional correlation was simultaneously measured with the same geometry and essentially the same electronics as K_{α}-γ_{131}.

Because the resolution of the large volume Ge(Li) detector was adequate, the peaks of interest were easily selected. The contribution to the coincidences due to the continuum beneath the peaks was negligible in comparison to the total coincidences. This trivial contribution was determined from separate runs in which the position of the energy windows were shifted off the peaks.

The K X-rays in coincidence with γ_{110} are shown in Figure 3-21. The coincidence spectrum itself closely resembles the one for K_{α}-γ_{131}. The random coincidences have not yet been subtracted in the spectrum shown. The unlabeled peak to the right of $K\beta_2$-γ_{110} was γ_{63}-γ_{110}. This peak was a combination of random γ_{63}-γ_{110} and legitimate γ_{63}-γ_{110} through the intermediate 198 keV transition. The peak disappeared when the random coincidences were subtracted.

The origin of the K_{α} in K_{α}-γ_{110} was not as unambiguous as the K_{α} in K_{α}-γ_{131}. For K_{α}-γ_{110} the K_{α} X-rays could have been due to K internal conversion of the 198 keV or the 261 keV transitions as well as due to the 177 keV or 240 keV

Figure 3-20. Position of the energy windows on the 110 keV and 131 keV gamma-rays.

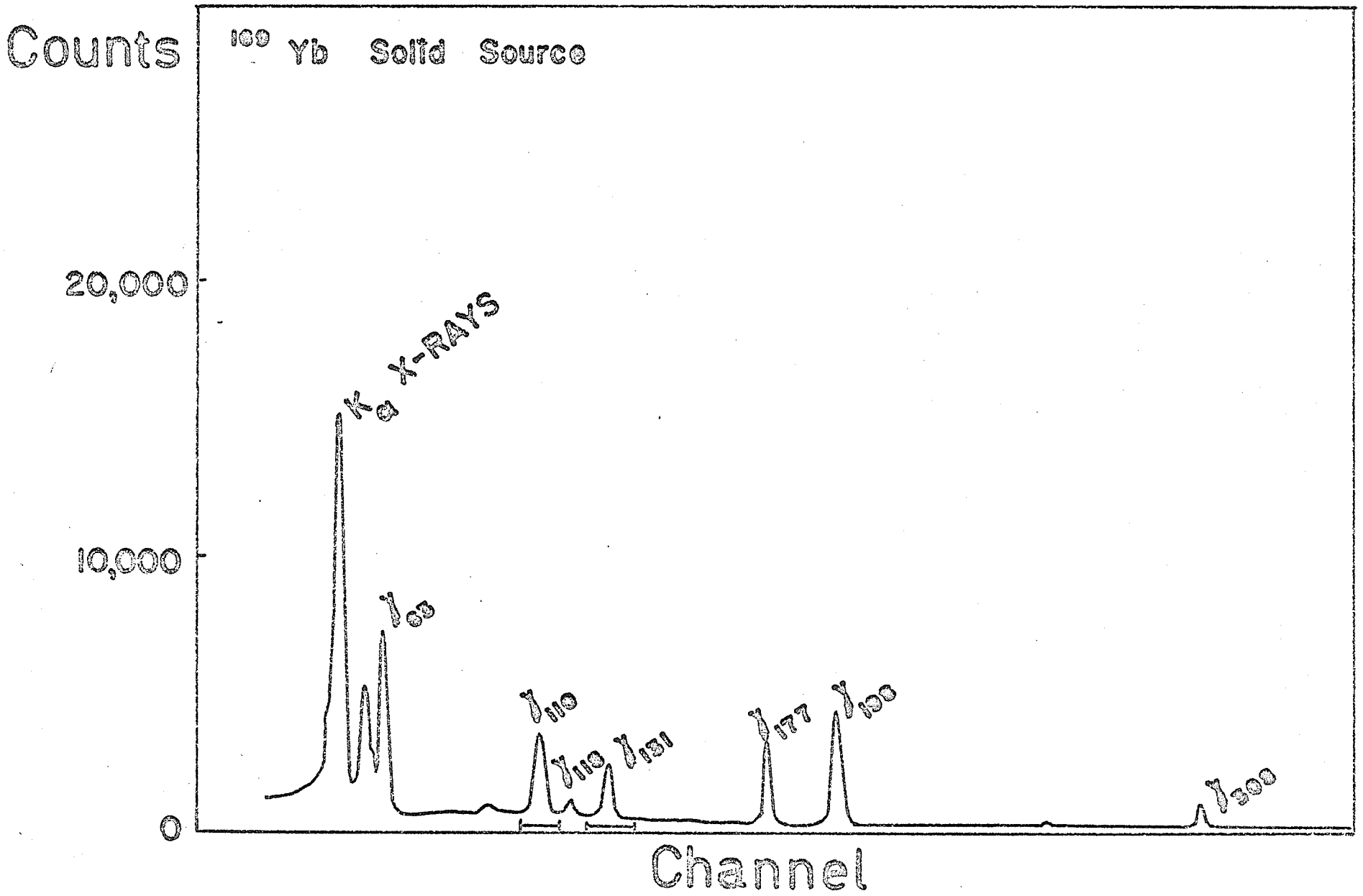
Counts
^{169} Yb Solid Source
20,000
10,000
0
K_α X-RAYS
γ_{63}
γ_{110}
γ_{109}
γ_{118}
γ_{131}
γ_{177}
γ_{198}
γ_{308}
Channel

Figure 3-21. Spectrum of K X-rays in coincidence with the 110 keV gamma-rays.

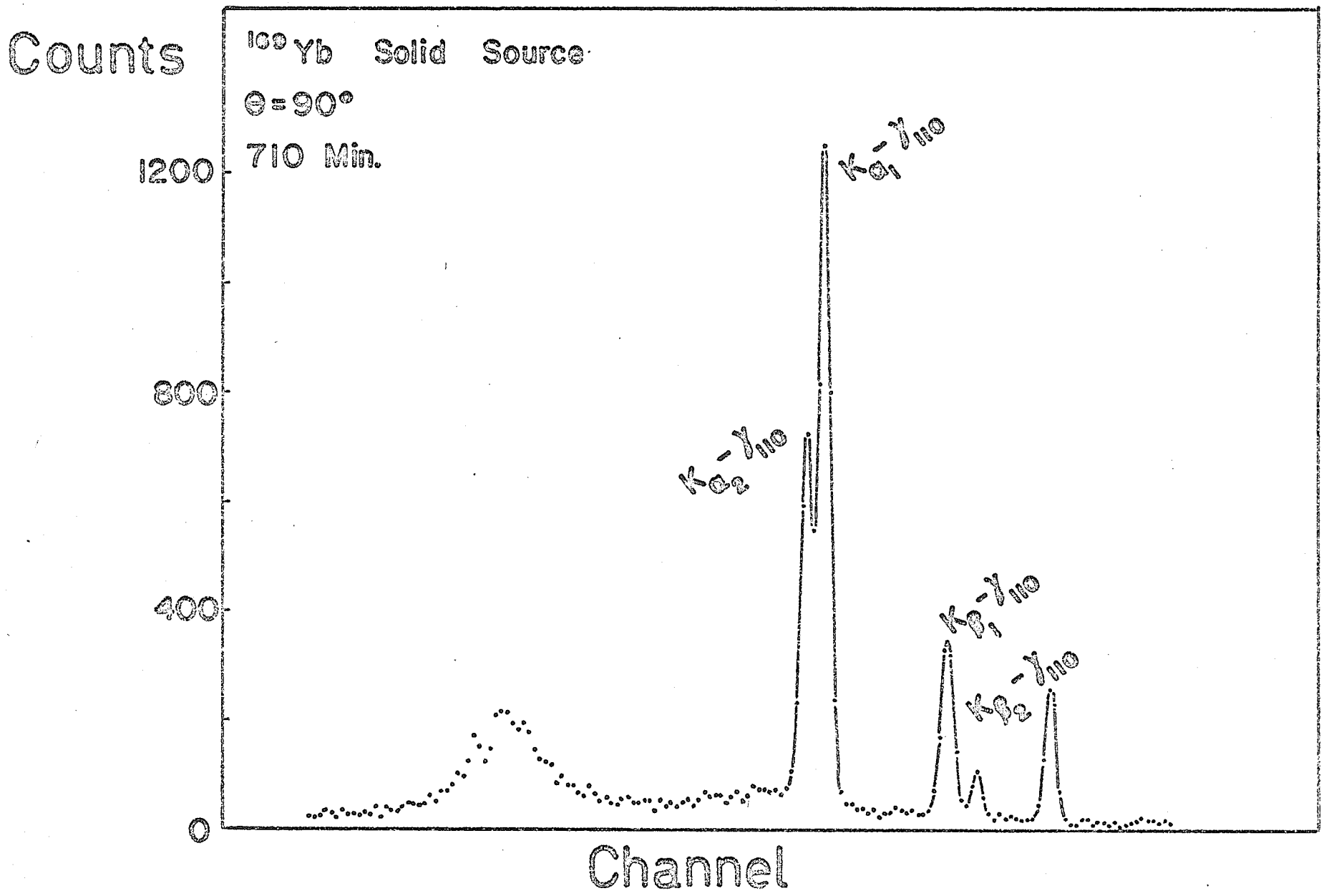
Counts
^{169}Yb Solid Source
θ = 90°
710 Min.
1200
800
400
0
$K\alpha_2 - \gamma_{110}$
$K\alpha_1 - \gamma_{110}$
$K\beta_1 - \gamma_{110}$
$K\beta_2 - \gamma_{110}$
Channel

transitions (see Figure 3-22). The latter two transitions would be in coincidence through the intermediate 20.7 keV transition which is itself not energetic enough to decay by K internal conversion. Fortunately, as it was shown for the K_α-γ_{131} case, the contribution from the 240 keV transition was insignificant in comparison to the 177 keV

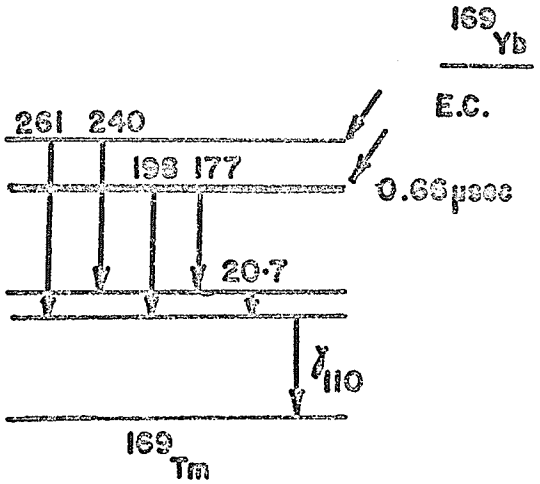

Figure 3-22. Simplified level scheme of ^{169}Tm showing the transitions in cascade with the 110 keV gamma-rays.

transition. The intensity ratio of $K_\alpha(e_{261K})$ to $K_\alpha(e_{198K})$ would be

$$\frac{K_\alpha(e_{261K})}{K_\alpha(e_{198K})} \simeq \frac{e_{261K}}{e_{198K}} = \frac{\gamma_{261}}{\gamma_{198}} \frac{\alpha_{261K}}{\alpha_{198K}} < 0.005$$

i.e. less than 0.5% and like the 240 keV transition, the 261 keV transition's contribution would be insignificant.

Thus the directional correlation measurement K_α-γ_{110} was actually $K_\alpha(e_{177K}+e_{198K})$-$\gamma_{110}$.

The K_α-γ_{110} directional correlation coefficients recorded with the liquid source were

$$A_{22}(K_\alpha(e_{177K}+e_{198K})-\gamma_{110}) = -0.038\pm0.015$$

$$A_{44}(K_\alpha(e_{177K}+e_{198K})-\gamma_{110}) = +0.023\pm0.016$$

The measurements taken with a solid source a half year later and with radioactive material from another supplier yielded

$$A_{22}(K_\alpha(e_{177K}+e_{198K})-\gamma_{110}) = -0.015\pm0.021$$

$$A_{44}(K_\alpha(e_{177K}+e_{198K})-\gamma_{110}) = -0.006\pm0.023$$

Although one would at first suspect attenuation of the anisotropy in the solid source, this could not be so. It must be remembered that there was no attenuation for the K_α-γ_{131} case. Furthermore the γ-γ directional correlations (to be reported later on) agreed with other unattenuated γ-γ measurements. Careful inspection of the above two sets of numbers show that they agree with each other within the experimental error, i.e. the solid source and the liquid source gave the same anisotropy.

The complete list of directional correlation coefficients involving K_α X-rays following internal conversion is given in Table III. Before the correlations involving the conversion electrons are discussed, the

TABLE III

DIRECTIONAL CORRELATION COEFFICIENTS INVOLVING K_α X-RAYS FOLLOWING INTERNAL CONVERSION

Directional Correlation	Source	Correlation Coefficients	
		A_{22}	A_{44}
K_α-γ_{131}	liquid	-0.053(13)	+0.021(13)
K_α-γ_{131}	solid	-0.051(23)	+0.011(24)
K_α-γ_{110}	liquid	-0.038(15)	+0.023(16)
K_α-γ_{110}	solid	-0.015(21)	-0.006(23)
K_α-e_{177K}	solid	-0.025(15)	+0.011(16)
K_α-e_{198K}	solid	-0.009(13)	+0.013(14)
γ_{177}-K_α [a]	sol.& liq. [b]	-0.017(26)	+0.001(28)
γ_{198}-K_α [a]	sol.& liq. [b]	-0.003(16)	+0.013(17)

a) For these measurements the energy window was set on K_α. In the other measurements the energy windows were set on the gamma-ray or conversion electron.

b) The directional correlation results from the liquid and solid sources were combined because of the relatively few coincidences (relative to the number of other coincidences in this experiment, viz. K_α-γ_{131}).

γ-γ measurements made will be investigated.

The X-ray detector was also sensitive to gamma-rays and hence it was possible to do γ-γ directional correlation measurements. For instance, recording the entire X-ray detector spectrum in coincidence with γ_{131}, one obtained K_α-γ_{131} and γ_{177}-γ_{131}. The latter was a γ-γ directional correlation which had been previously measured[14,26] and which would serve as a check on the validity of the K_α-γ_{131} measurement. Figure 3-23 is the intermediate energy (150-200 keV) gamma-rays in coincidence with γ_{131}. The only true coincidence was γ_{177}-γ_{131}. The peak on the right of γ_{177}-γ_{131} was due to random γ_{198}-γ_{131}. When the random coincidences were subtracted, this peak disappeared. Although the relative intensity of γ_{177} was about twice that of K_α following conversion of the 131 keV transition, the X-ray detector was over an order of magnitude less efficient at the higher energy. Hence there were fewer coincidences recorded for γ_{177}-γ_{131} than for K_α-γ_{131}. So the coincidences acquired with the solid source were combined with those from the liquid source to yield the final γ_{177}-γ_{131} directional correlation. Nevertheless, despite their large errors, the results from the solid were consistent with those from the liquid source.

The directional correlation coefficients derived for γ_{177}-γ_{131} were

$$A_{22}(\gamma_{177}\text{-}\gamma_{131}) = +0.258 \pm 0.039$$

$$A_{44}(\gamma_{177}\text{-}\gamma_{131}) = +0.120 \pm 0.042$$

Figure 3-23. Intermediate energy gamma-rays in coincidence with the 131 keV gamma-rays.

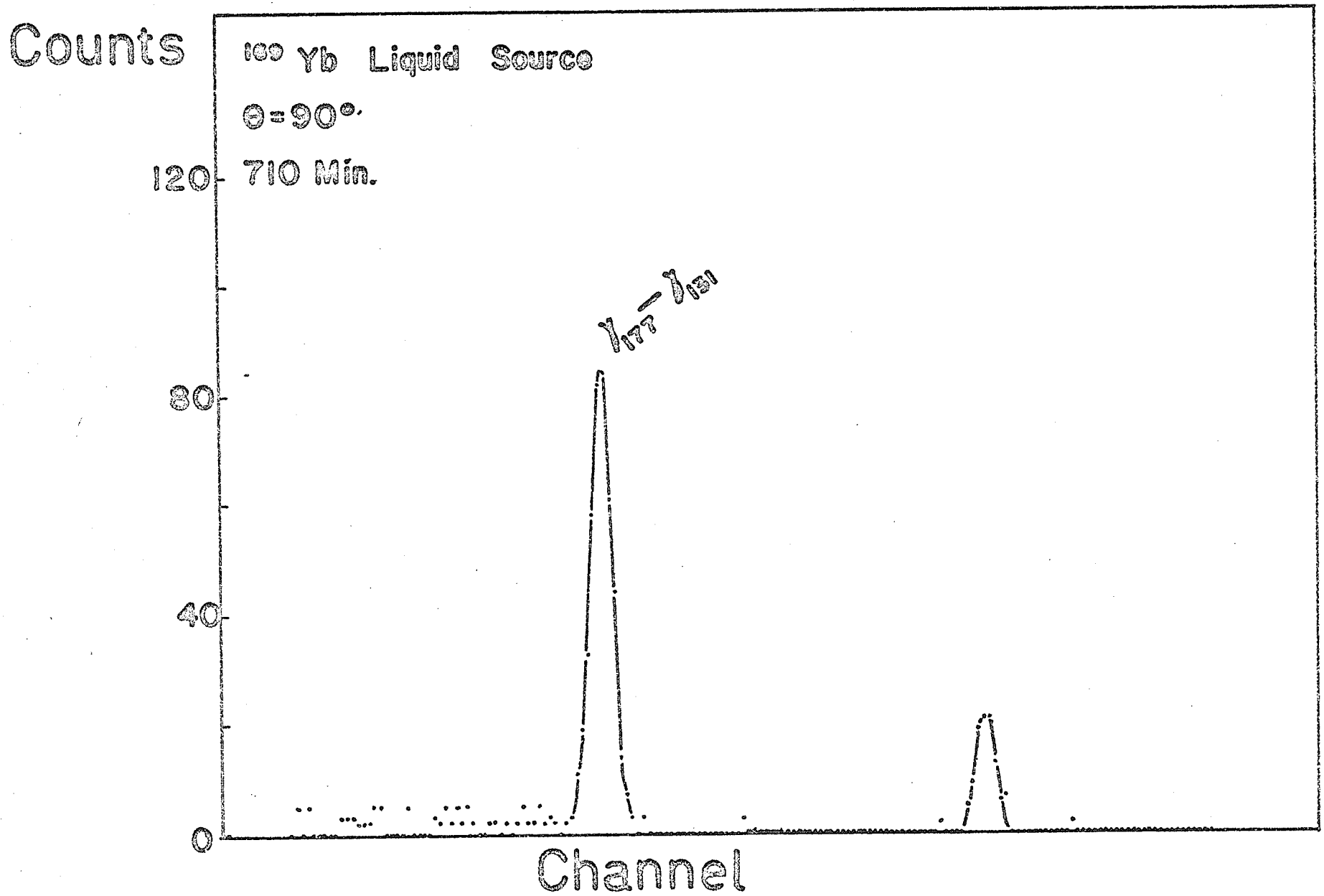
Counts
169 Yb Liquid Source
θ = 90°.
710 Min.
120
80
40
0
Channel
γ177 - γ131

These agreed with Becker et.al.'s[26] values of

$$A_{22}(\gamma_{177}-\gamma_{131}) = +0.253\pm0.008$$

$$A_{44}(\gamma_{177}-\gamma_{131}) = +0.036\pm0.010$$

Their measurements were made with Ge(Li) detectors. Grabowski et.al.[14] used scintillation detectors and their values were slightly higher at

$$A_{22}(\gamma_{177}-\gamma_{131}) = +0.275\pm0.007$$

The consistency of the present $\gamma_{177}-\gamma_{131}$ measurement with the other measurements inspired confidence in the present $K_\alpha-\gamma_{131}$ directional correlation measurements.

The agreement of all the present $\gamma-\gamma$ directional correlation measurements, not just $\gamma_{177}-\gamma_{131}$, with other investigations[14,26,27,28] was excellent (see Table IV). The other important correlation besides $\gamma_{177}-\gamma_{131}$ was $\gamma_{198}-\gamma_{110}$ (see Figure 3-24) for which the correlation coefficients were

$$A_{22}(\gamma_{198}-\gamma_{110}) = +0.335\pm0.052$$

$$A_{44}(\gamma_{198}-\gamma_{110}) = +0.066\pm0.057$$

These results agreed with the results of Becker et.al.[26] who obtained

$$A_{22}(\gamma_{198}-\gamma_{110}) = +0.338\pm0.007$$

$$A_{44}(\gamma_{198}-\gamma_{110}) = +0.018\pm0.011$$

Indeed all the evidence suggests that the directional

TABLE IV

GAMMA-GAMMA AND GAMMA-ELECTRON DIRECTIONAL CORRELATION COEFFICIENTS

Directional Correlation Coefficient	Present Work	Becker et.al.[a] (ref.26)	Grabowski et.al.[b] (ref.14)	Günther et.al.[c] (ref.27)	Kaufmann et.al.[d] (ref.28)
$A_{22}(\gamma_{177}-\gamma_{131})$	0.258(39)	0.253(8)	0.275(7)		
$A_{44}(\gamma_{177}-\gamma_{131})$	0.120(42)	0.036(10)	-0.005(16)		
$A_{22}(\gamma_{198}-\gamma_{110})$	0.335(52)	0.338(7)	0.295(7)	0.341(3)	0.347(6)
$A_{44}(\gamma_{198}-\gamma_{110})$	0.066(57)	0.018(11)	-0.013(17)	0.004(5)	
$A_{22}(\gamma_{131}-e_{177K})$	0.031(51)		0.002(7)		
$A_{44}(\gamma_{131}-e_{177K})$	-0.044(55)				
$A_{22}(\gamma_{110}-e_{198K})$	0.050(43)		0.001(8)		
$A_{44}(\gamma_{110}-e_{198K})$	0.029(45)				

a) Becker et.al. used two Ge(Li) gamma-ray detectors to measure the γ-γ directional correlation.
b) Grabowski et.al. used two NaI(Tl) scintillation detectors for the γ-γ directional correlation and a NaI(Tl) detector with a magnetic lens spectrometer for the γ-e directional correlation.
c) Günther et.al. used Ge(Li) detectors to measure the γ-γ directional correlation.
d) Kaufmann et.al. used a NaI(Tl) scintillation detector and a Ge(Li) detector for the γ-γ directional correlation.

Figure 3-24. Intermediate energy gamma-rays in coincidence with the 110 keV gamma-rays.

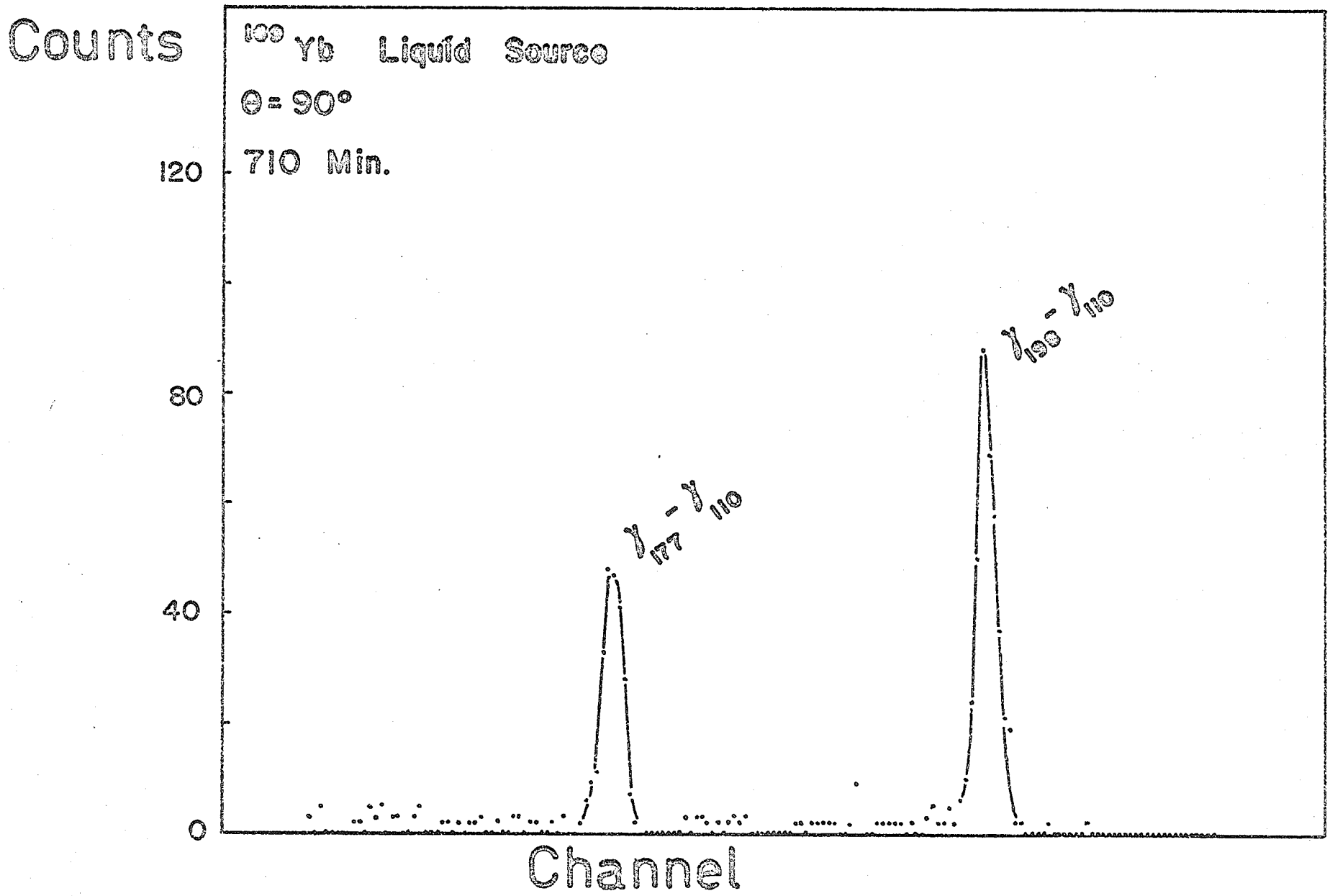
Counts
169 Yb Liquid Source
θ = 90°
710 Min.
120
80
40
0
$\gamma_{177} - \gamma_{110}$
$\gamma_{198} - \gamma_{110}$
Channel

correlation measurements involving the K_α X-rays following K internal conversion were valid and authentic.

The K X-rays in coincidence with K conversion electrons were looked at next. In particular, K_α-e_{177K} and K_α-e_{198K} directional correlations were measured. The source and source position for these measurements were the same as for the K_α-γ_{131} and K_α-γ_{110} solid source measurements (see Figure 2-1). The electron detector system was positioned prior to recording K_α-γ_{131} and K_α-γ_{110} and there was no change in the environment of the source when K_α-e_{177K} and K_α-e_{198K} was done.

Figure 3-25 is the spectrum of K X-rays in coincidence with e_{198K}. This coincidence spectrum closely resembles those spectra in which the energy window was set on γ_{131} or γ_{110} (see Figures 3-18 and 3-21). The only difference here was the fewer random coincidences than for the previous K_α-γ. The reason for this was the better time resolution of the coincidence electronics. For K_α-γ the resolution was a third longer than it was for K_α-e_K (about 40 nsec versus about 30 nsec).

The origin of K_α in K_α-e_{198K} was not clearly defined as for K_α-γ_{131} or even for K_α-γ_{110}. From Figure 3-26 it can be seen that the K_α in coincidence with e_{198K} could have come from the K conversion of the 110 keV or 118 keV transitions as well as from the 198 keV transition.

Figure 3-25. Spectrum of K X-rays in coincidence with the K conversion electrons of the 198 keV transition.

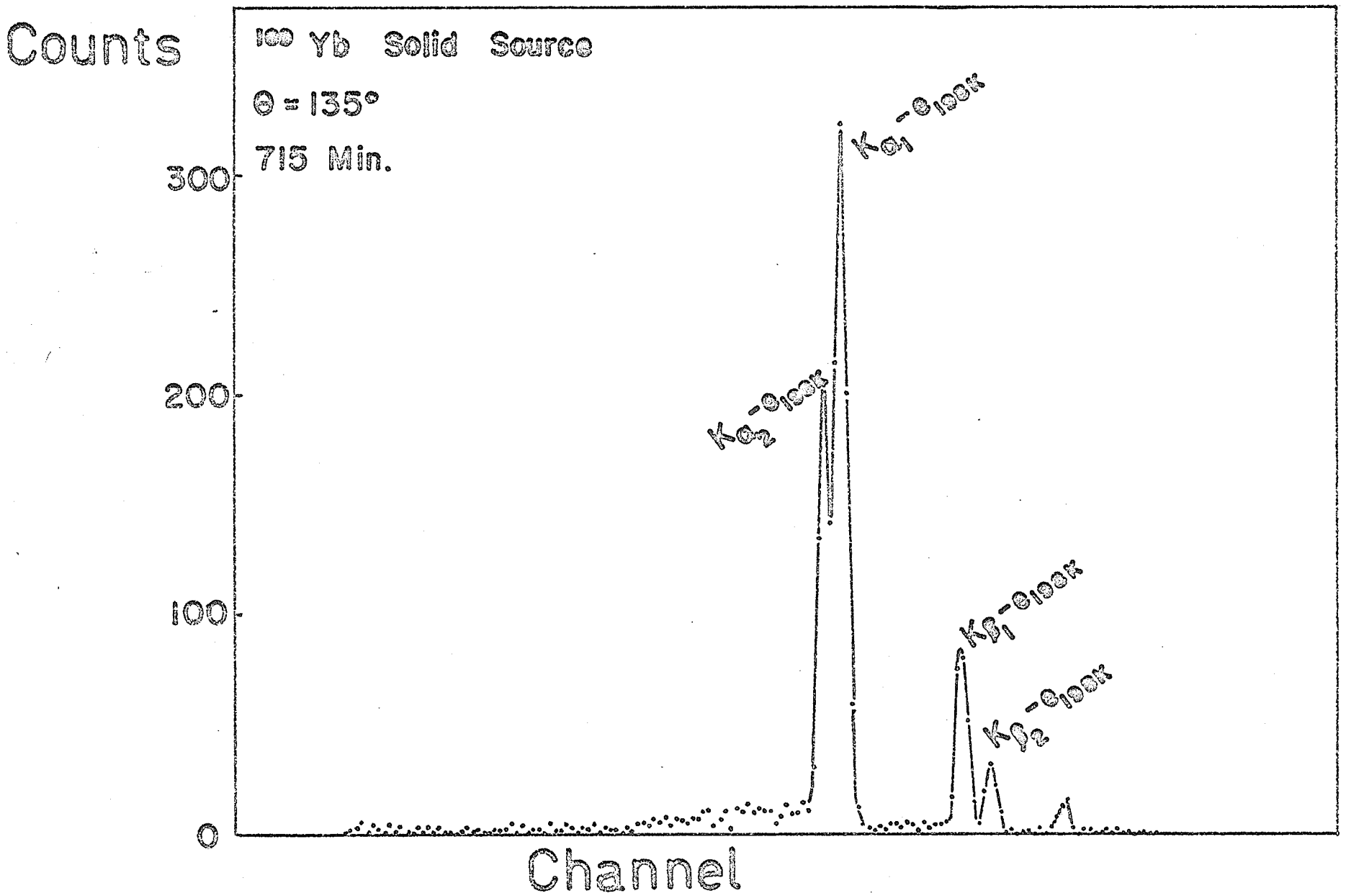
Counts
^{168} Yb Solid Source
θ = 135°
715 Min.
300
200
100
0
$K\alpha_1 - e_{190K}$
$K\alpha_2 - e_{190K}$
$K\beta_1 - e_{190K}$
$K\beta_2 - e_{190K}$
Channel

Fortunately the ratio of $K_\alpha(e_{118K})$ to $K_\alpha(e_{110K})$ was small as the following calculation shows

$$\frac{K_\alpha(e_{118K})}{K_\alpha(e_{110K})} \simeq \frac{e_{118K}}{e_{110K}} = \frac{\gamma_{118}}{\gamma_{110}} \cdot \frac{\alpha_{118K}}{\alpha_{110K}} < 0.08$$

Since any anisotropy involving K X-rays would be small - only a few percent at the most - and since the percentage of $K_\alpha(e_{118K})$ was small (less than 8%), any $K_\alpha(e_{118K})$-e_{198K} anisotropy would be insignificant. Thus the directional correlation measurement of K_α-e_{198K} was actually $K_\alpha(e_{198K}+e_{110K})$-$e_{198K}$.

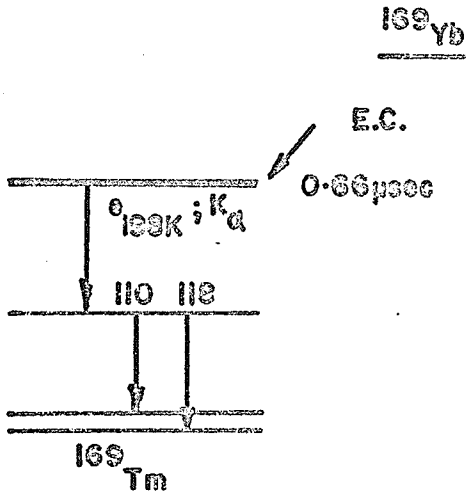

Figure 3-26. Simplified level scheme of ^{169}Tm showing the transitions in cascade with e_{198K}.

The directional correlation coefficients with the solid source were

$$A_{22}(K_\alpha(e_{198K}+e_{110K})-e_{198K}) = -0.009 \pm 0.013$$

$$A_{44}(K_\alpha(e_{198K}+e_{110K})-e_{198K}) = +0.013 \pm 0.014$$

Naturally no directional correlation measurements could be made with the liquid source.

Although the energy window on the e_{198K} peak was free from adjacent peaks, the e_{177K} window was not (see Figure 3-27). The e_{177K} energy window included part of the e_{131L} peak. This is an important factor because K_α X-rays from K conversion of the 177 keV transition could be in true coincidence with e_{131L} (see Figure 3-28). Of course from the actual coincidence spectrum one cannot differentiate between the origins of K_α.

The contribution of K_α following K conversion of the 118 keV transition was small as it was shown for K_α-e_{198K}. Nevertheless there were a number of other origins for K_α in K_α-e_{177K} which complicated things. Recognizing that some e_{131L} was included in the e_{177K} energy window, K_α-e_{177K} actually consisted of $K_\alpha(e_{177K}+e_{131K}+e_{110K})-e_{177K}$ + $K_\alpha(e_{177K})-e_{131L}$. Hence, the advantage of having the other relatively clean coincidences can be appreciated.

The directional correlation coefficients with the solid source were

$$A_{22}(K_\alpha(e_{177K}+e_{131K}+e_{110K})-e_{177K} + K_\alpha(e_{177K})-e_{131L}) = -0.025\pm0.015$$

$$A_{44}(K_\alpha(e_{177K}+e_{131K}+e_{110K})-e_{177K} + K_\alpha(e_{177K})-e_{131L}) = +0.011\pm0.016$$

Figure 3-27. Position of the energy windows on e_{177K} and e_{198K}.

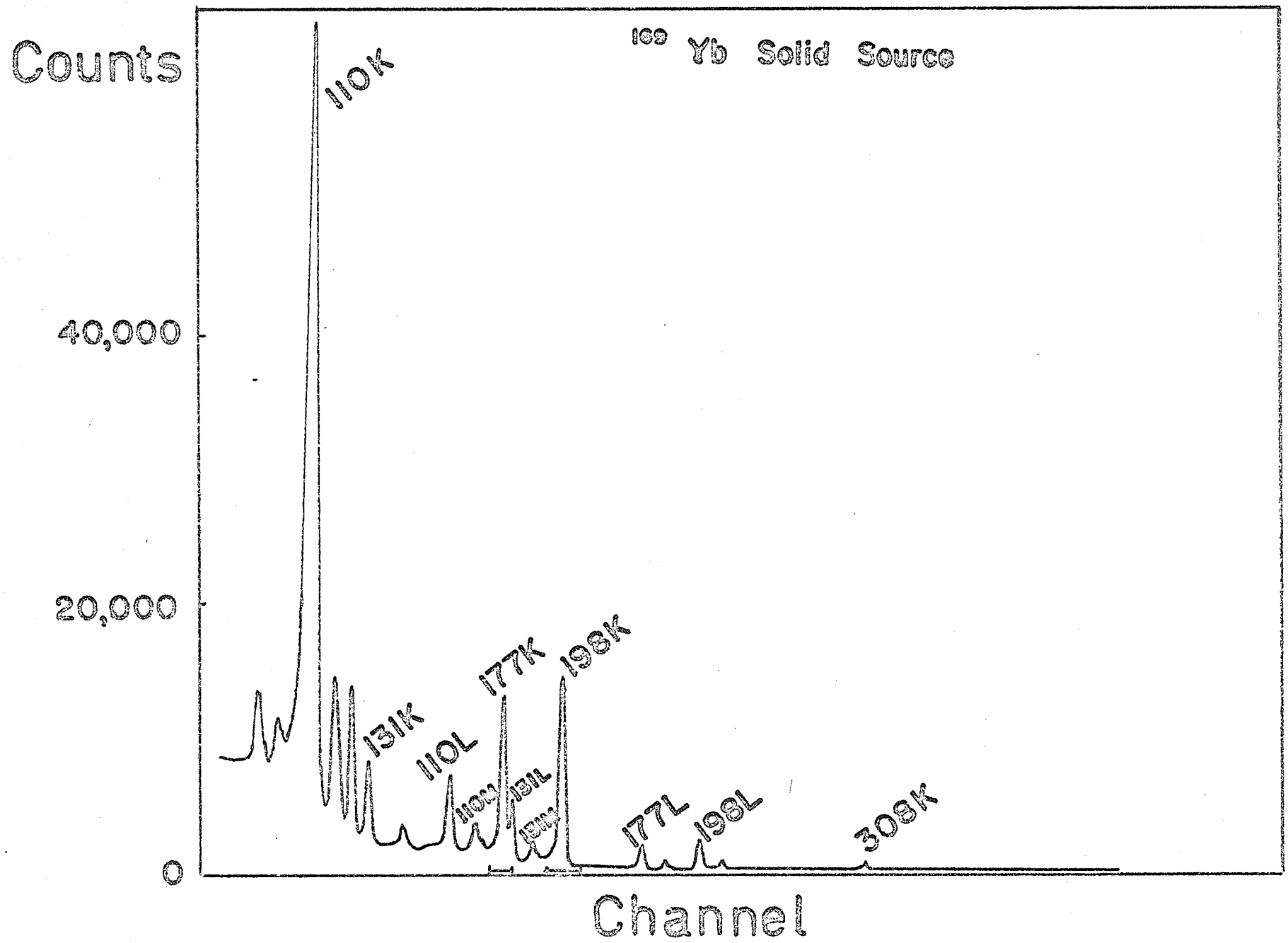
Counts
169 Yb Solid Source
110K
40,000
20,000
131K
110L
177K
198K
110M
131L
131M
177L
198L
308K
0
Channel

Again no directional correlation measurements could be made with the liquid source. A spectrum of K X-rays in coincidence with e_{177K} is shown in Figure 3-29.

Recording the entire X-ray detector spectrum in coincidence with the selected conversion electrons

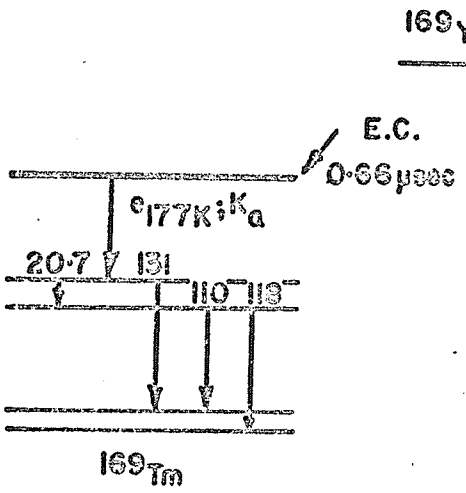

Figure 3-28. Simplified level scheme of ^{169}Tm showing the transitions in cascade with e_{177K}.

allowed one to measure γ-e_K directional correlations. Simultaneously with K_α-e_{198K} and K_α-e_{177K}, γ_{110}-e_{198K} and γ_{131}-e_{177K} were also recorded (see Figures 3-30 and 3-31). Hence γ_{110}-e_{198K} and γ_{131}-e_{177K} could be compared with the previous measurements,[14] and serve as an internal check on the validity of K_α-e_{198K} and K_α-e_{177K}. The directional correlation coefficients (with the solid

Figure 3-29. Spectrum of K X-rays in coincidence with e_{177K}.

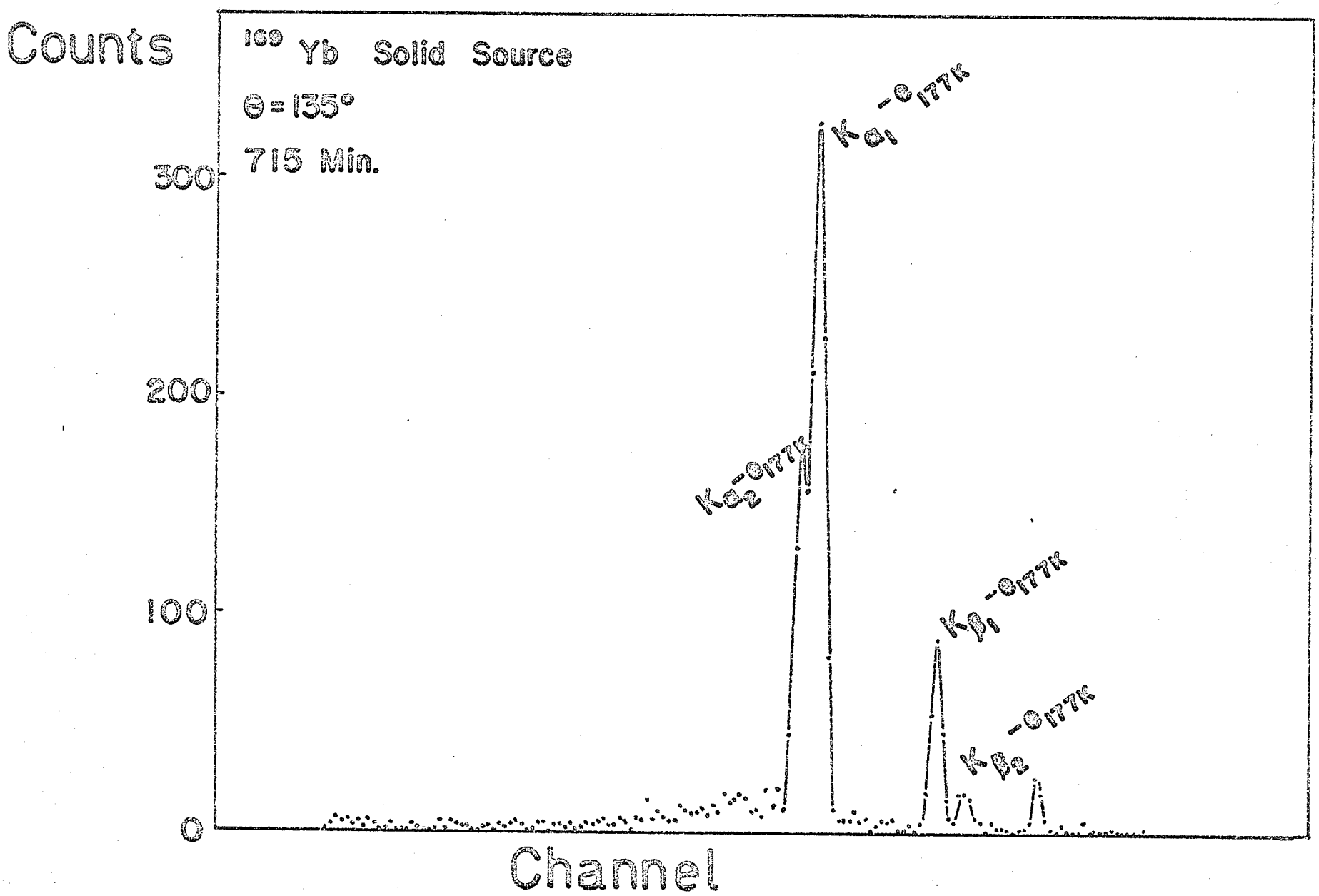
Counts
169 Yb Solid Source
θ = 135°
715 Min.
300
200
100
0
Kα1 - e177K
Kα2 - e177K
Kβ1 - e177K
Kβ2 - e177K
Channel

Figure 3-30. Intermediate energy gamma-rays in coincidence with e_{198K}.

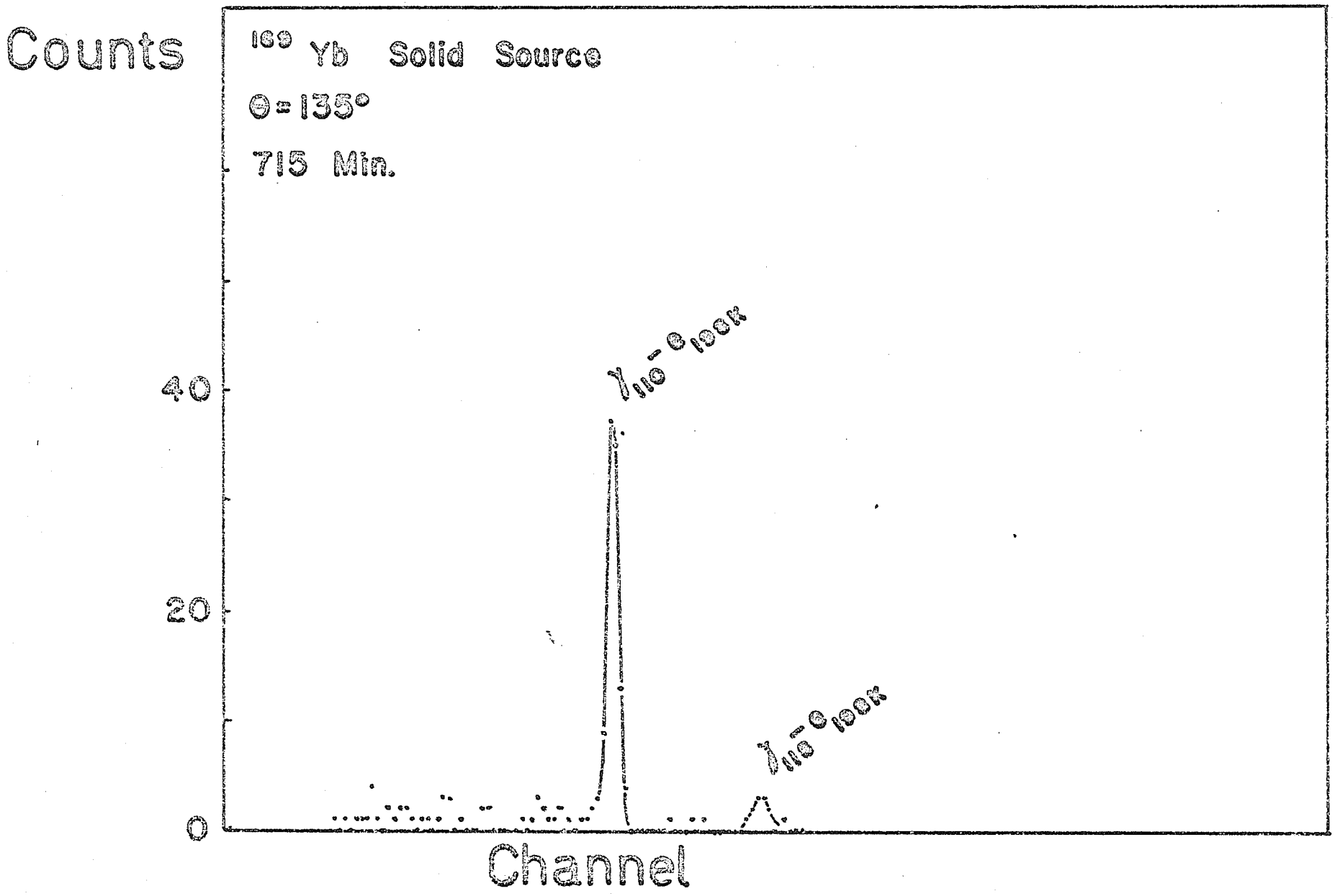
Counts
169 Yb Solid Source
θ = 135°
715 Min.
40
20
0
γ110 - e peak
γ110 - e peak
Channel

Figure 3-31. Intermediate energy gamma-rays in coincidence with e_{177K}.

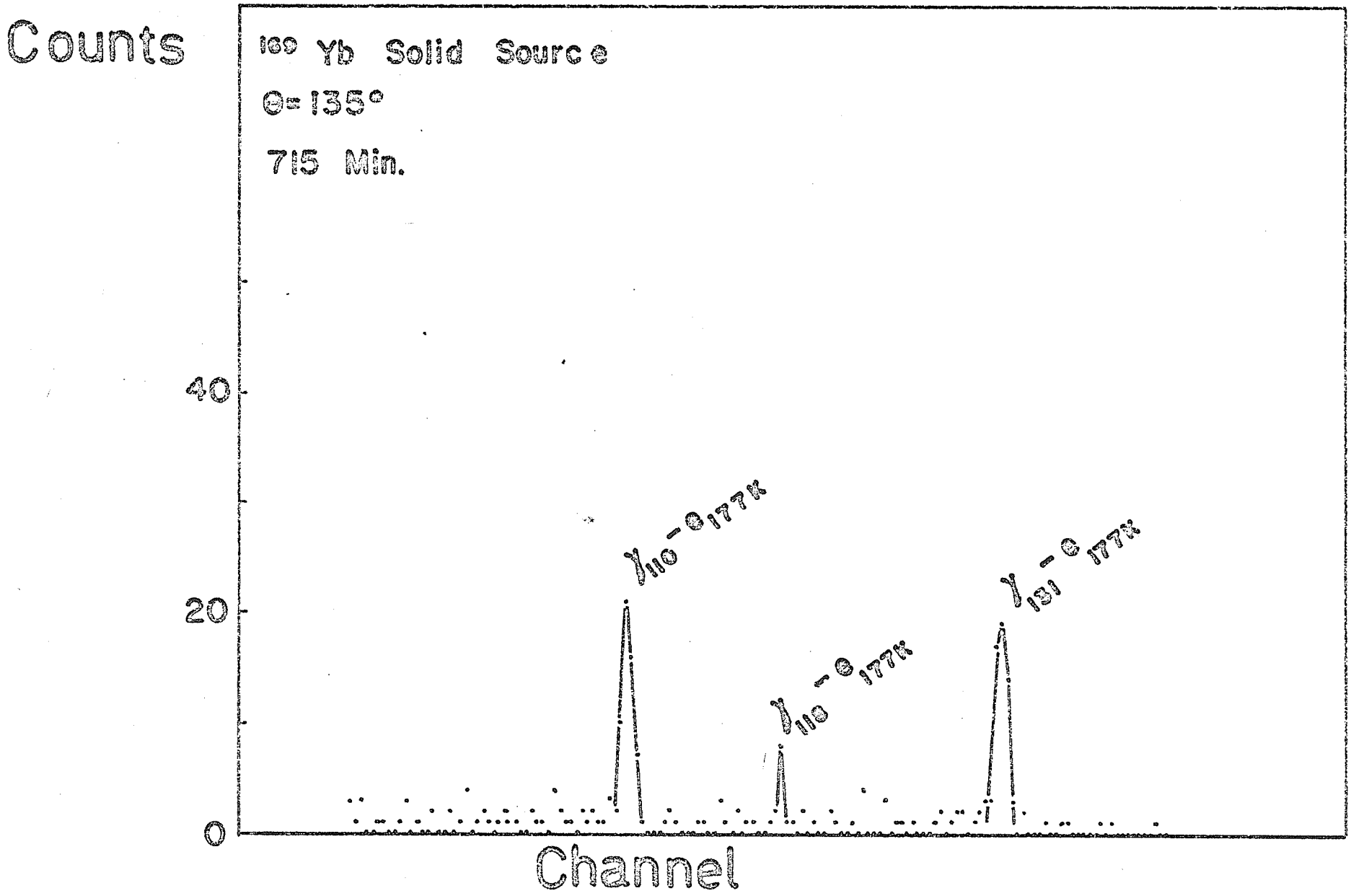
Counts
169 Yb Solid Source
θ= 135°
715 Min.
40
20
0
γ110 - θ177K
γ110 - θ177K
γ131 - θ177K
Channel

source) were

$$A_{22}(\gamma_{110}\text{-}e_{198K}) = +0.050\pm0.043$$

$$A_{22}(\gamma_{131}\text{-}e_{177K}) = +0.031\pm0.051$$

Unfortunately the error was not as small as one would like it to be but the coefficients still agreed with Grabowski et.al.'s values[14] of

$$A_{22}(\gamma_{110}\text{-}e_{198K}) = +0.001\pm0.008$$

$$A_{22}(\gamma_{131}\text{-}e_{177K}) = +0.002\pm0.007$$

Thus the γ-e_K directional correlation measurements lent credibility to the K_α-e_K directional correlation measurements.

Minor attention was paid to K_α-γ_{198} and K_α-γ_{177}. These coincidences differed from the previous ones only in that the energy window or gate was set on the K_α X-ray rather than on the gamma-ray. These measurements were important because the K_α in K_α-γ_{198} could arise only from K internal conversion of the 110 keV transition (see Figure 3-32); the contribution from the K internal conversion of the 118 keV transition would be very small. The correlation coefficients were

$$A_{22}(K_\alpha(e_{110K})\text{-}\gamma_{198}) = -0.003\pm0.016$$

$$A_{44}(K_\alpha(e_{110K})\text{-}\gamma_{198}) = +0.013\pm0.017$$

i.e. an isotropic distribution.

For K_a-γ_{177} the source of K_a were primarily from K internal conversion of the 131 keV transition with some contribution from the 110 keV transition. The correlation coefficients were

$$A_{22}(K_a(e_{131K}+e_{110K})-\gamma_{177}) = -0.017\pm0.026$$

$$A_{44}(K_a(e_{131K}+e_{110K})-\gamma_{177}) = +0.001\pm0.028$$

Again the directional distribution appeared isotropic.

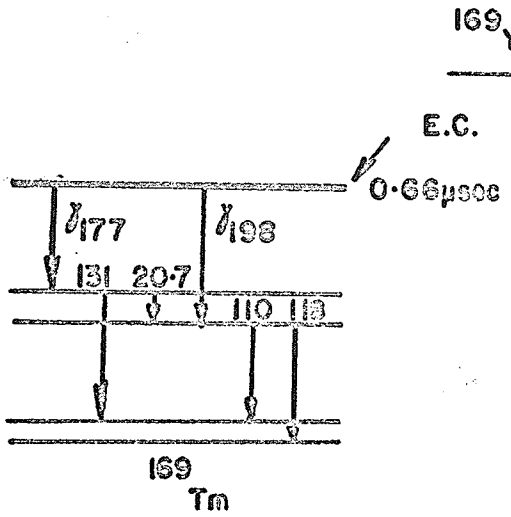

Figure 3-32. Simplified level scheme of ^{169}Tm showing the transitions in cascade with γ_{177} and γ_{198}.

The directional correlation coefficients were measured for the following six cascades in $^{169}Yb \rightarrow {}^{169}Tm$

$K_a(e_{177K})-\gamma_{131}$

$K_a(e_{177K}+e_{198K})-\gamma_{110}$

$K_\alpha(e_{198K}+e_{110K})-e_{198K}$

$K_\alpha(e_{177K}+e_{131K}+e_{110K})-e_{177K}$ + $K_\alpha(e_{177K})-e_{131L}$

$K_\alpha(e_{110K})-\gamma_{198}$

$K_\alpha(e_{110K}+e_{131K})-\gamma_{177}$

The authenticity of these measurements was confirmed with the consistency of simultaneous γ-γ and γ-e_K measurements with previous γ-γ and γ-e_K values. The authenticity of the measurements involving gamma-rays was further supported by the reproducibility of the measurements with solid and liquid sources.

^{207}Bi Source. A directional correlation measurement involving K_α X-rays was performed on $^{207}Bi \rightarrow {}^{207}Pb$. The ^{207}Bi source used was a vacuum-deposited aluminum-foil-backed one with a strength of about 1 μCi. The energy window was set on e_{1064K} (see Figure 3-33). Then the K_α in coincidence with e_{1064K} would be from the 1064 keV transition itself, as well as from any K_α following K conversion of the 570 keV transition. Figure 3-34 is the actual coincidence spectrum. The 0.80 sec isomeric level enabled one to separate the K_α above the level (mainly from K electron capture) from K_α below the level. The latter were almost solely from K internal conversion of the 1064 keV and 570 keV transitions.

Since K_α-e_{1064K} was actually $K_\alpha(e_{1064K}+e_{570K})-e_{1064K}$ the directional correlation coefficients obtained were

$$A_{22}(K_\alpha(e_{1064K}+e_{570K})-e_{1064K}) = +0.001\pm0.059$$

$$A_{44}(K_\alpha(e_{1064K}+e_{570K})-e_{1064K}) = -0.020\pm0.062$$

It appeared that there was no anisotropy, i.e. an isotropic distribution.

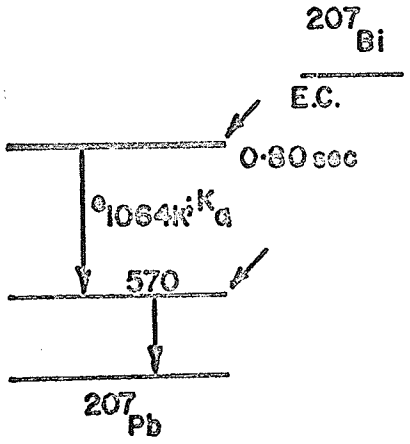

Figure 3-33. Simplified decay scheme of ^{207}Pb showing the transitions in coincidence with e_{1064K}.

The 1064 keV transition is an M4 transition while the 570 keV transition is an E2 transition. Both transitions do not penetrate the nucleus. Furthermore ^{207}Pb is certainly not noted for any large electric quadrupole moment (0.2×10^{-24} cm^2).[13] Hence the expected isotropic distribution. The A_{22} value of +0.001(59) adds further evidence to the authenticity of the anisotropy measured in

Figure 3-34. K X-rays in coincidence with e_{1064K}.

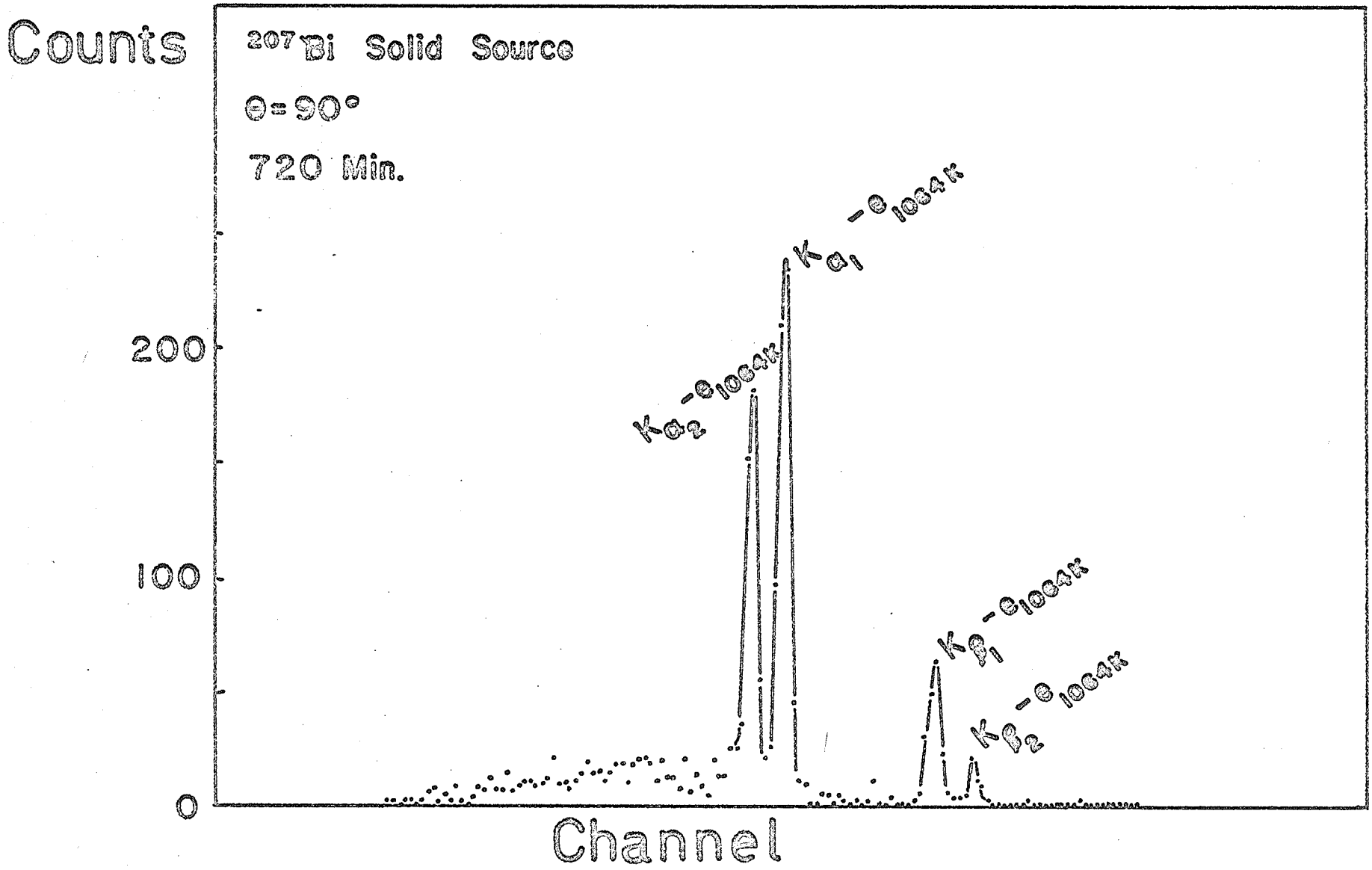
Counts
^{207}Bi Solid Source
θ = 90°
720 Min.
200
100
0
$K\alpha_2 - e_{1064K}$
$K\alpha_1 - e_{1064K}$
$K\beta_1 - e_{1064K}$
$K\beta_2 - e_{1064K}$
Channel

^{169}Tm. Although the experimental set-up was not identical in both cases, part of the electronics was the same as well as the method of analysis and the experimenter (i.e. the author).

CHAPTER IV

DICHOTOMIZATION OF THE DIRECTIONAL CORRELATION COEFFICIENTS

In the previous chapter, the directional correlation coefficients were given for the several measurements made. These coefficients will now be dichotomized. Generally $A_{22} = A_2^{(1)} \cdot A_2^{(2)}$ where $A_2^{(1)}$ is the contribution from the first element in the cascade and $A_2^{(2)}$ is the contribution from the second element of the cascade. Thus in the case of $A_{22}(K_\alpha(e_{177K})-\gamma_{131})$,

$$A_{22}(K_\alpha(e_{177K})-\gamma_{131}) = A_2(K_\alpha(e_{177K})) \cdot A_2(\gamma_{131})$$

or

$$A_2(K_\alpha(e_{177K})) = \frac{A_{22}(K_\alpha(e_{177K})-\gamma_{131})}{A_2(\gamma_{131})} \quad \frac{-0.053(11)}{A_2(\gamma_{131})} \quad \ldots(1)$$

$A_2(\gamma_{131})$ can easily be obtained from directional correlation tables.[29] Since it is a pure E2 transition from a $7/2^+$ level to a $3/2^+$ level the value is

$$A_2(\gamma_{131}) = F_2(7/2^+, 3/2^+, E2, E2) = -0.4676$$

Then equation (1) becomes

$$A_2(K_\alpha(e_{177K})) = +0.113(23)$$

This process can be applied to the other measured directional correlation coefficients. However the coefficients involving the 110 keV, 177 keV and 198 keV transitions are somewhat complicated because they are not

pure. For the mixed 110 keV transition

$$A_2(\gamma_{110}) = (F_2(5/2^+,3/2^+,M1,M1)+2\delta(E2/M1)F_2(5/2^+,3/2^+,M1,E2)+ +\delta^2(E2/M1)F_2(5/2^+,3/2^+,E2,E2))/(1+\delta^2(E2/M1))$$

where $\delta(E2/M1)$ is the mixing ratio. The mixing ratios adopted for this transition, as well as for the other transitions, were the appropriate weighted averages of recent measurements of the various δ's (see Table V).

An alternative to the directional correlation table was to extract $A_2(\gamma)$ from the gamma-gamma directional correlation coefficients. For instance using the tabulated $A_2(\gamma_{110})$ and the weighted average of $A_{22}(\gamma_{198}-\gamma_{110})$ from references 14, 26 and 27,

$$A_2(\gamma_{198}) = \frac{A_{22}(\gamma_{198}-\gamma_{110})}{A_2(\gamma_{110})} = +0.531(8) \qquad ...(2)$$

Similarly,

$$A_2(\gamma_{177}) = \frac{A_{22}(\gamma_{177}-\gamma_{131})}{A_2(\gamma_{131})} = -0.541(17) \qquad ...(3)$$

In the succeeding calculations, a weighted average for $A_2(\gamma_{198})$ from the directional correlation table[29] and equation (2) was adopted, i.e. $A_2(\gamma_{198}) = +0.540(6)$. However the result from equation (3) differed considerably from the results obtained from the directional correlation table. Just the result from equation (3) was used because only two measurements of the 177 keV mixing ratio (of

TABLE V

WEIGHTED AVERAGE MIXING RATIOS

Transition	δ(E2/M1)	δ^2(E2/M1)	$A_2(\gamma)$ [c]
110 keV	-0.152(2) [a]	0.0230(3)	+0.643(4)
177 keV	+0.450(17) [b]	0.202(8)	-0.604(7)
198 keV	+0.310(4) [a]	0.0953(10)	+0.543(5)

a) These values were the weighted averages of the results from references 26,27,28 and 30.
b) This value was the result from only references 27 and 30.
c) Taken from reference 29 using the weighted average mixing ratios.

possibly questionable validity) were available. Four measurements of the 198 keV mixing ratio were available.

Having established the values of the necessary $A_2(\gamma)$, $A_{22}(K_\alpha\text{-}\gamma_{110})$ was dichotomized;

$$A_{22}(K_\alpha(e_{177K}+e_{198K})\text{-}\gamma_{110}) = f_1 A_{22}(K_\alpha(e_{198K})\text{-}\gamma_{110}) + (1-f_1)A_{22}(K_\alpha(e_{177K})\text{-}\gamma_{110})$$

where f_1 was the fraction of the K_α X-rays in coincidence with the 110 keV transition following e_{198K} and $(1-f_1)$ was the remainder of the K_α X-rays in coincidence with the 110 keV transition following e_{177K} (see Figure 4-1). The fraction f_1 was derived from the feeding and bleeding of the appropriate levels,

$$f_1 = \frac{I_{e_{198K}}}{(\frac{I_{20.7}}{I_{20.7}+I_{131}})I_{e_{177K}+I_{e_{198K}}}} = 0.800(19)$$

Here $I_{e_{198K}}$ and $I_{e_{177K}}$ were the intensities of e_{198K} and e_{177K}.[31] $I_{20.7}$ and I_{131} were the total intensities of the 20.7 keV and 131 keV transitions respectively. Then

$$A_{22}(K_\alpha(e_{177K}+e_{198K})\text{-}\gamma_{110}) = f_1 A_2(K_\alpha(e_{198K}))\cdot A_2(\gamma_{110}) + (1-f_1)A_2(K_\alpha(e_{177K}))\cdot A_2(\gamma_{110})$$

or

$$A_2(K_\alpha(e_{198K})) = \frac{A_{22}(K_\alpha\text{-}\gamma_{110})}{f_1 A_2(\gamma_{110})} - \frac{(1-f_1)A_2(K_\alpha(e_{177K}))}{f_1}$$

$$= -0.086(26)$$

One could also consider

$$A_{22}(K_\alpha(e_{110K})\text{-}\gamma_{198}) = A_2(K_\alpha(e_{110K}))\cdot A_2(\gamma_{198})$$

or

$$A_2(K_\alpha(e_{110K})) = \frac{A_{22}(K_\alpha\text{-}\gamma_{198})}{A_2(\gamma_{198})} = -0.006(30)$$

If this equals zero, as it appears it does, the K_α X-rays associated with the 110 keV internal conversion are isotropically distributed.

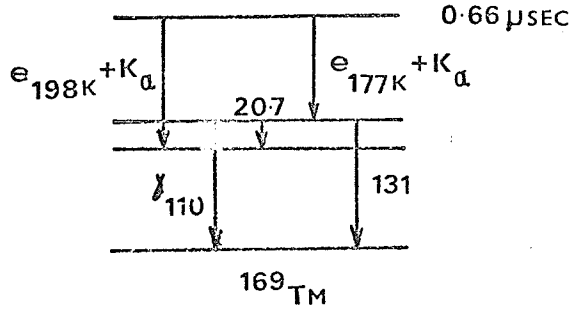

Figure 4-1. Abridged decay scheme showing the origin of the K_α X-rays in coincidence with γ_{110}. For simplicity the diagram assumed one K_α X-ray is generated for every conversion electron.

The next dichotomization was

$$A_{22}(K_\alpha(e_{131K}+e_{110K})\text{-}\gamma_{177}) = f_2A_{22}(K_\alpha(e_{131K})\text{-}\gamma_{177}) + (1-f_2)A_{22}(K_\alpha(e_{110K})\text{-}\gamma_{177})$$

where

$$f_2 = \frac{I_{e_{131K}}}{(\frac{I_{20.7}}{I_{20.7}+I_{198}})I_{e_{110K}}+I_{e_{131K}}} = 0.544(15),$$

the fraction of K_α X-rays in coincidence with the 177 keV transition following e_{131K} (see Figure 4-2). The total intensities of the 20.7 keV and 198 keV transitions were $I_{20.7}$ and I_{198} respectively. Again these intensities were derived from the feeding and the bleeding of the proper

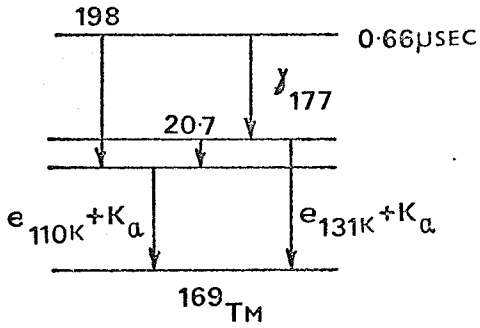

Figure 4-2. Simplified decay scheme showing the origin of the K_α X-rays in coincidence with γ_{177}. For simplicity the diagram assumes one K_α X-ray is generated for every conversion electron.

levels. The intensities of e_{131K} and e_{110K} were Ie_{131K} and $I_{e_{110K}}$. Thus,

$$A_{22}(K_\alpha(e_{131K}+e_{110K})-\gamma_{177}) = f_2A_2(K_\alpha(e_{131K}))\cdot A_2(\gamma_{177}) + (1-f_2)A_2(K_\alpha(e_{110K})\cdot A_2(\gamma_{177})$$

or

$$A_2(K_\alpha(e_{131K})) = \frac{A_{22}(K_\alpha-\gamma_{177})}{f_2 A_2(\gamma_{177})} - \frac{(1-f_2)A_2(K_\alpha(e_{110K}))}{f_2}$$

$$= +0.065(117)$$

It appeared that $K_\alpha(e_{131K})$ had an isotropic distribution.

The directional correlation involving K_α in coincidence with e_{198K} was next pursued (see Figure 4-3),

$$A_{22}(K_\alpha(e_{198K}+e_{110K})-e_{198K}) = f_3 A_2(K_\alpha(e_{198K})-e_{198K}) + (1-f_3)A_2(K_\alpha(e_{110K})-e_{198K}) \quad \ldots(4)$$

where

$$f_3 = \frac{1}{\left(\frac{a_{110K}}{a_{110K}+a_{110L,M,\ldots}+1}\right)+1} = 0.627$$

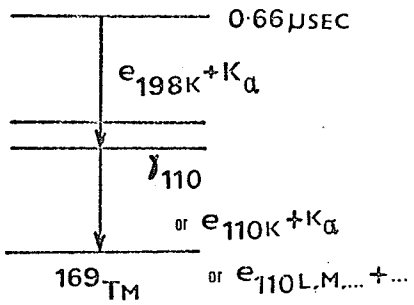

Figure 4-3. Abbreviated decay scheme showing the origin of the K_α X-rays in coincidence with e_{198K}.

f_3 was the fraction of K_α X-rays in coincidence with e_{198K} that followed e_{198K} (but not following e_{110K}). Equation (4)

was expanded

$$A_{22}(K_\alpha(e_{198K}+e_{110K})-e_{198K}) = f_3A_2(K_\alpha(e_{198K}))\cdot A_2(e_{198K}) + (1-f_3)A_2(K_\alpha(e_{110K}))\cdot A_2(e_{198K})$$

$$= f_3A_2(K_\alpha(e_{198K}))\cdot b_2(e_{198K})\cdot A_2(\gamma_{198}) + (1-f_3)A_2(K_\alpha(e_{110K}))\cdot b_2(e_{198K})\cdot A_2(\gamma_{198}) \quad \ldots(5)$$

The particle parameter for the 198 keV transition was

$$b_2(e_{198K}) = \frac{A_2(e_{198K})}{A_2(\gamma_{198})}$$

Equation (5) was used to solve for $b_2(e_{198K})$

$$b_2(e_{198K}) = (A_{22}(K_\alpha-e_{198K}))/(f_3A_2(K_\alpha(e_{198K}))\cdot A_2(\gamma_{198}) + (1-f_3)A_2(K_\alpha(e_{198K}))\cdot A_2(\gamma_{198}))$$

$$= +0.3(4)$$

This result was compared with the results of other directional correlation measurements[14)]

$$b_2(e_{198K}) = \frac{A_{22}(\gamma_{110}-e_{198K})}{A_{22}(\gamma_{110}-\gamma_{198})} = +0.003(24)$$

The two measurements were consistent. Unfortunately the present directional correlation measurements were not sufficiently accurate to improve the previously measured value of $b_2(e_{198K})$.

As has been indicated the directional correlation involving e_{177K} was complicated by the inclusion of a small portion of e_{131L} in the e_{177K} energy window. There

is a definite anisotropy whenever L conversion electrons are involved with K_α X-rays.[4] Hence the presence of $K_\alpha(e_{177K})$-e_{131L} could have contributed the entire anisotropy that was measured in K_α-e_{177K}. The directional correlation was

$$A_{22}(K_\alpha(e_{177K}+e_{131K}+e_{110K})-e_{177K}+K_\alpha(e_{177K})-e_{131L}) =$$
$$= f_4A_{22}(K_\alpha(e_{177K})-e_{177K}) + f_5A_{22}(K_\alpha(e_{131K})-e_{177K}) +$$
$$+ f_6A_{22}(K_\alpha(e_{110K})-e_{177K}) + f_7A_{22}(K_\alpha(e_{177K})-e_{131L}) \quad ...(6)$$

where f_4 was the fraction of the K_α which were in coincidence with e_{177K} and which followed e_{177K}. Similarly f_5 and f_6 were the fractions that followed e_{131K} and e_{110K} respectively; f_7 was the fraction of the K_α which were in coincidence with e_{131L} and which followed e_{177K}. If e_{131L} was not included in e_{177K} the fraction of the K_α's in coincidence with e_{177K} as a result of e_{177K} (see Figure 4-4) would be,

$$\text{fraction} = 1/\left(\left(\frac{I_{131}}{I_{20.7}+I_{131}}\right)\left(\frac{\alpha_{131K}}{\alpha_{131K}+\alpha_{131L,M,\ldots}+1}\right) + \right.$$
$$\left. +\left(\frac{I_{20.7}}{I_{20.7}+I_{131}}\right)\left(\frac{\alpha_{110K}}{\alpha_{110K}+\alpha_{110L,M,\ldots}+1}\right) + 1\right)$$

The internal conversion coefficients, α, were taken from reference 25. If a fraction p of the total e_{131L} was included within the e_{177K} energy window, the fraction of K_α's in coincidence with e_{177K} as a result of e_{177K} would become

$$f_4 = \text{fraction} \cdot \frac{I_{e177K}}{I_{e177K}+pI_{e131L}} = (0.725(16))\cdot(\frac{1.48}{1.48+p})$$

Furthermore,

$$f_5 = (0.128(12))\cdot(\frac{1.48}{1.48+p})$$

$$f_6 = (0.147(12))\cdot(\frac{1.48}{1.48+p})$$

$$f_7 = \frac{p}{1.48+p}$$

When these fractions were inserted into equation (6), along with the proper A_2's,

$$p = (84^{+16}_{-76})\%$$

Thus as little as 8% of the total e_{131L} in the e_{177K} energy window would have given the measured anisotropy. Experimentally, indications were that about 20% of the total e_{131L} peak was included.

Attention was next directed toward the A_4 coefficients. Repeating the style of analysis done on the A_2 coefficients

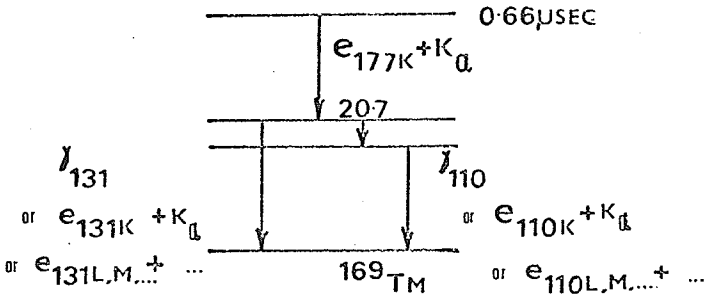

Figure 4-4. Simplified decay scheme showing the origin of the K_α X-rays in coincidence with e_{177K}.

on the A_4 coefficients, one obtained

$$A_4(K_\alpha(e_{177K})) = -0.053(31)$$

$$A_4(K_\alpha(e_{198K})) = +1.11(104)$$

The coefficients $A_4(K_\alpha(e_{110K}))$ and $A_4(K_\alpha(e_{131K}))$ were not calculated because the A_2's had indicated isotropy and the A_4's with their huge errors would have simply verified it.

The various coefficients involving the K_α's are collected in Table VI. These coefficients were a result of K_α X-rays following internal conversion and not electron capture. These coefficients were determined from an internally consistent set of measurements. Moreover the measurements were substantiated by simultaneous γ-γ and γ-e_K measurements.

TABLE VI

THE DIRECTIONAL CORRELATION COEFFICIENTS
FOR THE K_α X-RAYS FOLLOWING INTERNAL CONVERSION

A_2 Coefficients	A_4 Coefficients
$A_2(K_\alpha(e_{177K}))=+0.113(23)$	$A_4(K_\alpha(e_{177K}))=-0.053(31)$
$A_2(K_\alpha(e_{198K}))=-0.086(29)$	$A_4(K_\alpha(e_{198K}))=+1.11(104)$
$A_2(K_\alpha(e_{110K}))=-0.006(30)$	
$A_2(K_\alpha(e_{131K}))=+0.065(117)$	

CHAPTER V

DISCUSSION OF RESULTS

In the last chapter the experimental directional correlation coefficients, A_{22} and A_{44}, were dichotomized into A_2 and A_4 coefficients associated with K_α X-rays. Only the nonzero A_2 and A_4 coefficients will have consequential results. Hence this chapter will deal almost exclusively with them. Certainly abnormality always attracts more attention.

Normally only two of the possible three electron transitions are allowed from the L to the K shell (see Figure 5-1). The allowed transitions which generate the K_α X-rays are governed by the following selection rules for electric dipole radiation[34]

$\Delta \underline{l} = \pm 1$; $\Delta j = 0$ or ± 1

(the j-transition $0 \rightarrow 0$ is forbidden)

where $\Delta \underline{l}$ is the change in orbital angular momentum and Δj is the change in total angular momentum during the transition. The transition from $j = 3/2^-, \underline{l} = 1$ to $j = 1/2^+$, $\underline{l} = 0$ gives rise to the K_{α_1} X-rays; the other transition, $j = 1/2^-$, $\underline{l} = 1$ to $j = 1/2^+$, $\underline{l} = 0$ generates the K_{α_2} X-rays.

If the static electric quadrupole adds in states $d_{3/2}'$ and $d_{5/2}'$ to the normal $1s_{1/2}$ state (as suggested by Church and Weneser[12]) additional transitions would be

possible. These additional states, as has been mentioned, could arise because of an electric quadrupole interaction between the deformed nucleus and the K shell electrons. The resulting X-radiation could even be of E2 multipolarity for which the selection rules are[34]

$$\Delta l = 0 \text{ or } \pm 2; \quad \Delta j = 0, \pm 1 \text{ or } \pm 2$$

(the j-transitions $0 \rightarrow 0$, $1/2 \rightarrow 1/2$, $0 \rightarrow 1$ and $1 \rightarrow 0$ are forbidden)

With the additional $d_{3/2}'$ and $d_{5/2}'$ states, five additional

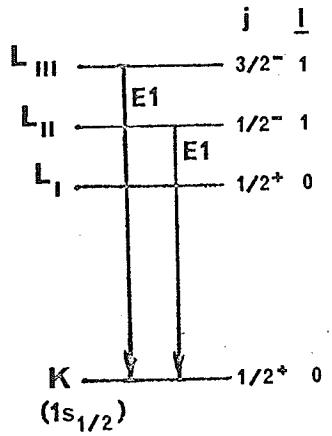

Figure 5-1. The allowed electron de-excitations which generate K_α X-rays for a normal atom.

transitions would be possible (see Figure 5-2). So one would have seven possible transitions, two normal and

five unusual ones from the electric quadrupole interaction. The presence of E2 X-radiation should not be startling since M1 X-radiation (arising from the forbidden L_I-to-K-shell transition) has been theoretically predicted[35] and experimentally found.[37]

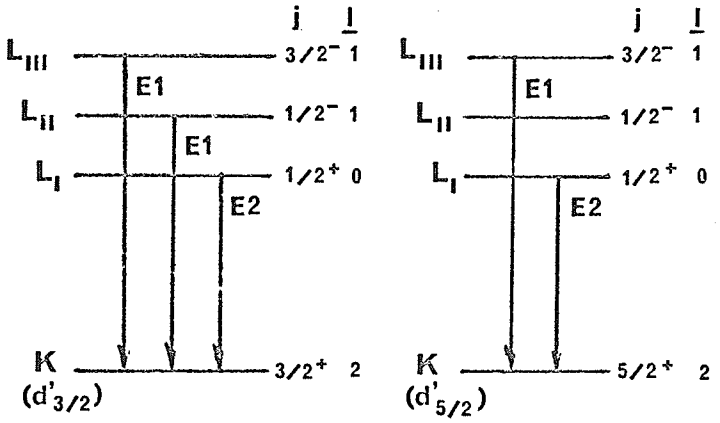

Figure 5-2. The additional allowed electron de-excitations which generate K X-rays for an atom with a K-shell spin of 3/2 or 5/2.

The anisotropy involving K_α X-rays associated with the conversion of the 177 keV transition differed from the K_α X-rays associated with the conversion of the 198 keV transition. Both of these nuclear transitions originated from the same $7/2^+$ nuclear level. Thus the static electric quadrupole interaction between the nucleus and the K shell electrons (due to the electric quadrupole

moment of the $7/2^+$ level) should be the same. One plausible explanation for the difference in the dichotomized directional correlation coefficients is that at least part of the anisotropy rose because of dynamic effects associated with the 177 keV and 198 keV transitions themselves. In order to keep the problem to a manageable size, an assumption was made - the dynamic effects just lead to additional $d_{3/2}'$ and $d_{5/2}'$ states (same as the static effects). The reason for making this assumption was that the measured directional correlation coefficients claim that the final state must include spins of 3/2 and 5/2. Certainly $s_{1/2}'$, $p_{1/2}'$ and $p_{3/2}'$ states would not satisfy this criteria; higher spin states than $d_{3/2}'$ and $d_{5/2}'$ would be less likely to occur.

Since all seven transitions previously mentioned may have occurred in these measurements, it explicitly was impossible from the correlation coefficients to determine the quantity of the $d_{3/2}'$ and $d_{5/2}'$ states mixed with the original $ls_{1/2}$ state. What could be done was to use the experimental results to specify the combinations or ratios of the various transitions that satisfied the measured anisotropy.

If one takes the 198 keV transition

$$A_4(K_\alpha(e_{198K})) = +1.11(104)$$

Since the error quoted was one standard deviation, there

was about a 30% chance that the A_4 coefficient was equal to about 0. For simplicity then, it was assumed that

$$A_4(K_\alpha(e_{198K})) = 0$$

Considering all the possible transitions,

$$\begin{aligned} A_4(K_\alpha(e_{198K})) &= 0 \\ &= f'(1/2^+,1/2^-,1)A_4(1/2^+,1/2^-,1) + \\ &\quad + f'(1/2^+,3/2^-,1)A_4(1/2^+,3/2^-,1) + \\ &\quad + f'(3/2^+,1/2^+,2)A_4(3/2^+,1/2^+,2) + \\ &\quad + f'(3/2^+,1/2^-,1)A_4(3/2^+,1/2^-,1) + \\ &\quad + f'(3/2^+,3/2^-,1)A_4(3/2^+,3/2^-,1) + \\ &\quad + f'(5/2^+,1/2^+,2)A_4(5/2^+,1/2^+,2) + \\ &\quad + f'(5/2^+,3/2^-,1)A_4(5/2^+,3/2^-,1) \\ &= f'(1/2^+,1/2^-,1)(0.0) + \\ &\quad + \ldots + \\ &\quad + f'(5/2^+,1/2^+,2)(-0.6172) + \\ &\quad + \ldots \\ &= f'(5/2^+,1/2^+,2)(-0.6172) \end{aligned}$$

or

$$f'(5/2^+,1/2^+,2) = 0.0 \qquad \ldots(7)$$

Here $f'(j_f,j_i,L)$ was the fraction of the K_α X-rays of multipolarity L that arose from the electron transition from the j_i level to the j_f level. The $A_4(j_f,j_i,L)$ were the tabulated directional correlation coefficients.[29)]

Since there were no transitions to the $5/2^+$ level from the $1/2^+$ level and it was an allowed transition, this suggested that it was unlikely that there were any transitions to the $5/2^+$ level from the $3/2^-$ level as well.

This implied that the total amount of $d_{5/2}'$ in the $1s_{1/2}$ wave during the 198 keV transition was very small or nonexistent. Next an attempt was made to get an estimate of the transitional probabilities $T(5/2^+,3/2^-,1)$ and $T(5/2^+,1/2^+,2)$ to see whether both were of the same order of magnitude. If they were, it would justify setting the $d_{5/2}'$ admixture to zero during the 198 keV transition. Now the absolute X-ray transition rates for electric multipole radiation are given by[35]

$$T(j_f,j_i,L) = 2\rho U\left(\frac{(2\underline{l}_i+1)(2\underline{l}_f+1)(2j_i+1)}{(2L+1)^2}\right)(C(\underline{l}_f\underline{l}_i L;00))^2\cdot$$

$$(W(j_f\underline{l}_f j_i\underline{l}_i;\tfrac{1}{2}L))^2\left(\left(\frac{L+1}{L}\right)^{\frac{1}{2}}((\mathbb{k}_i-\mathbb{k}_f)Q^{L-1(+)}_{\mathbb{k}_f\mathbb{k}_i}+LQ^{L-1(-)}_{\mathbb{k}_f\mathbb{k}_i}\right)+$$

$$-\left(\frac{L}{L+1}\right)^{\frac{1}{2}}((\mathbb{k}_i-\mathbb{k}_f)Q^{L+1(+)}_{\mathbb{k}_f\mathbb{k}_i}-(L+1)Q^{L+1(-)}_{\mathbb{k}_f\mathbb{k}_i}))^2$$

where

$$Q^{\lambda(\pm)}_{\mathbb{k}_f\mathbb{k}_i} = \int_o^\infty (G_{\mathbb{k}_f}H_{\mathbb{k}_i} \pm H_{\mathbb{k}_f}G_{\mathbb{k}_i})B^\lambda(Ur)dr$$

All quantities are expressed in rationalized relativistic units, i.e. $\hbar$ (Plancks constant/2π) = m_e (electron mass) = c (speed of light) = 1 and q^2 (electron charge) = ρ. The fine structure constant is ρ = 1/137; U is the X-ray energy. $\mathbb{k}$ is a quantum number given by Rose.[36] It has the values

$$\mathbb{k} = \underline{l},\ j = \underline{l}-\tfrac{1}{2}$$

$$\mathbb{k} = -(\underline{l}+1),\ j = \underline{l}+\tfrac{1}{2}$$

$C(l_f -l_i L;00)$ are Clebsch-Gordan coefficients and $W(j_f l_f j_i l_i;\frac{1}{2}L)$ are Wigner coefficients. $B^{\lambda}(Ur)$ are the spherical Bessel functions of the first kind. The computation of the radial integrals $Q^{\lambda(\pm)}_{k_f k_i}$ depends upon the radial wave functions G_k and H_k that are selected. The latter depend upon the atomic model.

As a first approximation, the relativistic hydrogen-like radial wavefunctions were used.[36] A complete list of the radial wavefunctions used is given in Appendix B.

To find the accuracy these wavefunctions would give, the following transition rate ratio was calculated,

$$\frac{T(1/2^+,3/2^-,1)}{T(1/2^+,1/2^-,1)} = 1.79$$

Experimentally the ratio was (100)/(55±2) = 1.82(7). The closeness was encouraging. Certainly one could not expect such accurate results with $T(5/2^+,3/2^-,1)/T(5/2^+,1/2^+,2)$ since the wavefunctions could be quite different from the relativistic hydrogen-like wavefunctions. The calculation yielded

$$\frac{T(5/2^+,3/2^-,1)}{T(5/2^+,1/2^+,2)} = 12.8$$

Then the probability of the $3/2^- \rightarrow 5/2^+$ transition was not much more predominant than the $1/2^+ \rightarrow 5/2^+$ transition. It will be shown later that the theoretical calculations were about 100% larger than the experimental value. Then

since $T(5/2^+,3/2^-,1)/T(5/2^+,1/2^+,2) \simeq 6$, the quantity of the $3/2^- \rightarrow 5/2^+$ in $A_4(K_\alpha(e_{198K}))$ should be very small. Hence the earlier expression of only a very small amount of $d_{5/2}'$ mixture in the $1s_{1/2}$ wave was quite appropriate.

Next the A_2 coefficient for the 198 keV transition was considered;

$$\begin{aligned} A_2(K_\alpha(e_{198K})) &= -0.86(29) \\ &= f'(1/2^+,1/2^-,1)A_2(1/2^+,1/2^-,1) + \\ &\quad + f'(1/2^+,3/2^-,1)A_2(1/2^+,3/2^-,1) + \\ &\quad + f'(3/2^+,1/2^+,2)A_2(3/2^+,1/2^+,2) + \\ &\quad + f'(3/2^+,1/2^-,1)A_2(3/2^+,1/2^-,1) + \\ &\quad + f'(3/2^+,3/2^-,1)A_2(3/2^+,3/2^-,1) + \\ &\quad + f'(5/2^+,1/2^+,2)A_2(5/2^+,1/2^+,2) + \\ &\quad + f'(5/2^+,3/2^-,1)A_2(5/2^+,3/2^-,1) \end{aligned}$$

Upon inserting the appropriate values and using the values of $f'(5/2^+,1/2^+,2)$ and $f'(5/2^+,3/2^-,1)$ determined from the A_4 coefficients, one got

$$f'(3/2^+,1/2^+,2)(-0.500) + f'(3/2^+,1/2^-,1)(0.500) + \\ + f'(3/2^+,3/2^-,1)(-0.400) = -0.086(29) \qquad \ldots(8)$$

As one could see, as many as three possible transitions could have been contributing to the measured anisotropy.

At this moment attention was focused upon the 177 keV transition. Ultimately the results from both transitions were analyzed together to extract as much information as was possible upon which to form conclusions.

For the 177 keV transition, the only nonzero A_4

coefficient was $A_4(5/2^+,1/2^+,2) = -0.6172$. Then

$$A_4(K_\alpha(e_{177K})) = -0.053(31)$$
$$= f(5/2^+,1/2^+,2)(-0.6172)$$

or

$$f(5/2^+,1/2^+,2) = 0.086(50) \qquad \ldots(9)$$

It should be recognized that these fractions for the 177 keV transitions are not primed and necessarily will not have the same values as the primed f's associated with the 198 keV transition.

Attention was turned toward the A_2 coefficient and only the nonzero coefficients were considered;

$$A_2(K_\alpha(e_{177K})) = +0.113(23)$$
$$= f(3/2^+,1/2^+,2)(-0.500) +$$
$$+ f(3/2^+,1/2^-,1)(0.500) +$$
$$+ f(3/2^+,3/2^-,1)(-0.400) +$$
$$+ f(5/2^+,3/2^-,1)(0.3742) +$$
$$+ f(5/2^+,1/2^+,2)(-0.5345)$$

or

$$f(3/2^+,1/2^+,2)(-0.500) + f(3/2^+,1/2^-,1)(0.500) +$$
$$+ f(3/2^+,3/2^-,1)(-0.400) + f(5/2^+,3/2^-,1)(0.3742) =$$
$$= +0.159(50) \qquad \ldots(10)$$

So one had a collection of the possible combinations of fractions of the various transitions given by equations (7) to (10). However all was not clouded beyond solution by the many possibilities. Three other experimental measurements were available which would shed some light on the problem. The other experimental values were the intensity ratios

$K_{\alpha_2}/K_{\alpha_1}$, $(K_{\alpha_2}-\gamma_{131})/(K_{\alpha_1}-\gamma_{131})$ and $(K_{\alpha_2}-\gamma_{110})/(K_{\alpha_1}-\gamma_{110})$. Fortunately the X-ray detector resolution just partially resolved the two K_α peaks and applying the $K\beta_1$ shape to the K_α peaks, the following values were obtained:

$$\frac{K_{\alpha_2}}{K_{\alpha_1}} = 0.55(2)$$

$$\frac{K_{\alpha_2}(e_{177K})-\gamma_{131}}{K_{\alpha_1}(e_{177K})-\gamma_{131}} = 0.45(4)$$

$$\frac{K_{\alpha_2}(e_{198K})-\gamma_{110}}{K_{\alpha_1}(e_{198K})-\gamma_{110}} = 0.49(6)$$

The last value was calculated from the experimental value since part of the K_α's in the original coincidences were from e_{177K}. The three ratios each were an average of the ratios at the angles of 90°, 135° and 180°. In the stated experimental ratios, any transitions from the L_I shell to the K shell would be included in the K_{α_2} peak. The very fact that the coincidence ratios were statistically different from the singles' ratio were themselves a suggestion of abnormality.

All the experimental evidence combined with the theoretical transition probabilities were used in an attempt to definitely determine the amount of $d_{3/2}'$ and $d_{5/2}'$ wave mixtures in the K shell wave during the 177 keV and the 198 keV transitions.

The process to give definite mixtures was an iterative

one. First it was assumed that only a $d_{5/2}'$ admixture occurred during the 177 keV transition. The experimental-to-theoretical ratio was determined for the transition rates from the $3/2^-$ and $1/2^+$ levels to the $5/2^+$ level. This correction factor was applied to calculations for transitions from the $3/2^-$ and $1/2^+$ levels to the $3/2^+$ level. Next the intensity ratio for transitions to the $3/2^+$ level from the $1/2^-$ level was calculated from the experimental data involving the 198 keV transition. Returning to the 177 keV case, the $d_{3/2}'$ admixture was included and the intensity ratios determined from the 198 keV case were applied here. A new comparison was made of the experimental-to-theoretical ratio and the new correction factor was applied to the 198 keV case. The process was repeated until reasonable values were obtained.

First $A_2(K_\alpha(e_{177K}))$ was considered. It was assumed that only a $d_{5/2}'$ admixture (no $d_{3/2}'$ admixture) was present. The directional correlation coefficients yielded

$$f(5/2^+,3/2^-,1) = 0.43(14)$$

Then

$$\frac{f(5/2^+,3/2^-,1)}{f(5/2^+,1/2^+,2)} = 4.9(32)$$

This was compared with the theoretical prediction of 12.8, i.e.

$$\frac{\text{Actual}}{\text{Theoretical}}\left(\frac{f(5/2^+,3/2^-,1)}{f(5/2^+,1/2^+,2)}\right) = 0.38(25)$$

It was next assumed that the ratio

$$\frac{\text{Actual}}{\text{Theoretical}}\left(\frac{f(3/2^+,3/2^-,1)}{f(3/2^+,1/2^+,2)}\right)$$

also equalled 0.38(25). Then the modified theoretical value for the X-ray transition probabilities during the 198 keV transition became

$$\frac{f'(3/2^+,3/2^-,1)}{f'(3/2^+,1/2^+,2)} = (0.38(25))(4.68) = 1.78(117)$$

This value was inserted where ever possible into the experimental measurements involving the 198 keV transition. Four independent equations and four unknowns resulted.

One equation was from the results of $A_2(K_\alpha(e_{198K}))$ (from equation (8)).

$$(-0.500)(0.56(37))f'(3/2^+,3/2^-,1) + \\ + (0.500)f'(3/2^+,1/2^-,1) + (-0.400)f'(3/2^+,3/2^-,1) = \\ = 0.086(29) \qquad \ldots(11)$$

The second equation was the $K_{\alpha_2}/K_{\alpha_1}$ singles' ratio.

$$f'(1/2^+,1/2^-,1) = (0.55(2))f'(1/2^+,3/2^-,1) \qquad \ldots(12)$$

The ratio $(K_{\alpha_2}(e_{198K})-\gamma_{110})/(K_{\alpha_1}(e_{198K})-\gamma_{110})$ gave the third equation.

$$\frac{f'(3/2^+,1/2^+,2) + f'(1/2^+,1/2^-,1) + f'(3/2^+,1/2^-,1)}{f'(1/2^+,3/2^-,1) + f'(3/2^+,3/2^-,1)} = \\ = 0.49(6) \qquad \ldots(13)$$

Finally the fourth equation arose because the fractions all had to add up to one.

$$f'(3/2^+,1/2^+,2) + f'(1/2^+,1/2^-,1) + f'(3/2^+,1/2^-,1) + + f'(1/2^+,3/2^-,1) + f'(3/2^+,3/2^-,1) = 1.000 \quad ...(14)$$

Algebraically manipulating these four equations (equations (11) to (14)), one obtained

$$f'(3/2^+,3/2^-,1) = 0.096(51)$$

$$f'(3/2^+,1/2^-,1) = 0.028(28)$$

$$f'(3/2^+,1/2^+,2) = 0.054(46)$$

Using the ratio

$$\frac{f'(3/2^+,1/2^-,1)}{f'(3/2^+,3/2^-,1)} = 0.29(33),$$

returning to the experimental results associated with the 177 keV transition and including the $d_{3/2}'$ admixture, one found a value for $f(5/2^+,3/2^-,1)$. This fraction was combined with $f(5/2^+,1/2^+,2)$ to be used in an estimate of the new error in the theoretical values. The iteration was repeated. The results after each iteration for three iterations are shown in Table VII.

The fraction, $f(5/2^+,3/2^-,1)$, oscillated as the iteration process proceeded, i.e. 0.43(14) to 0.19(27) to 0.83(83). The oscillation must have been about the correct value and it did not appear that repeating the iteration process would lead to convergence. What was done was to select a weighted average of the results from the first two iterations as the most likely values of the fractions f and f'. When that was done, the results shown in Table VIII

TABLE VII

FRACTIONS OF THE DIFFERENT K_α TRANSITIONS IN THE ITERATION PROCESS

177 keV Transition	198 keV Transition
1 Iteration:	
$f(3/2^+,1/2^+,2) = 0.0$	$f'(3/2^+,1/2^+,2) = 0.054(46)$
$f(3/2^+,1/2^-,1) = 0.0$	$f'(3/2^+,1/2^-,1) = 0.028(28)$
$f(3/2^+,3/2^-,1) = 0.0$	$f'(3/2^+,3/2^-,1) = 0.096(51)$
$f(5/2^+,1/2^+,2) = 0.086(50)$	
$f(5/2^+,3/2^-,1) = 0.43(14)$	
2 Iterations:	
$f(3/2^+,1/2^+,2) = 0.024(34)$	$f'(3/2^+,1/2^+,2) = 0.044(77)$
$f(3/2^+,1/2^-,1) = 0.012(18)$	$f'(3/2^+,1/2^-,1) = 0.005(6)$
$f(3/2^+,3/2^-,1) = 0.042(42)$	$f'(3/2^+,3/2^-,1) = 0.035(32)$
$f(5/2^+,1/2^+,2) = 0.086(50)$	
$f(5/2^+,3/2^-,1) = 0.19(27)$	
3 Iterations:	
$f(5/2^+,1/2^+,2) = 0.086(50)$	
$f(5/2^+,3/2^-,1) = 0.83(83)$	

TABLE VIII

FRACTIONS OF THE ABNORMAL K_α TRANSITIONS

177 keV Transition	198 keV Transition
$f(3/2^+,1/2^+,2) = 0.012(17)$	$f'(3/2^+,1/2^+,2) = 0.005(5)$
$f(3/2^+,1/2^-,1) = 0.006(9)$	$f'(3/2^+,1/2^-,1) = 0.058(39)$
$f(3/2^+,3/2^-,1) = 0.021(21)$	$f'(3/2^+,3/2^-,1) = 0.050(56)$
Total $d_{3/2}' = 0.04(5)$	Total $d_{3/2}' = 0.11(10)$
$f(5/2^+,1/2^+,2) = 0.086(50)$	
$f(5/2^+,3/2^-,1) = 0.35(19)$	
Total $d_{5/2}' = 0.44(24)$	

were obtained.

One can see that from the iterative approach used, actual values for $d_{3/2}'$ and $d_{5/2}'$ admixtures were obtained. The results suggested that (11±10)% of the K shell wave during and after the 198 keV nuclear transition was a $d_{3/2}'$ wave; that, during and after the 177 keV nuclear transition, the K shell wave consisted of $(4^{+5}_{-4})\%$ $d_{3/2}'$ wave and (44±24)% $d_{5/2}'$ wave.

CHAPTER VI

CONCLUSION

Presented in this dissertation were the consistent experimental results of evidence of electric quadrupole interaction on the K shell electron wavefunction by a deformed nucleus. The evidence presented suggested that when the ^{169}Tm nucleus is in the excited $7/2^+$ level and while decaying from that level, through retarded transitions, it interacts with the K shell electron wavefunction. The interaction must impart to the normal $1s_{1/2}$ wavefunction spins as high as $3/2^+$ and $5/2^+$ at least part of the time. It was assumed that the interaction was exclusively an electric quadrupole interaction and that it added just $d_{3/2}'$ and $d_{5/2}'$ states to the normal $1s_{1/2}$ wavefunction. Then admixtures of (11±10)% $d_{3/2}'$ after the retarded 198 keV transition and (4±5)% $d_{3/2}'$ and (44±24)% $d_{5/2}'$ after the retarded 177 keV transition were consistent with the experimental results. There was no evidence of similar interaction when the nucleus decayed by unretarded transitions.

Experimentally, the interaction was detected by measuring the directional distribution of K_α X-rays following internal conversion of the nuclear transition.

A reference direction was specified with the aid of a cascading gamma-ray or conversion electron. The distribution would have been isotropic if the K shell wavefunction was the normal $1s_{1/2}$ wavefunction (spin of $1/2^+$). Since the K_α X-ray distribution was not isotropic in two cases, the K shell wavefunction must have had a spin greater than $1/2^+$. To account for the actual directional distributions, in these two cases the wavefunction must have had a spin as high as $5/2^+$ part of the time. As a summary, the anisotropies measured ($A = (C(180^\circ)-C(90^\circ))/C(90^\circ)$) are listed in Table IX.

TABLE IX

MEASURED ANISOTROPY

Coincidence	Anisotropy	Significant
K_α-γ_{131}	-0.065(19)	Yes
K_α-γ_{110}	-0.038(22)	Yes
K_α-(e_{177K}+e_{131L})	-0.031(28)	No
K_α-e_{198K}	-0.006(26)	No
K_α-γ_{177}	-0.022(53)	No
K_α-γ_{198}	-0.002(17)	No

When technology presents X-ray detectors with resolutions of better than 350 eV at 50 keV, K_{α_2} and K_{α_1} X-rays could then be easily separated from any transition

from the L_I shell to the K shell. A coincidence between K_α X-rays and γ_{131} should yield very precise values for the ratios

$$(f(3/2^+,1/2^+,2)+f(5/2^+,1/2^+,2))/(f(3/2^+,1/2^-,1))$$

$$(f(3/2^+,3/2^-,1)+f(5/2^+,3/2^-,1))/(f(3/2^+,1/2^-,1))$$

This should produce more accurate fractions than those derived by the iterative process. Such a measurement would not however give the absolute magnitude of the fractions which the directional correlation measurements have given.

Until further experimental evidence is available, the possibility now exists (because of the present research) that the fluorescence yields are not unique for a given atom but may also depend upon the state the nucleus is in. Furthermore it has been demonstrated that in the cases when K_α X-rays do have a directional distribution, K_α-e_K directional correlation measurements can be used to measure the electron particle parameter of e_K.

The present research has exhibited evidence of the electric quadrupole interactions on the K shell electron wavefunction. It has also pointed out some of the practical applications of a new way to explore the nucleus and atomic structure.

BIBLIOGRAPHY

1) E. Bodenstedt, Lectures on Hyperfine Interactions, A Field Between Nuclear Physics and Solid State Physics, given at University of Leuven (1969).
2) P. Kusch and V. Hughes, in Handbuch der Physik, Vol.37 (1959).
3) H. Frauenfelder and R.M. Steffen, in Alpha-, Beta-, and Gamma-Ray Spectroscopy, edited by K. Siegbahn, North-Holland, Amsterdam (1966) 997.
4) A.Z. Dolginov, JETP Letters 34 (7), 4 (1958) 644.
5) V.V. Perepelkin, JETP Letters 5 (1967) 81.
6) J. Fechner, C. Günther, H. Hübel, R.S. Raghavan, K.-H. Speidel, H. Toschinski and B. Wolbeck, Phys. Lett. 26B, 6 (1968) 374.
7) M.K. Ranaswamy, Bull. Am. Phys. Soc. 13, 11 (1968) 1450.
8) D.S. Murty, K.V. Ramana Rao, P. Jagam and V. Lakshminarayana, Can. J. Phys. 48, 12 (1970) 1514.
9) M. McDonnell and M.K. Ranaswamy, Phys. Rev. 171, 4 (1968) 1278.
10) J.B. Brannan, Thesis, Columbus, Ohio (1969).
11) S.K. Sen, in Proceedings of the Conference on the Electron Capture and Higher Order Processes in Nuclear Decays, Debrecen, Hungary (1968) 406.
12) E.L. Church and J. Weneser, Annual Rev. of Nucl. Sci., 10 (1960) 193.
13) C.M. Lederer, J.M. Hollander and I. Perlman, Table of Isotopes, 6th Edition (1967).
14) Z. Grabowski, J. Thun, M. El-Nesr and W. Hamilton, Z. Physik 167 (1962) 111.
15) F. Asaro, F.S. Stephens, J. Hollander and I. Perlman, Phys. Rev. 117 (1960) 492.
16) S.G. Nilsson and S.G. Rasmussen, Nucl. Phys. 5 (1958) 617.
17) M. Kalvius, P. Kienle, H. Eicher, W. Wiedemann and C. Schüler, Z. Physik 172 (1963) 231.
18) R.L. Cohen, Phys. Rev. 134A (1964) 94.
19) G. Alaga, K. Alder, A. Bohr and B.R. Mottelson, Dan. Mat.-Fys. Medd. 29 (1955) 9.
20) M.C. George, Ph.D. Dissertation, University of Alabama (1967).
21) Z.N. Miminoshvili, V.V. Murav'eva and A.A. Sorokin, Soviet J. of Nucl. Phys. 10, 2 (1970) 113.
22) P. Alexander and F. Boehm, Nucl. Phys. 46, 1 (1963) 108.
23) H. Frauenfelder, Ann. Rev. of Nucl. Sci. 2 (1953) 129.
24) D.H. White, Nucl. Instr. & Meth. 21 (1965) 209.
25) R.S. Hager and E.C. Seltzer, Nucl. Data A4 (1968) 1.

26) A.J. Becker and R.M. Steffen, Bull. Am. Phys. Soc. 12 (1967) 716.
27) C. Günther, H. Hübel, A. Kluge, K. Krien and H. Toschinski, Nucl. Phys. A123 (1969) 386.
28) E.N. Kaufmann, J.D. Bowman and S.K. Bhattacherjee, Nucl. Phys. A119 (1968) 417.
29) M. Ferentz and N. Rosenzweig, in Alpha-, Beta-, and Gamma-Ray Spectroscopy, edited by K. Siegbahn, North-Holland, Amsterdam (1966) 1687.
30) V.M. Kel'man, R.Ya. Metskhvarishvili, B.K. Preobrazhenskii, V.A. Romanov and V.V. Tuchkevich, J. Expt. Theoret. Phys. (USSR) 37(1959) 639. English Translation: Soviet Physics, JETP 37 (1960) 456.
31) J.W. Mihelich, T.J. Ward and K.P. Jacob, Phys. Rev. 103, 5 (1956) 1285.
32) V.R. Potnis, G.P. Agin, C.E. Mandeville and R. Rogow, Bull. Am. Phys. Soc. 17, 1 (1972) 28.
33) A.J. Becker, K.S. Krane and R.M. Steffen, Bull. Am. Phys. Soc. 17, 1 (1972) 138.
34) A. Sandstrom in Handbuch der Physik, edited by S. Flügge, Springer-Verlag, Berlin (1957) 78.
35) H.R. Rosner and C.P. Bhalla, Z. Physik 231 (1970) 347.
36) M.E. Rose, Relativistic Electron Theory, John Wiley & Sons, Inc. (1961) 169.
37) O.W.B. Schult, Z. Naturforsch. 26A (1971) 368.

APPENDIX

APPENDIX A

DERIVATION OF THE ERROR IN THE DIRECTIONAL CORRELATION COEFFICIENTS

Generally the unnormalized directional correlation coefficients, a_n, are

$$a_n = \sum_i P_{ni}^{-1} C(\theta_i)$$

where $A_{22} = a_2/a_0$ and $A_{44} = a_4/a_0$. P_{ni}^{-1} is the inverse matrix of the Legendre Polynomial matrix P_{in} and $C(\theta_i)$ are the total true coincidence counts at the angle θ_i. For the case of coincidences measured at the three angles of θ_1, θ_2 and θ_3,

$$P_{in} = \begin{bmatrix} P_0(\cos\theta_1) & P_2(\cos\theta_1) & P_4(\cos\theta_1) \\ P_0(\cos\theta_2) & P_2(\cos\theta_2) & P_4(\cos\theta_2) \\ P_0(\cos\theta_3) & P_2(\cos\theta_3) & P_4(\cos\theta_3) \end{bmatrix}$$

If θ_1, θ_2 and θ_3 are 90°, 135° and 180° respectively

$$P_{in} = \begin{bmatrix} 1 & -1/2 & 3/8 \\ 1 & 1/4 & -13/32 \\ 1 & 1 & 1 \end{bmatrix}$$

and

$$P_{ni}^{-1} = \frac{1}{105}\begin{bmatrix} 42 & 56 & 7 \\ -90 & 40 & 50 \\ 48 & -96 & 48 \end{bmatrix}$$

The variance of a_n is

$$\sigma^2(a_n) = G^{-1}_{nn}$$

where

$$G_{nm} = \sum_i \frac{P_{in}P_{im}}{\sigma^2(\mu_i)}$$

Here the coincidence counting rate is $\mu_i = C(\theta_i)/t$;
t is the length of time for collecting coincidences.
Using the notation of White[24]

$$\sigma^2(\mu_i) = \frac{C^+(\theta_i)^2}{t^2}$$

where $C^+(\theta_i)$ is the gross coincidences at angle θ_i before background is subtracted. Then

$$G_{nm} = t^2 \sum_i \frac{P_{in}P_{im}}{C^+(\theta_i)^2}$$

For coincidences at the three angles of 90°, 135° and 180°, the errors in the directional correlation coefficients are then

$$A_{22} = \frac{1}{105a_0}\left[C^+(90^\circ)^2((90)^2+(42\frac{a_2}{a_0})^2)+C^+(135^\circ)^2\cdot\right.$$
$$\left.\cdot((40)^2+(56\frac{a_2}{a_0})^2)+C^+(180^\circ)^2((50)^2+(7\frac{a_2}{a_0})^2)\right]^{\frac{1}{2}}$$

and

$$A_{44} = \frac{1}{105a_0}\left[C^+(90^\circ)^2((48)^2+(42\frac{a_4}{a_0})^2+C^+(135^\circ)^2\cdot\right.$$
$$\left.\cdot((96)^2+(56\frac{a_4}{a_0})^2)+C^+(180^\circ)^2((48)^2+(7\frac{a_4}{a_0})^2)\right]^{\frac{1}{2}}$$

where

$$a_0 = \frac{1}{105}(42C(90^\circ)+56C(135^\circ)+7C(180^\circ))$$

$$a_2 = \frac{1}{105}(-90C(90^\circ)+40C(135^\circ)+50C(180^\circ))$$

$$a_4 = \frac{1}{105}(48C(90^\circ)-96C(135^\circ)+48C(180^\circ))$$

APPENDIX B

RELATIVISTIC HYDROGEN-LIKE RADIAL WAVEFUNCTIONS

The following wavefunctions were derived from the general forms given in reference 36. They are expressed in rationalized relativistic units.

K shell, $j=1/2^+$ $(1s_{1/2})$	$H_{k=-1} = -0.209r^{0.8640}e^{-0.5035r}$
	$G_{k=-1} = +0.774r^{0.8640}e^{-0.5035r}$
L_I shell, $j=1/2^+$ $(2s_{1/2})$	$H_{k=-1} = (-0.0831+0.0118r)r^{0.8640}e^{-0.2556r}$
	$G_{k=-1} = (0.308-0.0892r)r^{0.8640}e^{-0.2556r}$
L_{II} shell, $j=1/2^-$ $(2p_{1/2})$	$H_{k=1} = (-0.0724+0.00668r)r^{0.8640}e^{-0.2556r}$
	$G_{k=1} = (-0.0196-0.0503r)r^{0.8640}e^{-0.2556r}$
L_{III} shell, $j=3/2^-$ $(2p_{3/2})$	$H_{k=-2} = -0.00529r^{1.937}e^{-0.2518r}$
	$G_{k=-2} = 0.0417r^{1.937}e^{-0.2518r}$
K shell, $j=3/2^+$ $(d_{3/2}')$	$H_{k=2} = (-2.45\times10^{-3}+8.39\times10^{-5}r)r^{1.937}e^{-0.1690r}$
	$G_{k=2} = (-3.05\times10^{-4}-9.86\times10^{-4}r)r^{1.937}e^{-0.1690r}$
K shell, $j=5/2^+$ $(d_{5/2}')$	$H_{k=-3} = -7.82\times10^{-5}r^{2.957}e^{-0.1678r}$
	$G_{k=-3} = 9.25\times10^{-4}r^{2.957}e^{-0.1678r}$